

1 **A marine bacterial community that degrades poly(ethylene**
2 **terephthalate) and polyethylene**

3 Rongrong Gao^{1,2,3,4}, Chaomin Sun^{1,2,4*}

4 ¹Key Laboratory of Experimental Marine Biology, Institute of Oceanology, Chinese
5 Academy of Sciences, Qingdao, China

6 ²Laboratory for Marine Biology and Biotechnology, Qingdao National Laboratory
7 for Marine Science and Technology, Qingdao, China

8 ³College of Earth Science, University of Chinese Academy of Sciences, Beijing,
9 China

10 ⁴Center of Ocean Mega-Science, Chinese Academy of Sciences, Qingdao, China

11

12 * Corresponding author

13 Chaomin Sun Tel.: +86 532 82898857; fax: +86 532 82898857.

14 E-mail address: sunchaomin@qdio.ac.cn

15

16 **Keywords:** ocean, plastics, bacterial community reconstitution, degradation,
17 pollution

18 **Running title:** A marine bacterial community degrades PET and PE

19

20

21

22

23

24

25

26

27

28

29 **Abstract**

30 Plastic wastes have become the most common form of marine debris and present a
31 growing global pollution problem. Recently, microorganisms-mediated degradation
32 has become a most promising way to accomplish the eventual bioremediation of
33 plastic wastes due to their prominent degradation potentials. Here, a marine bacterial
34 community which could efficiently colonize and degrade both poly (ethylene
35 terephthalate) (PET) and polyethylene (PE) was discovered through a screening with
36 hundreds of plastic waste associated samples. Using absolute quantitative 16S rRNA
37 sequencing and cultivation methods, we obtained the abundances and pure cultures
38 of three bacteria mediating plastic degradation. We further reconstituted a tailored
39 bacterial community containing above three bacteria and demonstrated its efficient
40 degradation of PET and PE through various techniques. The released products from
41 PET and PE degraded by the reconstituted bacterial community were determined by
42 the liquid chromatography-mass spectrometry. Finally, the plastic degradation process
43 and potential mechanisms mediated by the reconstituted bacterial community were
44 elucidated through transcriptomic methods. Overall, this study establishes a stable and
45 effective marine bacterial community for PET and PE degradation and sheds light on
46 the degradation pathways and associated mechanistic processes, which paves a way to
47 develop a microbial inoculant against plastic wastes.

48

49

50

51

52

53

54

55

56

57 **Introduction**

58 Plastics have been found widespread in the world's oceans¹⁻⁴. It has been reported that
59 about 4.8 to 12.7 million tons of plastic debris per year enter the ocean⁵. Plastics in the
60 marine environment are of increasing concern because of their persistence and effects
61 on the oceans⁶, wildlife⁷, and, potentially, humans³. An estimated one million birds
62 and ten thousand marine animals die each year as a result of ingestion of or trapping
63 by plastics in the oceans^{8,9}. Moreover, after weathering, mechanical wear and
64 ultraviolet radiation, the large plastic may be broken into fragmentation, when it is
65 smaller than 5 mm in diameter, it was commonly defined as microplastics¹⁰. Of note,
66 microplastics also negatively impact upon marine biota and can be ingested and
67 accumulated along trophic webs until top predators^{11,12}.

68 Among various types of plastic wastes, poly (ethylene terephthalate) (PET) and
69 polyethylene (PE) constitute the major 46.5% portion of the tremendous amount of
70 plastic pollution debris¹³. PET is a type of semi-aromatic thermoplastic co-polymer
71 resin from polyester family, which has aromatic groups heteroatoms in the main
72 chain¹⁴. PE has a carbon-carbon backbone which is solely built of carbon atoms and
73 has high resistance against various degradation processes, due to non-hydrolyzable
74 covalent bonds¹⁵. Both PET and PE have properties such as lower density, long
75 hydrocarbon chain, high molecular weight and tensile strength, low permeability to
76 gases, durability to physical and chemical degradation, non-biodegradable
77 compound¹⁶⁻¹⁸.

78 Landfilling, incineration, recycling and biodegradation are the principal strategies
79 to solve the plastic waste problem⁸. As an environmentally friendly alternative to
80 conventional plastic waste management methods, microorganisms-mediated
81 degradation is the most promising way to accomplish an eventual bioremediation of
82 plastic wastes. Microbial degradation of plastics is usually an enzymatic activity that
83 catalyzes the cleavage of polymer bond into monomer entity^{19,20}. Thus far, PET
84 hydrolyzing activity has been reported for members of the cutinase, lipase and

85 esterase²⁰. PE, as one of the most abundant plastics in the ocean, shows obvious signs
86 of degradation when incubated with specific microorganisms under controlled
87 laboratory conditions²¹⁻²³. However, as compared to the extensive studies about PET-
88 degrading bacteria and enzymes^{14,18,19,24-26}, the researches about PE degradation
89 mediated by microorganisms lag well behind and the degradation efficiency using a
90 single strain or enzyme is still too low to meet the industrial applications requirements.
91 Alternatively, using microbial community to degrade PE might be a good choice
92 given their inherent multiple robust function among synergistic effect of different
93 species²⁷. Actually, the construction of artificial microbial consortia has opened a new
94 horizon in environment bioremediation in terms of removing hard biodegradable
95 harmful compounds²⁸.

96 Herein, a marine bacterial community efficiently degrading both PET and PE
97 was obtained by a large-scale screening. Three bacteria driving plastic degradation
98 were isolated and reconstituted to an artificial bacterial community with a similar
99 degradation capability to that of the original bacterial flora. The degradation effects
100 and possible products of PET and PE treated by this reconstituted bacterial
101 community were further clarified by various techniques. Lastly, the potential
102 degradation process and associated enzymes were disclosed through transcriptomics
103 methods.

104 **Results**

105 **Discovery of a marine bacterial community efficiently degrading both PET and**
106 **PE.** To obtain potential marine bacteria degrading PET or PE, we collected about 300
107 sediment samples contaminated by plastic debris from different locations of a bay of
108 China. Using these samples, we initiated to screen microorganisms that could use
109 plastic drink bottles (whose main component is PET) or commercial PE bags as major
110 carbon sources for growth. With that, a distinct consortium derived from one of the
111 plastic debris samples could efficiently colonize on both PET (Supplementary Fig. 1b)
112 and PE films (Supplementary Fig. 1d). Scanning electronic microscopy (SEM)

113 observation confirmed that the consortium could evidently colonize on PET
114 (Supplementary Fig. 1f) and PE films (Supplementary Fig.1i). Of note, these
115 colonizers formed an obvious biofilm layer and closely interacted each other with
116 filament-like structures on PET (Supplementary Fig. 1g) and PE films
117 (Supplementary Fig.1j). After removing the microbial layer from the films, significant
118 morphological changes in both PET (Supplementary Figs. 2b-2d) and PE films were
119 observed by SEM, especially for PE which showed large amount of heavy cracks and
120 deep holes in the surface and even the inside of the film (Supplementary Figs. 2f-2h).

121 Given the fact that most commercial plastics contain various additives (such as
122 dyes, plasticizer, antistatic agents etc.), it is necessary to make sure that the
123 consortium indeed degraded the plastics rather than the additives. We thus repeated
124 the degradation test by the above consortium with the PET and PE films without any
125 additives. Consistently, both PET and PE films were evidently degraded after 4 weeks
126 treatment by the consortium even observed by eyes (Figs. 1b, 1d), and the four
127 corners of both films lost sharp morphology as that shown in the control (Figs. 1a, 1c).
128 Similar to the results obtained with the additive-containing plastics, SEM observation
129 revealed that the consortium could efficiently colonize on the surface of films (Figs.
130 1f, 1i) and caused obvious degradation by forming pits, cracks or holes in the surface
131 and inside of PET (Fig. 1g) and PE film (Fig. 1j). Similar to additive-containing
132 plastics, the consortium prefers to degrade pure PE than PET. Overall, we conclude
133 that this consortium could efficiently degrade both PET and PE, and is worthy of
134 further study.

135 **Isolation of the key degraders and reconstitution of the functional community**
136 **capable of plastic degradation.** To figure out the composition and dynamics of the
137 above microbial community during the course of plastics degradation, we performed
138 an absolute quantitative analysis of 16S rRNA sequences on this microbial flora. The
139 growth curve of this microbial flora showed that it took about 10 h to enter the
140 stationary phase and kept a stable population quantity after 7 d- or even longer

141 incubation (Supplementary Fig. 3a). Meanwhile, we monitored the degradation effects
142 on plastics in five different growth stages as shown in Supplementary Fig. 3a through
143 SEM. The SEM observation showed that the thickness and density of the microbial
144 layer on plastic films increased along with the culturing time (Supplementary Figs.
145 3b-3e). Obvious cracks in the films were observed after 7 days incubation
146 (Supplementary Fig. 3f), indicating the plastics had been degraded in this stage.
147 Therefore, we further performed an absolute quantitative analysis of 16S rRNA
148 sequences of bacteria within the microbial community at the 7-day incubation stage.
149 The sequencing results revealed five bacterial general ranked in the top 5 at this time
150 phase, which were *Idiomarina* (~50%), *Marinobacter* (~28%), *Exiguobacterium*
151 (~18%), *Halomonas* (~2%), *Ochrobactrum* (~1%) (Fig. 2a and Supplementary Table
152 1). To obtain the pure cultures of these bacteria, the cells attached to the films were
153 further isolated. As expected, bacterial strains belonging to above five genera were
154 obtained. However, only three of them (*Exiguobacterium* sp., *Halomonas* sp.,
155 *Ochrobactrum* sp.) showed both significant degradation capabilities against PET (Figs.
156 2b, 2d, 2f) and PE (Figs. 2c, 2e, 2g), indicating the other two bacteria might prefer to
157 form biofilms on the surface but not degradation of plastics even though their high
158 abundance within the bacterial community. Notably, SEM observations indicated that
159 the mixture of three above bacteria had a greater degradation efficiency on both PET
160 (Fig. 2h) and PE (Fig. 2i), suggesting that the bacterial community had a better
161 capability than single isolate for plastics degradation. With this, we reconstituted a
162 novel bacterial community containing these three bacteria in the proportion 1:1:1 and
163 further tested its plastic degradation efficiency. Surprisingly, after two weeks
164 incubation, both PET (Fig. 3b) and PE (Fig. 3d) were totally degraded to small pieces,
165 especially for PE. SEM observations further confirmed that the reconstituted bacterial
166 community had good colonization and degradation abilities on both PET (Figs. 3e-3g)
167 and PE (Figs. 3h-3j).

168 **Verification of the degrading effects of the reconstituted bacterial community on**
169 **PET and PE films.** To further verify the degradation effects of the reconstituted
170 bacterial community on PET and PE, we performed multiple techniques to clarify the
171 degradation efficiency and products led by this bacterial community. First, Fourier
172 Transform Infrared (FTIR) imaging was used to analyze the changes of the surface
173 chemical components and function groups of PET and PE treated by this reconstituted
174 bacterial community for four weeks. The FTIR spectra showed that the treated PET
175 had a distinct peak observed at a wave number at 3318 cm^{-1} (Fig. 4a), which was
176 attributed to the carboxylic acid and alcohol functional groups (R-OH stretching,
177 $3000\text{-}3500\text{ cm}^{-1}$)²⁹. On the other hand, FTIR spectra of treated PE showed two
178 different peaks compared with the control group (Fig. 4e), one was observed in the
179 vicinity of 1715 cm^{-1} and assigned to the carbonyl band (-C=O-), the other was
180 observed at a wave number at 3318 cm^{-1} and was attributed to the hydroxyl group¹⁵
181 (Fig. 4e). Thus, it is reasonable to see that the reconstituted bacterial community has a
182 better degradation efficiency on PE than PET due to the dysfunction of more key
183 bonds of PE. Overall, according to the FTIR spectra, the formation of carboxylic acid
184 end groups and carbonyl bands suggested the hydrolysis reaction of PET and PE,
185 which led to a reduction in molecular weight of the main polymer and cleavage of the
186 ester bond of PET polymer and carbon-carbon bond of PE.

187 Furthermore, the molecular weight distribution (MWD) changes for PET and PE
188 treated by the reconstituted bacterial community for four weeks were analyzed by Gel
189 Permeation Chromatography (GPC). The MWD of the treated PET showed an
190 obvious depolymerization trend (Fig. 4c), and two peaks appeared in the curve, one
191 representing the range of molecular weight of 98,451-399,162 Da (accounting for
192 1.55%), the other representing the range of molecular weight of 126-33,575 Da
193 (accounting for 98.44%). By comparison, the MWD curve of control had three peaks
194 (Fig. 4b), representing the range of molecular weight of 2,824-472,417 Da
195 (accounting for 75%), 170-1,617 Da (accounting for 10.64%) and 51-140 Da

196 (accounting for 14.17%), respectively. Clearly, the GPC results indicated the treated
197 PET had a significant reduction in the proportion of large molecules, and an obvious
198 increase in the scale of small molecules. Similarly, the MWD of the treated PE
199 decreased from 231,017Da to 122,388Da (Figs. 4f, 4g). Consistently, according to a
200 peak-differentiating and imitating calculation analyzed by X-Ray Diffraction (XRD),
201 the relative value of crystallinity degree reduced from 92.55% to 89.85% for treated
202 PET for four weeks (Fig. 4d), and decreased from 49.10% to 29.50% for treated PE
203 (Fig. 4h) for four weeks. Together, in combination of the results of SEM observation,
204 FTIR, GPC and XRD analyses, we conclude that the reconstituted bacterial
205 community indeed possesses a strong capability of degrading both PET and PE.

206 Next, the degraded products by the reconstituted bacterial community were
207 analyzed by High-performance liquid chromatography-Mass spectrometry (HPLC-
208 MS). For PET, terephthalic acid (TPA), ethylene glycol (EG), mono-(2-hydroxyethyl)
209 terephthalate (MHET) and bis (2-hydroxyethyl) terephthalate (BHET) have been
210 identified as the main enzymatic degradation products¹⁹. Consistently, TPA (Figs. 5a,
211 5b) and MHET (Figs. 5c, 5d) were identified as hydrolysis products after PET was
212 treated by the reconstituted bacterial community for four weeks. The degradation
213 products of PE after a 14-day treatment were also analyzed by HPLC-MS. The results
214 showed significant differences in the abundance and categories of the eluted
215 compounds as compared with the control group (Fig. 5e), especially in the end of the
216 mass spectrum graph, strongly suggesting PE was decomposed to novel substances.
217 Unfortunately, the chemical identity of these degradation compounds was not
218 confirmed due to lack of standard samples but their presence supports the hypothesis
219 of PE degradation by the reconstituted bacterial community.

220 **Transcriptomic profiling of the plastic degradation process and mechanism led**
221 **by the reconstituted bacterial community.** To explore the plastic degradation
222 process and potential mechanisms mediated by the reconstituted bacterial community,
223 we performed a macro transcriptome analysis of this flora in the presence of PET or

224 PE. Based on our above results, we chose three time points (8 h, 7 d and 14 d) for
225 further transcriptome analysis. According to the analysis of genes differential
226 expression after 8 h incubation with PET or PE, the significantly up-regulated genes
227 in the three bacteria (*Exiguobacterium* sp., *Halomonas* sp., *Ochrobactrum* sp.) were
228 mainly associated with energy production and cell growth regardless of the plastic
229 type, such as citrate cycle and ribosomal biosynthesis (Fig. 6a). Clearly, in the first 8 h
230 incubation time, bacteria mainly utilized the easily available nutrient in the original
231 minimal medium to quickly multiply. When extending the incubation time to 7 d or
232 14 d, most markedly up-regulated genes were closely related to biofilm formation
233 (such as quorum sensing, bacterial chemotaxis, flagellar assembling and two-
234 component system), bacterial secretion system, and cell growth and reproduction
235 (such as citrate cycle, carbon metabolism, fatty acid degradation and ribosomal
236 biosynthesis), regardless of plastic type and incubation time (Fig. 6b). Based on the
237 growth assay of the bacterial community shown in this study, with 7 d- or longer
238 incubation time, the population quantity of the community is still stable in the
239 presence of plastics (Supplementary Fig. 3a), suggesting the bacteria could still obtain
240 enough nutrient to support cell growth. Given very little carbon source provided in the
241 original minimal medium, it is reasonable to propose that bacteria are forced to
242 colonize and thereby degrading and utilizing the plastics-the only available nutrient
243 source in the environment. To better occupy the surface of plastics, the best choice is
244 to form biofilm, which could explain why the expression of large amount genes
245 associated with biofilm formation were significantly up-regulated, and this result also
246 consists well with the observation of huge biofilm formation in the plastic surface
247 (Figs. 1-3). Once the bacterial community successfully colonizes on the targets, they
248 might secret diverse enzymes to degrade the plastics. As shown in Figs. 6c and 6d, the
249 expression of many genes encoding potential plastics degrading enzymes was
250 evidently up-regulated, such as lipase, esterase, cutinase and hydrolase. With this, the
251 bacteria could obtain energy for growth and reproduction through degradation and

252 utilization of plastics, as revealed by the transcriptomic results that the expressions of
253 many genes associated with energy production and carbon metabolism were
254 significantly increased (Fig. 6b).

255 **Discussion**

256 Plastics have become a global concern as the accumulation in the world's oceans and
257 their impacts on marine organisms and human health^{2-4,30}. Therefore, much effort has
258 been exerted to reduce plastic wastes. To remove plastic wastes and recycle plastic-
259 based materials, biocatalytic degradation might be applied as an ecofriendly
260 method^{18,19}. Microbes have potentials to degrade plastics with ester bond via
261 enzymatic hydrolysis through colonization onto the surfaces of materials^{18,19,21}.
262 Because some marine bacteria have the ability to degrade hydrocarbons which
263 possessing similar chemical structure with plastics, it has been suggested that a certain
264 fraction of the microbial community colonizing plastics might have capability of
265 degrading plastics^{31,32} and thereby using as a carbon matrix. However, it remains
266 unclear whether and to what extent marine prokaryotic communities are capable of
267 degrading plastic in the ocean. For the first time, this study investigated the
268 community structures of marine microbial biofilms attached to two different plastics
269 (PET and PE) (Fig. 2 and Supplementary Table 1), successfully reconstituted a
270 tailored bacterial community possessing significant plastic degrading capabilities
271 (Figs. 3, 4), and clarified the degradation process and products eventually (Figs. 5, 6).
272 Therefore, our results answer the question that whether oceanic bacteria are capable to
273 degrade plastics, and clearly show that plastic waste associated bacteria in the marine
274 environment have great potentials to develop plastic degradation bio-products.

275 Indeed, we obtained the functional bacterial community efficiently degrading
276 plastics from a bay heavily contaminated by plastic waste, while we failed to find any
277 potential plastic-degrading bacterial flora from the deep-sea sediment samples,
278 indicating that it is advisable to screen potential degraders in the plastic polluted
279 locations in the future. Similarly, several researchers have obtained microplastic-

280 associated bacterial community having plastic-degrading potentials in the field
281 investigation. For example, the plastisphere bacterial communities on PET surfaces in
282 the North Sea³³, bacterial biofilms associated with PE, PP and glass during an *in-situ*
283 incubation experiment taking place in the northern Adriatic Sea²⁷. However, these
284 studies mainly focus on the community structures and dynamics of bacteria on the
285 surfaces of plastics, the metabolic pathways and associated mechanistic processes
286 involved in the biodegradation of plastics are yet to be characterized. In the present
287 study, we disclosed the degradation details through transcriptomics methods,
288 revealing three potential steps including biofilm formation, degradation and utilization
289 involved in the degradation process exerting by bacterial esterase, cutinase and
290 hydrolase (Fig. 6). Overall, our study paves a way to obtain plastic degraders in
291 marine environments and a good candidate to explore plastic degradation mechanisms
292 in the future.

293 Of note, in the present study, we adopted community but not individual bacterium
294 for plastic degradation given the better degradation effect of three bacteria over single
295 bacterium against plastic waste (Fig. 2). Indeed, the efficiency for biodegradation and
296 bioremediation of environmental pollutants using single strains is still very low and
297 restricted²⁸. In contrast, mixed flora has stronger environmental adaptability, higher
298 degradation efficiency and more ample scope for the greater use of biotechnologies in
299 biodegradation compared with single pure bacterium due to the synergistic effect of
300 different microorganisms among them²⁸. Therefore, more and more attention has been
301 shifted towards microbial consortia, since their inherent multiple function, robust and
302 adaptable characteristics. Actually, great achievements have obtained in the
303 bioremediation fields with microbial consortia, such as treatment of wastewater
304 eutrophication³⁴, removal of heavy metals³⁵, degradation of dyes³⁶. By comparison,
305 there is rarely report on plastic degradation led by bacterial community, especially the
306 reconstituted functional consortium. Our study pioneered a way to advance the
307 development of high-efficient, stable and controllable synthetic microbial consortia

308 against different plastic waste. Notably, three bacteria within the reconstituted
309 bacterial community belong to the genera of *Exiguobacterium*, *Halomonas* and
310 *Ochrobactrum*, which are all easily cultured and fast grown bacteria, providing a great
311 advantage for the future application.

312 In addition, the present bacterial community prefers to act on PE and enables to
313 degrade the intact PE film to debris (Fig. 3d), showing a great capability to solve the
314 PE degradation problem. It is known that PE is largely utilized in packaging,
315 representing ~40% of total demand for plastic products (www.plasticseurope.org)
316 with over a trillion plastic bags used every year¹⁵. PE comprises a linear backbone of
317 carbon atoms and holds the highly stable carbon-carbon (C-C) bonds, which is
318 resistant to degradation and has become a big challenge for plastic waste
319 biodegradation. PE biodegradation has been observed with an extreme long
320 incubation time (up to couples of months), given appropriate conditions. For example,
321 modest degradation of PE was observed after a combination of nitric acid treatment
322 and 3-month incubation with the fungus *Penicillium simplicissimum*³⁷. Even slower
323 PE degradation was also recorded after 4 to 7 months exposure to the bacterium
324 *Nocardia asteroides*³⁸. Excitedly, our reconstituted bacterial community could lead a
325 significant degradation towards PE (e.g. ubiquitous cracks in the surface and damages
326 in the four corners of PE film) within several days, and totally degrade the PE film to
327 very small pieces within 2 weeks. Undoubtedly, given the fast rate of biodegradation
328 reported here, these findings have potential for significant biotechnological
329 applications. Further investigation is also required to explore the detailed nature of the
330 products derived from degraded PE exerted by this reconstituted bacterial community,
331 and determine what enzymes responsible for PE/PET degradation predicted in this
332 study.

333 **Methods**

334 **Screening of microbial community degrading PET and PE.** About 300 sediment
335 samples contaminated by plastic debris from different locations of Huiquan Bay

336 (Qingdao, China) were collected and kept in the plastics container until using for
337 screening. Three kinds of PET plastic were used for degradation assays in the present
338 study, including plastic drink bottle, type ES301450 (0.25 mm in thickness) and type
339 ES301005 (0.0005 mm in thickness), the latter two were purchased from the Good
340 Fellow Company (UK). Similarly, three kinds of PE plastic were also used in the
341 present study, including commercial PE bags, type ET311350 (0.25mm in thickness)
342 and type ET311126 (0.025mm in thickness), the latter two were also purchased from
343 the Good Fellow Company (UK). None additives were contained in the films
344 purchased from the Good Fellow Company according to the manufacturer's standard
345 (Q/SH3180014). All PET and PE films used in this study were treated in 75% ethanol,
346 and then air-dried in a laminar-flow clean bench prior to use. For screening microbial
347 community degrading plastics, PET or PE films were all cut into 30 mm × 20 mm
348 square sheets and incubated in minimal medium (0.5 g yeast extract, 1 g peptone, in 1
349 L filtered sea water, and PH is adjusted to 7.0.) containing different plastics-
350 contaminated samples for couples of weeks to months before checking the
351 degradation effects.

352 **Absolute quantification of individual bacterial abundance in the community.** The
353 original bacterial community cultivated in the minimal medium without the
354 supplement of any plastics was set as a control group. Correspondingly, the culture
355 supplement with PET (type ES301450) or PE (type ET311350) was set as
356 experimental groups. The samples was collected in five different growth stages (group
357 A: $OD_{600}=0.3$, cultivated for 4.5 h; group B: $OD_{600}=0.58$, cultivated for 7.5 h, group C:
358 $OD_{600}=0.85$, cultivated for 8.5 h; group D: $OD_{600}=1.05$, cultivated for 9.5 h; group E:
359 $OD_{600}=1.13$, cultivated for 7 d). Three parallel groups were set for absolute
360 quantification of 16S rRNA sequences. The analyses were performed by Genesky
361 Biotechnologies Inc. (Shanghai, China). Briefly, total genomic DNAs of different
362 samples were extracted by using the QIAamp Rapid DNA Kit (Qiagen, Germany).
363 The DNA concentration and integrity were measured by a NanoDrop2000

364 spectrophotometer (Thermo Fisher Scientific, USA) and agarose gel electrophoresis,
365 respectively. The spike-in sequences contained conserved regions identical to those of
366 natural 16S rRNA genes and artificial variable regions were distinct from those found
367 in nucleotide sequences in public databases. These served as internal standards and
368 facilitated absolute quantification across samples. Appropriate mixtures with known
369 copy numbers of spike-in sequences were added to the sample DNAs. The V4-V5
370 regions of the 16S rRNA genes and spike-in sequences were amplified and sequenced
371 using Illumina HiSeq.

372 **Scanning Electron Microscopy (SEM) observation.** PET and PE films were
373 collected from each sample and observed through SEM to examine the degradation
374 effects by different bacterial community. After treated by bacteria, the PET or PE
375 films were soaked in 5% glutaraldehyde for cell fixation, then were dehydrated in 30-
376 100% graded ethanol for 15 min each and critical-point-dried with CO₂³⁹. Dried
377 specimens were sputter coated for 5 min with gold and platinum (10 nm) using a
378 Hitachi MC1000 Ion Sputter (Japan), and were examined using a field emission
379 scanning electron microscope (Hitachi S-3400N) operating at an accelerating voltage
380 of 5 kV. The PET and PE films treated with or without bacterial community were
381 washed in ultrasonic cleaner with 1% SDS, distilled water, and then ethanol¹⁹. The
382 film was air-dried, coated with gold and platinum (10 nm) using a Hitachi MC1000
383 Ion Sputter, and subjected to SEM observation.

384 **Fourier Transform Infrared (FTIR) analysis.** The PET and PE plastics exposed to
385 the microbial consortia were recovered after an incubation period of four weeks, then
386 were carefully rinsed in ultrasonic cleaner with 1% SDS, distilled water, and then
387 ethanol^{29,40}. After air dried, the plastic films treated with or without bacterial
388 community were recorded over the wavelength range 450-4000 cm⁻¹ at a resolution of
389 1 cm⁻¹ using a Nicolet-360 FTIR (Waltham, USA) spectrometer operating in ATR
390 mode^{37,38}. Thirty two scans were taken for each spectrum.

391 **Gel Permeation Chromatography (GPC) Analysis.** The molecular weight of PET
392 films treated with or without bacterial community was determined by GPC, which
393 were carried out on an instrument of model Shimadzu GPC-20A (Japan) equipped
394 with LC20 columns and operating at 35 °C⁴¹. Trichlorobenzene was used as mobile
395 phase (1 mL/min) after calibration with polystyrene standards of known molecular
396 mass. A sample concentration of 1 mg/mL was employed⁴². The molecular weight of
397 the PE films treated with or without bacterial community was determined by GPC on
398 an Agilent PL-GPC220 equipped with Agilent PLgel Olexis 300 × 7.5 mm columns
399 and operating at 150 °C^{43,44}. Trichlorobenzene was used as mobile phase (1 mL/min)
400 after calibration with polystyrene standards of known molecular mass. A sample
401 concentration of 1 mg/mL was employed^{38,45}.

402 **X-Ray Diffraction (XRD) analysis.** XRD was carried out by using the Bruker D8
403 Advance instrument with a wavelength of 1.5406 angstrom of CuK α ray. The XRD
404 tube current was set as 40 mA, and the tube voltage was set as 40 kV. The
405 measurements for PET were set in the angle range from $2\theta = 5^\circ$ to $2\theta = 45^\circ$ at a rate
406 of $1^\circ/\text{min}$ ^{46,47}. The measurements for PE were set in the angle range from $2\theta = 3^\circ$ to
407 $2\theta = 50^\circ$ at a rate of $1^\circ/\text{min}$ ⁴⁸.

408 **High-performance liquid chromatography-Mass spectrometry (HPLC-MS)**
409 **analysis.** HPLC-MS for PET was performed on an API QTRAP 5500 LCMS system
410 equipped with a XB-C18 100A analytical column (2.1× 250 mm, 2.6 μm). The mobile
411 phase was methanol at a flow rate of 0.5 mL/min, and the effluent was monitored at a
412 wavelength of 240 nm. The typical elution condition was followed as: 0 to 1 min, 10%
413 (v/v) methanol; 1 to 2 min, 10-50% methanol linear gradient; 2 to 2.5 min, 50-95%
414 (v/v) methanol; 4.5 to 4.6 min, 95-10% methanol linear gradient. The reaction mixture
415 supernatant was diluted with the mobile phase toward to the calibration range,
416 acidified with concentrated HCl (37%) and centrifuged to remove any
417 precipitation^{19,49}. Standard curves of TPA and BHET were prepared in a concentration
418 range from 0.17 to 1 mM and showed no significant difference.

419 HPLC-MS samples for PE biodegradation were submerged in acetonitrile and
420 sonicated for around 1 minute. The soluble products were then dissolved in 1 mL
421 fresh acetonitrile, which was then transferred to a microcentrifuge tube and spun
422 down for 2 minutes. Then, 2 μ L of supernatant was used for LC-MS (Waters
423 ACQUITY SQD, USA) analysis. The degradation products were detected by LC-MS
424 equipped with a ACQUITY UPLC BEH C18 analytical column (2.1 \times 50 mm, 1.7 μ m)
425 at 50-1500 m/z¹⁵. The column temperature was 30 °C, and the flow rate was 0.300
426 mL/min during operation. The typical elution condition was set as: 0 to 3 min, 90%
427 water, 10% acetonitrile; 3 to 4 min, 10-90% acetonitrile linear gradient; 4 to 8 min, 90%
428 (v/v) acetonitrile; 8 to 8.5min, 90-10% acetonitrile linear gradient; 8.5 to 10 min, 10%
429 (v/v) acetonitrile⁵⁰. The difference between the traces, untreated and treated is the MS
430 peak observed at 0.581 minutes.

431 **Isolation and genome sequencing of three bacteria leading plastics degradation.**

432 To isolate the bacteria in the community, the biofilm attached to the films were
433 collected and plated on the 2216E solid medium (containing 5 g/L peptone, 1 g/L
434 yeast extract, 1 L filtered seawater, 15 g agar, pH adjusted to 7.4-7.6). The visible
435 colony was further purified several times until it was considered to be axenic. The
436 purity of bacterial strains was confirmed by repeated partial sequencing of the 16S
437 rRNA gene. Using this method, five pure cultures were obtained and three of them
438 could degrade plastic, which were *Exiguobacterium* sp., *Halomonas* sp., and
439 *Ochrobactrum* sp, which were further incubated and performed genomic sequencing
440 as described previously⁵¹. Sequencing libraries were generated using NEBNext®
441 Ultra™ DNA Library Prep Kit for Illumina (NEB, USA) following manufacturer's
442 recommendations and index codes were added to attribute sequences to each sample⁵².
443 Seven databases were used to predict gene functions, including GO⁵³, KEGG⁵⁴,
444 COG⁵⁵, NR⁵⁶ and Swiss-Prot⁵⁷.

445 **Transcriptomics analysis.** The reconstituted bacterial community cultivated in the
446 minimal medium without supplement of any plastics was set as a control group.

447 Correspondingly, the culture supplement with PET (type ES301450) or PE (type
448 ET311350) was set as experimental groups. With this, we collected the control or
449 experimental samples grown for 8 h, 7 d, 14 d, respectively. Transcriptomics analysis
450 was performed by Novogene (Tianjin, China). Briefly, total RNAs of all samples were
451 extracted using TRIzol reagent (Invitrogen, USA) and the DNA contamination was
452 ruled out with MEGA clear Kit (Life technologies, USA). Sequencing libraries were
453 generated using NEBNext[®] Ultra[™] Directional RNA Library Prep Kit for Illumina[®]
454 (NEB, USA) following manufacturer's recommendations and index codes were added
455 to attribute sequences to each sample. rRNA is removed using a specialized kit that
456 leaves the mRNA. Fragmentation was carried out using divalent cations under
457 elevated temperature in NEBNext First Strand Synthesis Reaction Buffer (5×). The
458 clustering of the index-coded samples was performed on a cBot Cluster Generation
459 System using TruSeq PE Cluster Kit v3-cBot-HS (Illumia) according to the
460 manufacturer's instructions⁵⁸. After cluster generation, the library preparations were
461 sequenced on an Illumina HiSeq platform and paired-end reads were generated. Raw
462 data of fastq format were firstly processed through in-house perl scripts. In this step,
463 clean data were obtained by removing reads containing adapter, reads containing
464 ploy-N and low quality reads from raw data. At the same time, Q20, Q30 and GC
465 content the clean data were calculated. All the downstream analyses were based on
466 the clean data with high quality. Differential expression analysis of two
467 conditions/groups was performed using the DESeq R package (1.18.0). Then,
468 KOBAS software was used to test the statistical enrichment of differential expression
469 genes in KEGG pathways. GO enrichment analysis of differentially expressed genes
470 was implemented by the Goseq R package, in which gene length bias was corrected.
471 GO terms with corrected *P* value less than 0.05 were considered significantly enriched
472 by differential expressed genes^{59,60}.

473 **Data availability.** The complete genome sequences of *Halomonas* sp.,
474 *Exiguobacterium* sp. and *Ochrobactrum* sp. have been deposited at GenBank under

475 the accession numbers PRJNA673668, PRJNA673665 and PRJNA673670,
476 respectively.

477 **Acknowledgements**

478 This work is funded by the China Ocean Mineral Resources R&D Association Grant
479 (Grant No. DY135-B2-14), National Key R and D Program of China (Grant No.
480 2018YFC0310800), Strategic Priority Research Program of the Chinese Academy of
481 Sciences (Grant No. XDA22050301), the Taishan Young Scholar Program of
482 Shandong Province (tsqn20161051), and Qingdao Innovation Leadership Program
483 (Grant No. 18-1-2-7-zhc) for Chaomin Sun.

484 **Author Contributions**

485 RG and CS conceived and designed the study. RG performed all the experiments. RG
486 and CS analyzed the data. RG wrote the manuscript. CS revised the manuscript. All
487 authors read and approved the final manuscript.

488 **Conflict of interest**

489 The authors have no conflict of interest.

490 **References**

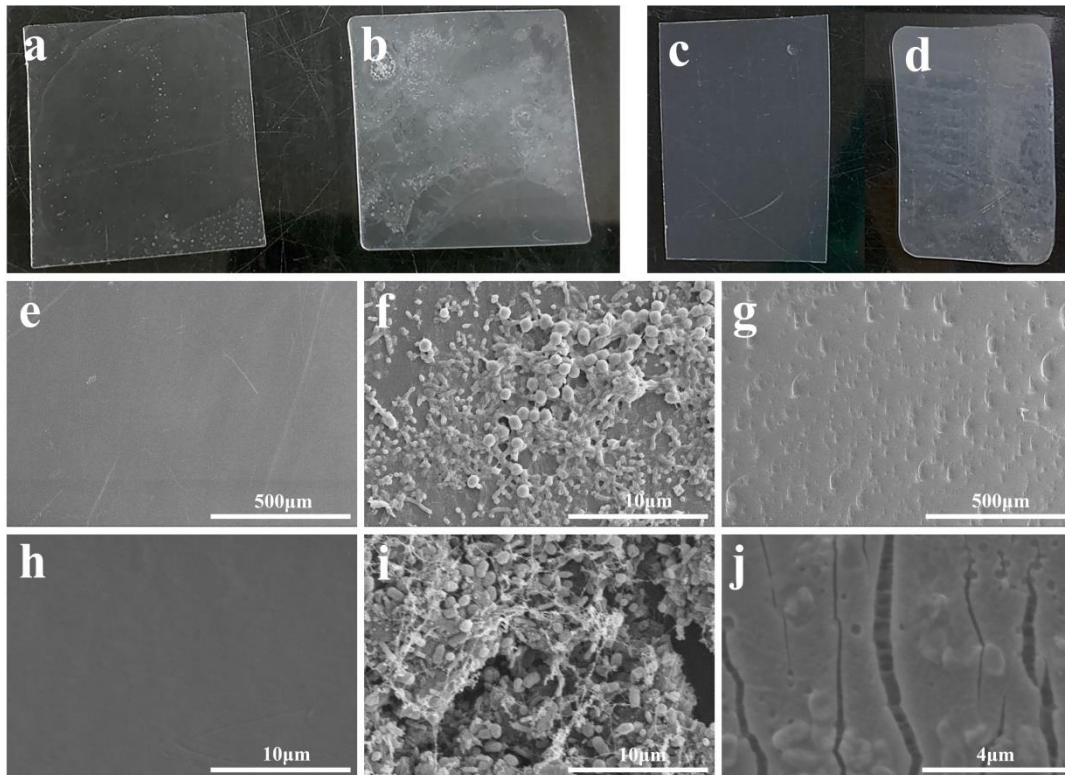
- 491 1. Law, K. L. et al. Plastic accumulation in the North Atlantic subtropical gyre. *Science* **329**, 1185-
492 1188 (2010).
- 493 2. Cozar, A. et al. Plastic debris in the open ocean. *P Natl Acad Sci USA* **111**, 10239-10244 (2014).
- 494 3. Jambeck, J. R. et al. Plastic waste inputs from land into the ocean. *Science* **347**, 768-771 (2015).
- 495 4. Lamb, J. B. et al. Plastic waste associated with disease on coral reefs. *Science* **359**, 460-462 (2018).
- 496 5. Barnes, D. K., Galgani, F., Thompson, R. C. & Barlaz, M. Accumulation and fragmentation of
497 plastic debris in global environments. *Philos Trans R Soc Lond B Biol Sci* **364**, 1985-1998 (2009).
- 498 6. Green, D. S., Boots, B., Blockley, D. J., Rocha, C. & Thompson, R. Impacts of discarded plastic
499 bags on marine assemblages and ecosystem functioning. *Environ Sci Technol* **49**, 5380-5389
500 (2015).
- 501 7. Li, W. C., Tse, H. F. & Fok, L. Plastic waste in the marine environment: A review of sources,
502 occurrence and effects. *Sci Total Environ* **566**, 333-349 (2016).
- 503 8. Webb, H. K., Arnott, J., Crawford, R. J. & Ivanova, E. P. Plastic degradation and its environmental
504 implications with special reference to Poly(ethylene terephthalate). *Polymers-Basel* **5**, 1-18 (2013).

- 505 9. Green, D. S., Boots, B., Blockley, D. J., Rocha, C. & Thompson, R. Impacts of discarded plastic
506 bags on marine assemblages and ecosystem functioning. *Environ Sci Technol* **49**, 5380-5389
507 (2015).
- 508 10. Hale, R. C., Seeley, M. E., La Guardia, M. J., Mai, L. & Zeng, E. Y. A global perspective on
509 microplastics. *J Geophys Res-Oceans* **125** (2020).
- 510 11. Carson, H. S., Nerheim, M. S., Carroll, K. A. & Eriksen, M. The plastic-associated microorganisms
511 of the North Pacific Gyre. *Mar Pollut Bull* **75**, 126-132 (2013).
- 512 12. Wang, J. D., Tan, Z., Peng, J. P., Qiu, Q. X. & Li, M. M. The behaviors of microplastics in the
513 marine environment. *Mar Environ Res* **113**, 7-17 (2016).
- 514 13. Geyer, R., Jambeck, J. R. & Law, K. L. Production, use, and fate of all plastics ever made. *Sci Adv*
515 **3**, e1700782 (2017).
- 516 14. Koshti, R., Mehta, L. & Samarth, N. Biological recycling of Polyethylene Terephthalate: a mini-
517 review. *J Polym Environ* **26**, 3520-3529 (2018).
- 518 15. Bombelli, P., Howe, C. J. & Bertocchini, F. Polyethylene bio-degradation by caterpillars of the
519 wax moth *Galleria mellonella*. *Curr Biol* **27**, R292-R293 (2017).
- 520 16. Ghosh, S. K., Pal, S. & Ray, S. Study of microbes having potentiality for biodegradation of plastics.
521 *Environ Sci Pollut R* **20**, 4339-4355 (2013).
- 522 17. Gewert, B., Plassmann, M. M. & MacLeod, M. Pathways for degradation of plastic polymers
523 floating in the marine environment. *Environ Sci-Proc Imp* **17**, 1513-1521 (2015).
- 524 18. Joo, S. et al. Structural insight into molecular mechanism of poly (ethylene terephthalate)
525 degradation. *Nat Commun* **9** (2018).
- 526 19. Yoshida, S. et al. A bacterium that degrades and assimilates poly(ethylene terephthalate). *Science*
527 **351**, 1196-1199 (2016).
- 528 20. Danso, D., Chow, J. & Streit, W. R. Plastics: environmental and biotechnological perspectives on
529 microbial degradation. *Appl Environ Microb* **85** (2019).
- 530 21. Paco, A. et al. Biodegradation of polyethylene microplastics by the marine fungus *Zalerion*
531 *maritimum*. *Sci Total Environ* **586**, 10-15 (2017).
- 532 22. Harshvardhan, K. & Jha, B. Biodegradation of low-density polyethylene by marine bacteria from
533 pelagic waters, Arabian Sea, India. *Mar Pollut Bull* **77**, 100-106 (2013).
- 534 23. Restrepo-Florez, J. M., Bassi, A. & Thompson, M. R. Microbial degradation and deterioration of
535 polyethylene - A review. *Int Biodeter Biodegr* **88**, 83-90 (2014).
- 536 24. Danso, D. et al. New insights into the function and global distribution of Polyethylene
537 Terephthalate (PET)-degrading bacteria and enzymes in marine and terrestrial metagenomes. *Appl*
538 *Environ Microb* **84** (2018).
- 539 25. Eberl, A. et al. Enzymatic surface hydrolysis of poly(ethylene terephthalate) and
540 bis(benzoyloxyethyl) terephthalate by lipase and cutinase in the presence of surface active
541 molecules. *J Biotechnol* **143**, 207-212 (2009).
- 542 26. Brueckner, T., Eberl, A., Heumann, S., Rabe, M. & Guebitz, G. M. Enzymatic and chemical
543 hydrolysis of poly(ethylene terephthalate) fabrics. *J Polym Sci Pol Chem* **46**, 6435-6443 (2008).
- 544 27. Pinto, M. et al. Putative degraders of low-density polyethylene-derived compounds are ubiquitous
545 members of plastic-associated bacterial communities in the marine environment. *Environ*
546 *Microbiol* (2020).

- 547 28. Qian, X. J. et al. Biotechnological potential and applications of microbial consortia. *Biotechnol Adv*
548 **40** (2020).
- 549 29. Sammon, C., Yarwood, J. & Everall, N. A FTIR-ATR study of liquid diffusion processes in PET
550 films: comparison of water with simple alcohols. *Polymer* **41**, 2521-2534 (2000).
- 551 30. Ostle, C. et al. The rise in ocean plastics evidenced from a 60-year time series. *Nat Commun* **10**
552 (2019).
- 553 31. Rosato, A. et al. Microbial colonization of different microplastic types and biotransformation of
554 sorbed PCBs by a marine anaerobic bacterial community. *Sci Total Environ* **705** (2020).
- 555 32. Xu, X. Y. et al. Marine microplastic-associated bacterial community succession in response to
556 geography, exposure time, and plastic type in China's coastal seawaters. *Mar Pollut Bull* **145**, 278-
557 286 (2019).
- 558 33. Oberbeckmann, S., Osborn, A. M. & Duhaime, M. B. Microbes on a bottle: substrate, season and
559 geography influence community composition of microbes colonizing marine plastic debris. *Plos*
560 *One* **11** (2016).
- 561 34. Mujtaba, G., Rizwan, M. & Lee, K. Removal of nutrients and COD from wastewater using
562 symbiotic co-culture of bacterium *Pseudomonas putida* and immobilized microalga *Chlorella*
563 *vulgaris*. *J Ind Eng Chem* **49**, 145-151 (2017).
- 564 35. Shafique, M., Jawaid, A. & Rehman, Y. As(V) reduction, As(III) oxidation, and Cr(VI) reduction
565 by multi-metal-resistant *Bacillus subtilis*, *Bacillus safensis*, and *Bacillus cereus* species isolated
566 from wastewater treatment plant. *Geomicrobiol J* **34**, 687-694 (2017).
- 567 36. Shanmugam, B. K., Easwaran, S. N., Lakra, R., Deepa, P. R. & Mahadevan, S. Metabolic pathway
568 and role of individual species in the bacterial consortium for biodegradation of azo dye: A
569 biocalorimetric investigation. *Chemosphere* **188**, 81-89 (2017).
- 570 37. Yamada-Onodera, K., Mukumoto, H., Katsuyaya, Y., Saiganji, A. & Tani, Y. Degradation of
571 polyethylene by a fungus, *Penicillium simplicissimum* YK. *Polym Degrad Stabil* **72**, 323-327
572 (2001).
- 573 38. Bonhomme, S. et al. Environmental biodegradation of polyethylene. *Polym Degrad Stabil* **81**, 441-
574 452 (2003).
- 575 39. Mumtaz, T., Khan, M. R. & Hassan, M. A. Study of environmental biodegradation of LDPE films
576 in soil using optical and scanning electron microscopy. *Micron* **41**, 430-438 (2010).
- 577 40. Kardas, I., Lipp-Symonowicz, B. & Sztajnowski, S. The influence of enzymatic treatment on the
578 surface modification of PET fibers. *J Appl Polym Sci* **119**, 3117-3126 (2011).
- 579 41. Shiono, S. Separation and identification of poly(ethylene-terephthalate) oligomers by gel-
580 permeation chromatography. *J Polym Sci Pol Chem* **17**, 4123-4127 (1979).
- 581 42. Collins, M. J., Zeronian, S. H. & Marshall, M. L. Analysis of the molecular-weight distributions of
582 aminolyzed poly(ethylene-terephthalate) by using gel-permeation chromatography. *J Macromol Sci*
583 *Chem* **A28**, 775-792 (1991).
- 584 43. Kaufman, H. S. & Walsh, E. K. Molecular weight and molecular weight distribution of high
585 density linear polyethylene. *J Polym Sci* **26**, 124-125 (1957).
- 586 44. Huang, H. H. et al. Direct comparison of IR and DRI detector for HT-GPC of polyolefins.
587 *Macromol Symp* **356**, 95-109 (2015).

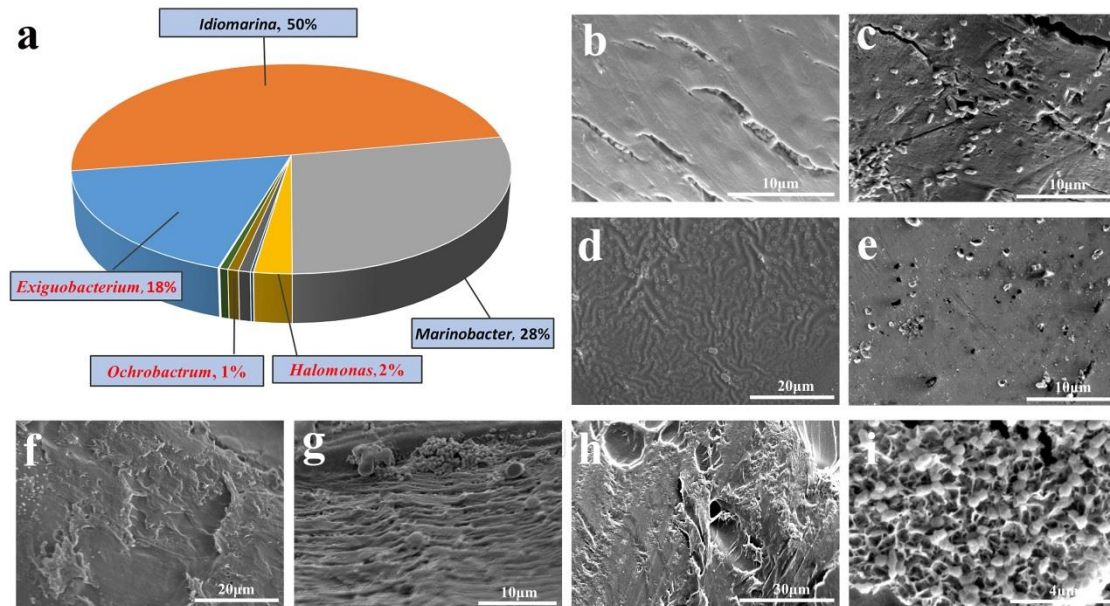
- 588 45. Tung, L. H. & Buckser, S. The effect of molecular weight on the crystallinity of polyethylene. *J*
589 *Phys Chem-US* **62**, 1530-1534 (1959).
- 590 46. Gaonkar, A. A., Murudkar, V. V. & Deshpande, V. D. Comparison of crystallization kinetics of
591 polyethylene terephthalate (PET) and reorganized PET. *Thermochim Acta* **683** (2020).
- 592 47. Farrow, G. & Preston, D. Measurement of crystallinity in drawn polyethylene terephthalate fibres
593 by X-Ray diffraction. *Brit J Appl Phys* **11**, 353-358 (1960).
- 594 48. Xiao, Z. C. & Akpalu, Y. A. New insights into the characteristics of early stage crystallization of a
595 polyethylene. *Polymer* **48**, 5388-5397 (2007).
- 596 49. Barth, M. et al. Effect of hydrolysis products on the enzymatic degradation of polyethylene
597 terephthalate nanoparticles by a polyester hydrolase from *Thermobifida fusca*. *Biochem Eng J* **93**,
598 222-228 (2015).
- 599 50. Ren, L. et al. Biodegradation of polyethylene by *Enterobacter* sp. D1 from the guts of wax moth
600 *Galleria mellonella*. *Int J Env Res Pub He* **16** (2019).
- 601 51. Zhang, J. et al. A novel bacterial thiosulfate oxidation pathway provides a new clue about the
602 formation of zero-valent sulfur in deep sea. *ISME J.* **14**, 2261-2274 (2020).
- 603 52. Bankevich, A. et al. SPAdes: a new genome assembly algorithm and its applications to single-cell
604 sequencing. *J Comput Biol* **19**, 455-477 (2012).
- 605 53. Ashburner, M. et al. Gene Ontology: tool for the unification of biology. *Nat Genet* **25**, 25-29
606 (2000).
- 607 54. Kanehisa, M., Goto, S., Kawashima, S., Okuno, Y. & Hattori, M. The KEGG resource for
608 deciphering the genome. *Nucleic Acids Res* **32**, D277-D280 (2004).
- 609 55. Galperin, M. Y., Makarova, K. S., Wolf, Y. I. & Koonin, E. V. Expanded microbial genome
610 coverage and improved protein family annotation in the COG database. *Nucleic Acids Res* **43**,
611 D261-D269 (2015).
- 612 56. Saier, M. H., Reddy, V. S., Tamang, D. G. & Vastermark, A. The transporter classification
613 database. *Nucleic Acids Res* **42**, D251-D258 (2014).
- 614 57. Bairoch, A. & Apweiler, R. The SWISS-PROT protein sequence database and its supplement
615 TrEMBL in 2000. *Nucleic Acids Res* **28**, 45-48 (2000).
- 616 58. Cock, P. J. A., Fields, C. J., Goto, N., Heuer, M. L. & Rice, P. M. The Sanger FASTQ file format
617 for sequences with quality scores, and the Solexa/Illumina FASTQ variants. *Nucleic Acids Res* **38**,
618 1767-1771 (2010).
- 619 59. Subramanian, A. et al. Gene set enrichment analysis: A knowledge-based approach for interpreting
620 genome-wide expression profiles. *P Natl Acad Sci USA* **102**, 15545-15550 (2005).
- 621 60. Garber, M., Grabherr, M. G., Guttman, M. & Trapnell, C. Computational methods for
622 transcriptome annotation and quantification using RNA-seq. *Nat Methods* **8**, 469-477 (2011).
- 623
624
625
626
627
628
629

630 **Figures**



631

632 **Fig. 1 Observation of the colonization and degradation effects of a marine**
633 **bacterial community on PET and PE films. a,** Morphology of PET film without
634 treatment. **b,** Morphology of PET film treated by the marine bacterial community for
635 seven days. **c,** Morphology of PE film without treatment. **d,** Morphology of PE film
636 treated by the marine bacterial community for seven days. **e,** SEM observation of PET
637 film without treatment. **f,** SEM observation of the colonization of the marine bacterial
638 community on the PET film after seven days incubation. **g,** SEM observation of the
639 degradation effects of PET film treated by the marine bacterial community for seven
640 days. **h,** SEM observation of PE film without treatment. **i,** SEM observation of the
641 colonization of the marine bacterial community on the PE film after seven days
642 incubation. **j,** SEM observation of the degradation effects of PE film treated by the
643 marine bacterial community for seven days. The type of PET film used for this assay
644 is ES301450 (0.25 mm in thickness). The type of PE film used for this assay is
645 ET311350 (0.25mm in thickness).



646

647 **Fig. 2 Abundance quantification and plastic degradation of three core bacteria**
648 **derived from the original marine bacterial community.** **a**, Absolute abundance
649 quantification of bacteria within the original community with plastic-degrading
650 capability through 16S rRNA sequencing method after 5-day incubation with plastics.
651 The top 5 high abundance general names were shown. The abundance of each genus
652 was indicated after corresponding name. The general names for three core bacteria are
653 highlighted with red color. SEM observation of PET (**b**) and PE (**c**) treated by
654 *Exiguobacterium* sp. for 14 days. SEM observation of PET (**d**) and PE (**e**) treated by
655 *Halomonas* sp. for 14 days. SEM observation of PET (**f**) and PE (**g**) treated by
656 *Ochrobactrum* sp. for 14 days. SEM observation of PET (**h**) and PE (**i**) treated by the
657 mixture of *Exiguobacterium* sp., *Halomonas* sp. and *Ochrobactrum* sp. for 7 days.

658

659

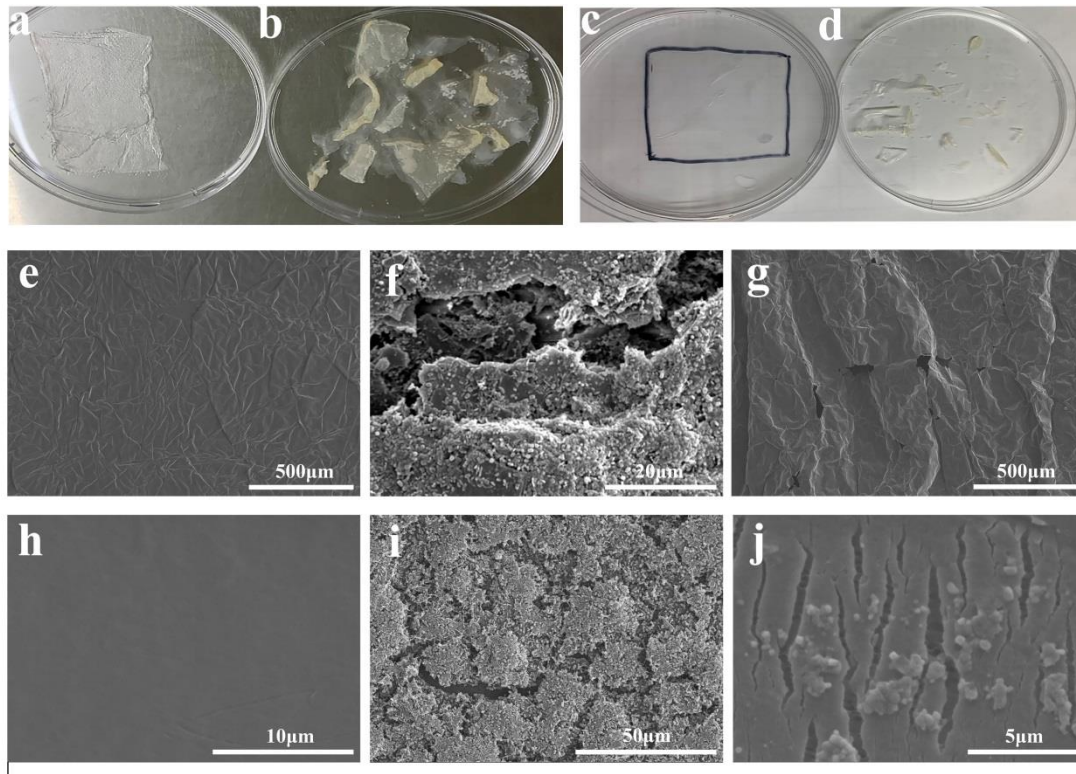
660

661

662

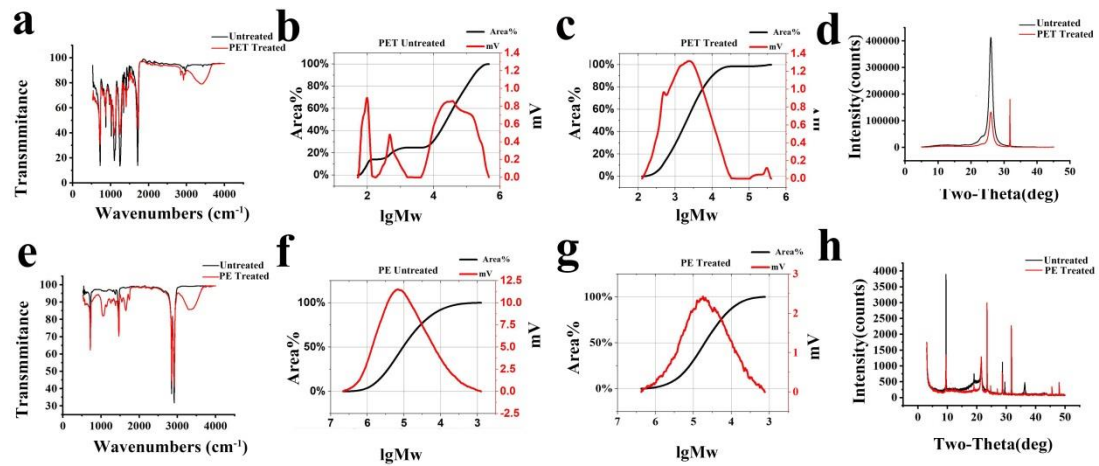
663

664



665

666 **Fig. 3 Observation of the colonization and degradation effects of the**
667 **reconstituted bacterial community on PET and PE films. a,** Morphology of PET
668 film without treatment. **b,** Morphology of PET film treated by the reconstituted
669 bacterial community for 14 days. **c,** Morphology of PE film without treatment. **d,**
670 Morphology of PE film treated by the reconstituted bacterial community for 14 days.
671 **e,** SEM observation of PET film without treatment. **f,** SEM observation of the
672 colonization of the reconstituted bacterial community on the PET film after 14 days
673 incubation. **g,** SEM observation of the degradation effects of PET film treated by the
674 reconstituted bacterial community for 14 days. **h,** SEM observation of PE film
675 without treatment. **i,** SEM observation of the colonization of the reconstituted
676 bacterial community on the PE film after 14 days incubation. **j,** SEM observation of
677 the degradation effects of PE film treated by the reconstituted bacterial community for
678 14 days. The type of PET film used for this assay is ES301005 (0.0005 mm in
679 thickness). The type of PE film used for this assay is ET311350 ET311126 (0.025mm
680 in thickness).



681

682

Fig. 4 Validation of PET and PE degradation by the reconstituted bacterial

683

community. a, FTIR analysis of untreated and treated PET film by the reconstituted

684

bacterial community for 28 days. **b,** GPC analysis of untreated PET film. **c,** GPC

685

analysis of PET film treated by the reconstituted bacterial community for 28 days. **d,**

686

XRD analysis of untreated and treated PET film by the reconstituted bacterial

687

community for 28 days. **e,** FTIR analysis of untreated and treated PE film by the

688

reconstituted bacterial community for 28 days. **f,** GPC analysis of untreated PE film.

689

g, GPC analysis of PE film treated by the reconstituted bacterial community for 28

690

days. **h,** XRD analysis of untreated and treated PET film by the reconstituted bacterial

691

community for 28 days. The type of PET film used for this assay is ES301005

692

(0.0005 mm in thickness). The type of PE film used for this assay is ET311350

693

ET311126 (0.025mm in thickness).

694

695

696

697

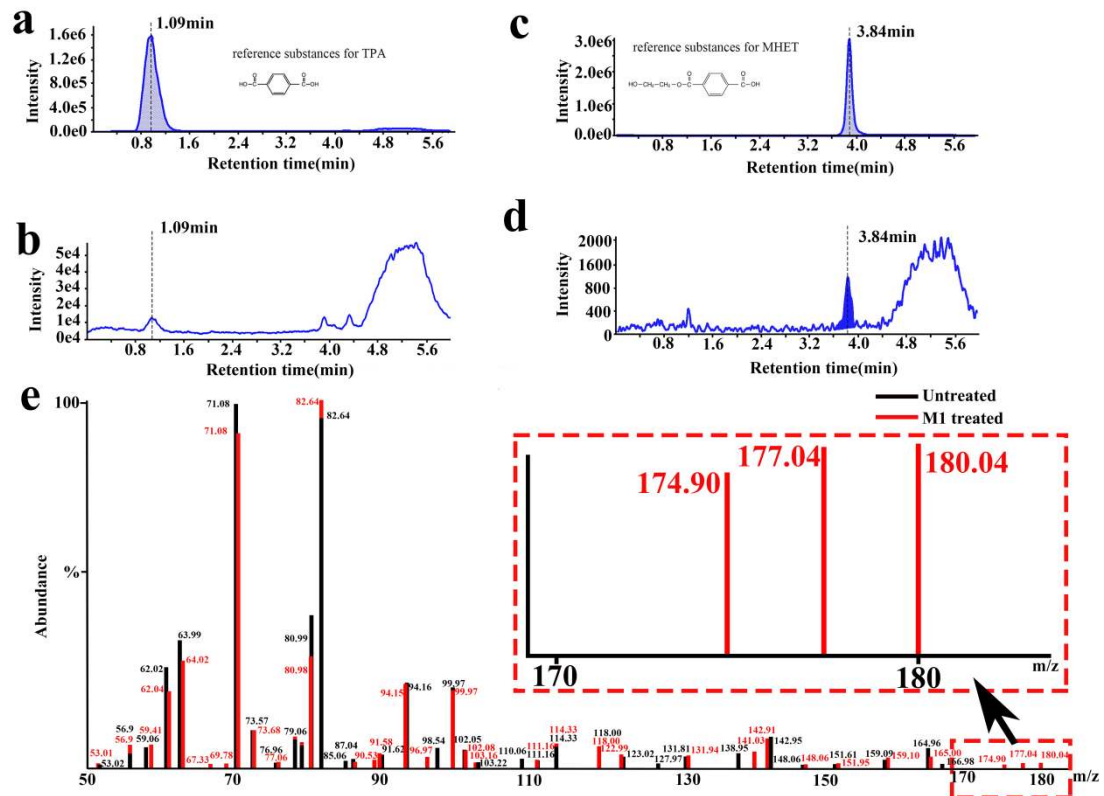
698

699

700

701

702



703

704

705

706

707

708

709

710

711

712

713

714

715

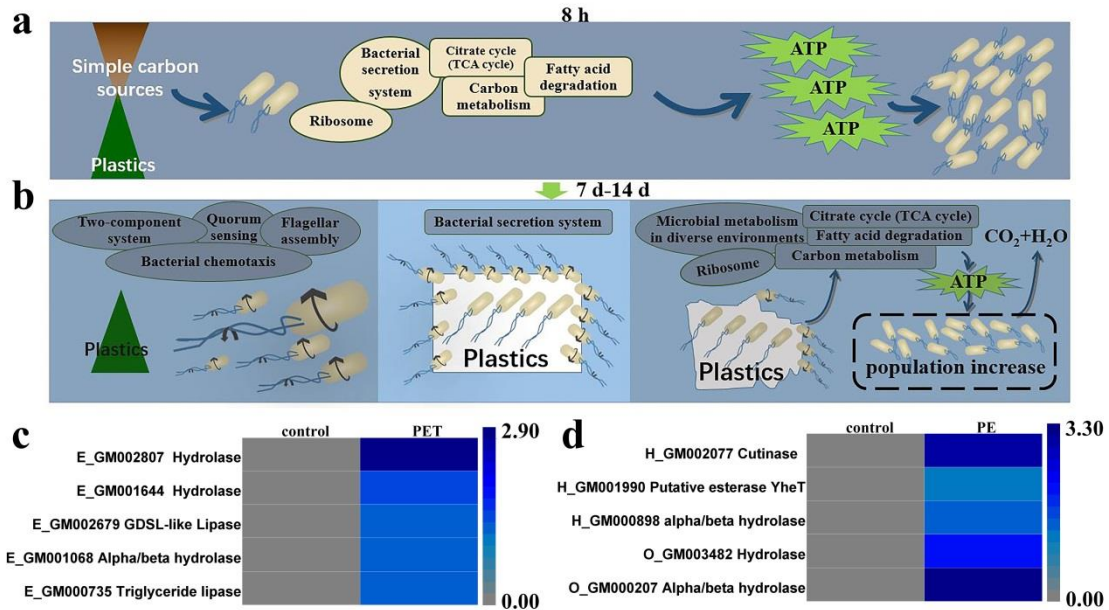
716

717

718

719

Fig. 5 Analysis of the released products from PET and PE films treated by the reconstituted bacterial community. a, HPLC spectrum of the standard terephthalic acid (TPA). **b,** HPLC spectrum of the product (prediction as TPA) released from the PET film treated by the reconstituted bacterial community for 28 days. **c,** HPLC spectrum of the standard mono-(2-hydroxyethyl) terephthalate (MHET). **d,** HPLC spectrum of the product (prediction as MHET) released from the PET film treated by the reconstituted bacterial community for 28 days. **e,** HPLC-MS spectrum of the products released from the PE film treated by the reconstituted bacterial community for 14 days. Magnification of the area is indicated by a dashed rectangle. The type of PET film used for this assay is ES301005 (0.0005 mm in thickness). The type of PE film used for this assay is ET311126 (0.025mm in thickness).



720

721 **Fig. 6 Transcriptomic analysis of the plastic degradation process and**

722 **mechanisms mediated by the reconstituted bacterial community. a,** Growth status

723 of the reconstituted bacterial community cultured in the minimal medium for 8 hours

724 supplemented with PET or PE film. **b,** The proposed model of plastic degradation and

725 utilization mediated by the reconstituted bacterial community cultured in the minimal

726 medium for 7 or 14 days supplemented with PET or PE film. The proposed growth

727 and metabolic pathways were referred to the transcriptomic results. The type of PET

728 film used for this assay is ES301005 (0.0005 mm in thickness). The type of PE film

729 used for this assay is ET311350 ET311126 (0.025mm in thickness). **c,** Heat map

730 showing the predicted PET-degradation enzymes derived from the reconstituted

731 bacterial community. **d,** Heat map showing the predicted PE-degradation enzymes

732 derived from the reconstituted bacterial community. All the transcriptomic data

733 associated with this figure are shown in the Supplementary information

734 (Supplemental Figs. 4-63) and uploaded in the public database.

735

736

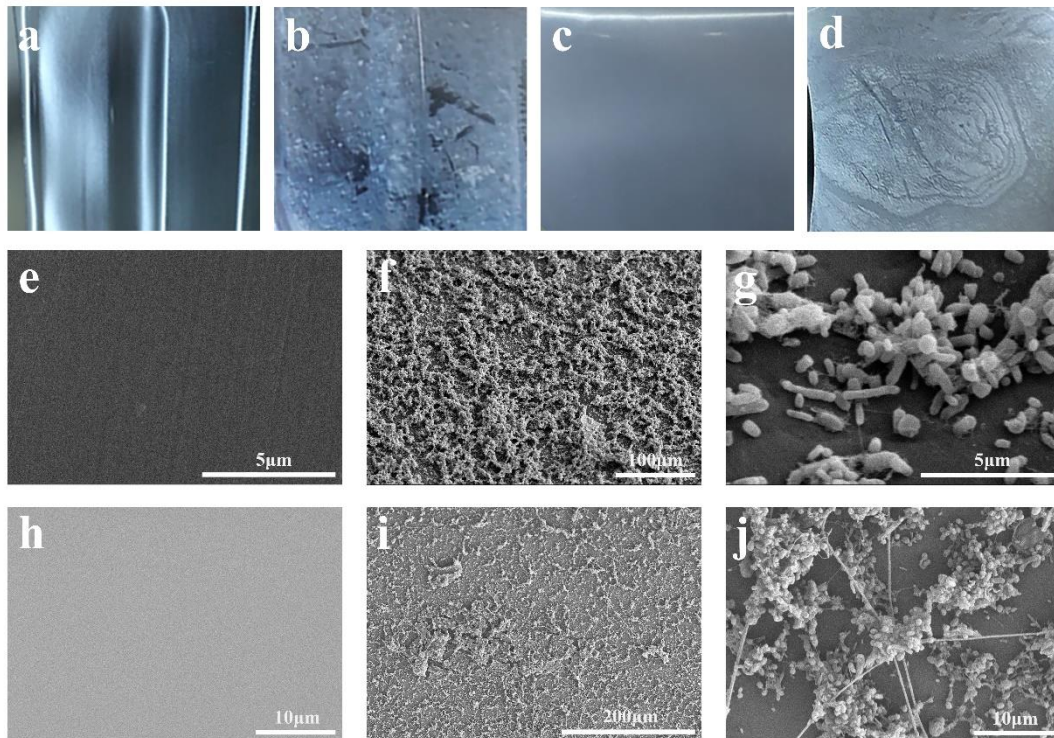
737

738

739

740

741 **Supplemental Figures**

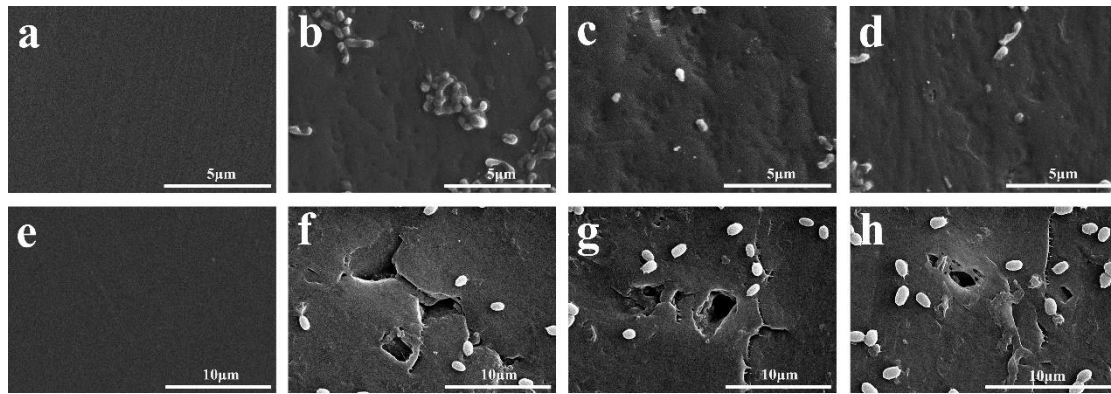


742

743 **Supplementary Fig. 1. Observation of the colonization and degradation effects**
744 **of a marine bacterial community on PET and PE films. a,** Morphology of PET
745 film without treatment. **b,** Morphology of PET film treated by the marine bacterial
746 community for seven days. **c,** Morphology of PE film without treatment. **d,**
747 Morphology of PE film treated by the marine bacterial community for seven days. **e,**
748 SEM observation of PET film without treatment. **f, g,** SEM observation of the
749 colonization of the bacterial community on the PET film after seven days incubation.
750 **h,** SEM observation of PE film without treatment. **i, j,** SEM observation of the
751 colonization of the bacterial community on the PE film after seven days incubation.
752 The type of PET film used for this assay is derived from the drink bottle containing
753 additives. The type of PE film used for this assay is derived from the commercial PE
754 bags containing additives.

755

756



757

758 **Supplementary Fig. 2. SEM observation of degradation effects on PET and PE**
759 **films by the marine bacterial community. a**, SEM observation of PET film without
760 treatment. **b-d**, SEM observation of the degradation effects on the PET film by the
761 marine bacterial community after seven days incubation. **e**, SEM observation of PE
762 film without treatment. **f-h**, SEM observation of the degradation effects on the PE
763 film by the marine bacterial community after seven days incubation. The type of PET
764 film used for this assay is derived from the drink bottle containing additives. The type
765 of PE film used for this assay is derived from the commercial PE bags containing
766 additives.

767

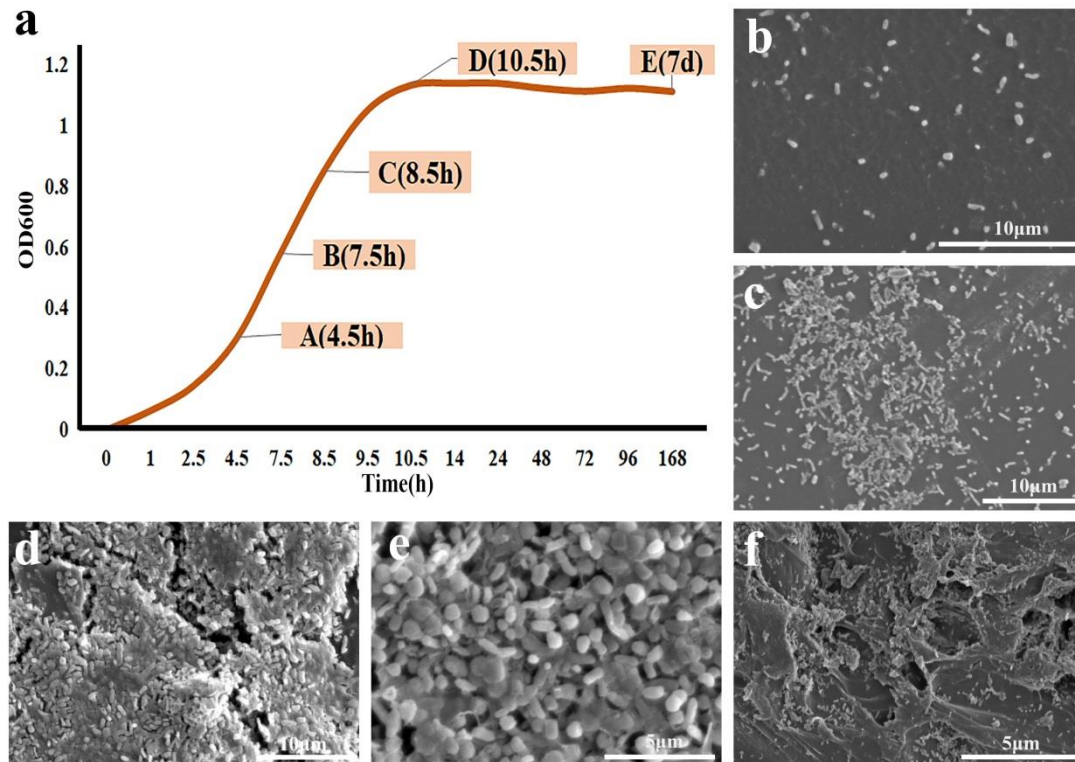
768

769

770

771

772



773

774 **Supplementary Fig. 3. Growth assay, colonization and degradation effects of the**

775 **marine bacterial community towards PET and PE films. a,** Growth assay of the

776 marine bacterial community in the presence of PET and PE films in five stages

777 including OD₆₀₀=0.3 (cultivated for 4.5 h), OD₆₀₀=0.58 (cultivated for 7.5 h),

778 OD₆₀₀=0.85 (cultivated for 8.5 h), OD₆₀₀=1.05 (cultivated for 9.5 h), OD₆₀₀=1.13

779 (cultivated for 7 d). **b,** SEM observation of the colonization of the marine bacterial

780 community on the plastic surface after cultivation for 4.5 h. **c,** SEM observation of the

781 colonization of the marine bacterial community on the plastic surface after cultivation

782 for 7.5 h. **d,** SEM observation of the colonization of the marine bacterial community

783 on the plastic surface after cultivation for 8.5 h. **e,** SEM observation of the

784 colonization of the marine bacterial community on the plastic surface after cultivation

785 for 10.5 h. **f,** SEM observation of the degradation effects of the marine bacterial

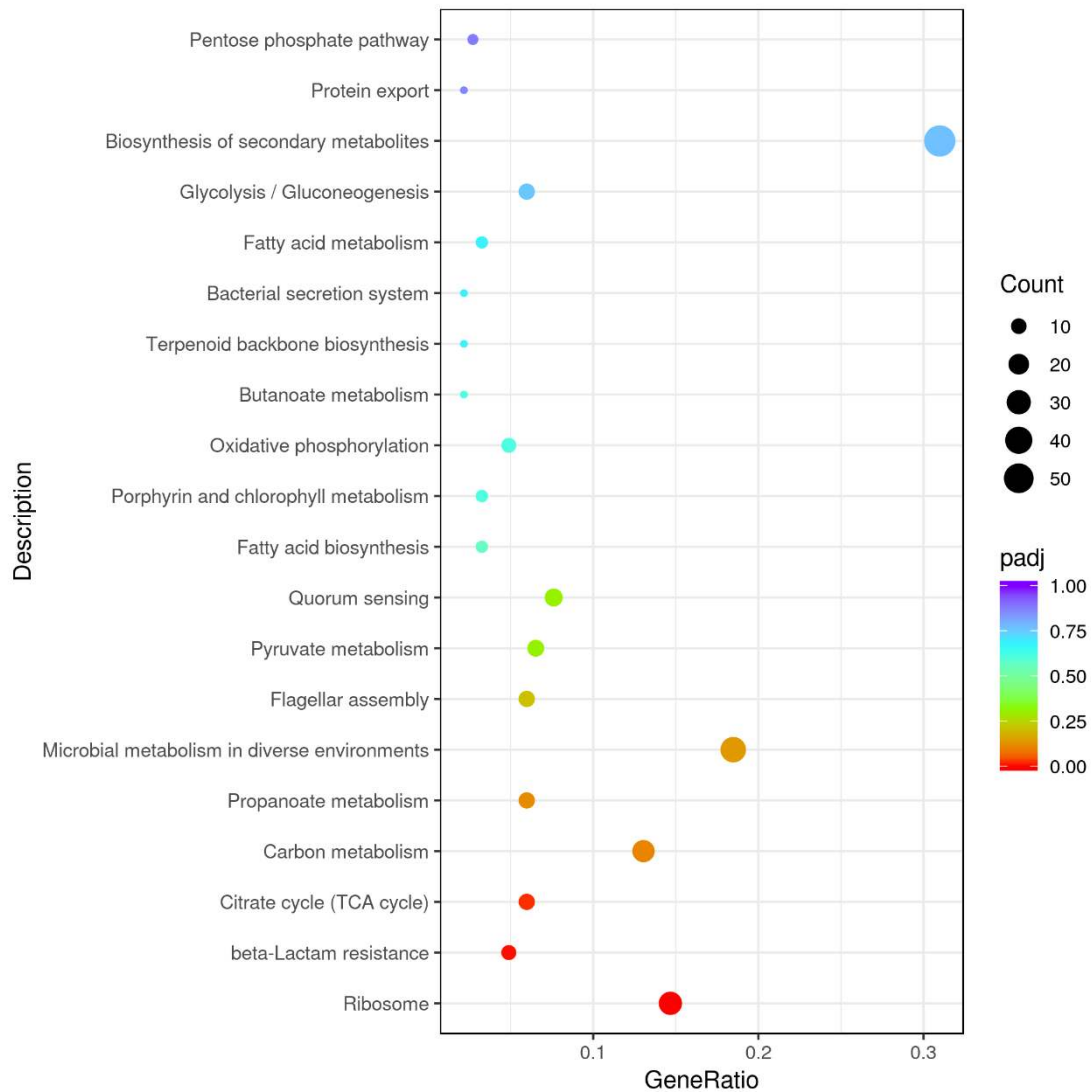
786 community on the plastic after cultivation 7 d. The type of PET film used for this

787 assay is ES301450 (0.25 mm in thickness). The type of PE film used for this assay is

788 ET311350 (0.25mm in thickness).

789

790

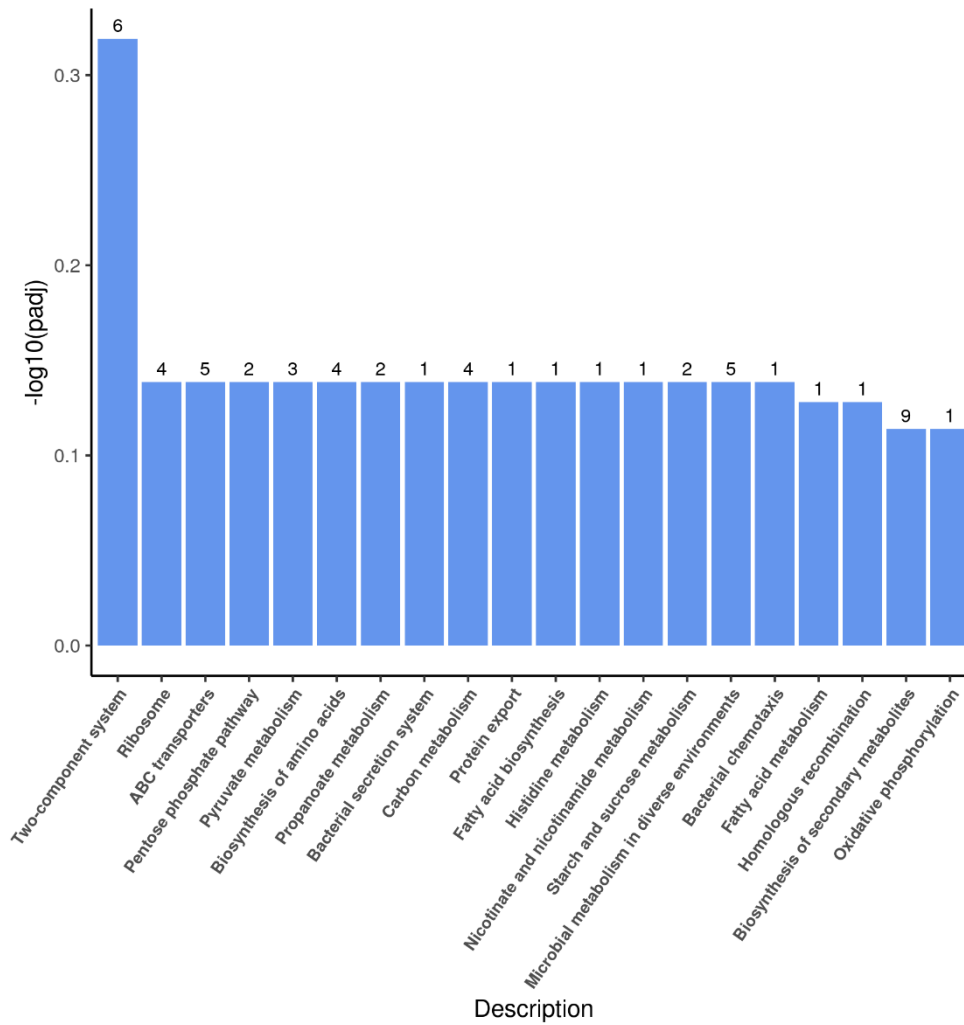


791

792 **Supplementary Fig. 5. Up-regulation KEGG pathways enrichment (scatter plot)**

793 **based on the transcriptomic analysis of PET degradation by *Exiguobacterium* sp.**

794 **for 8 h.**



795

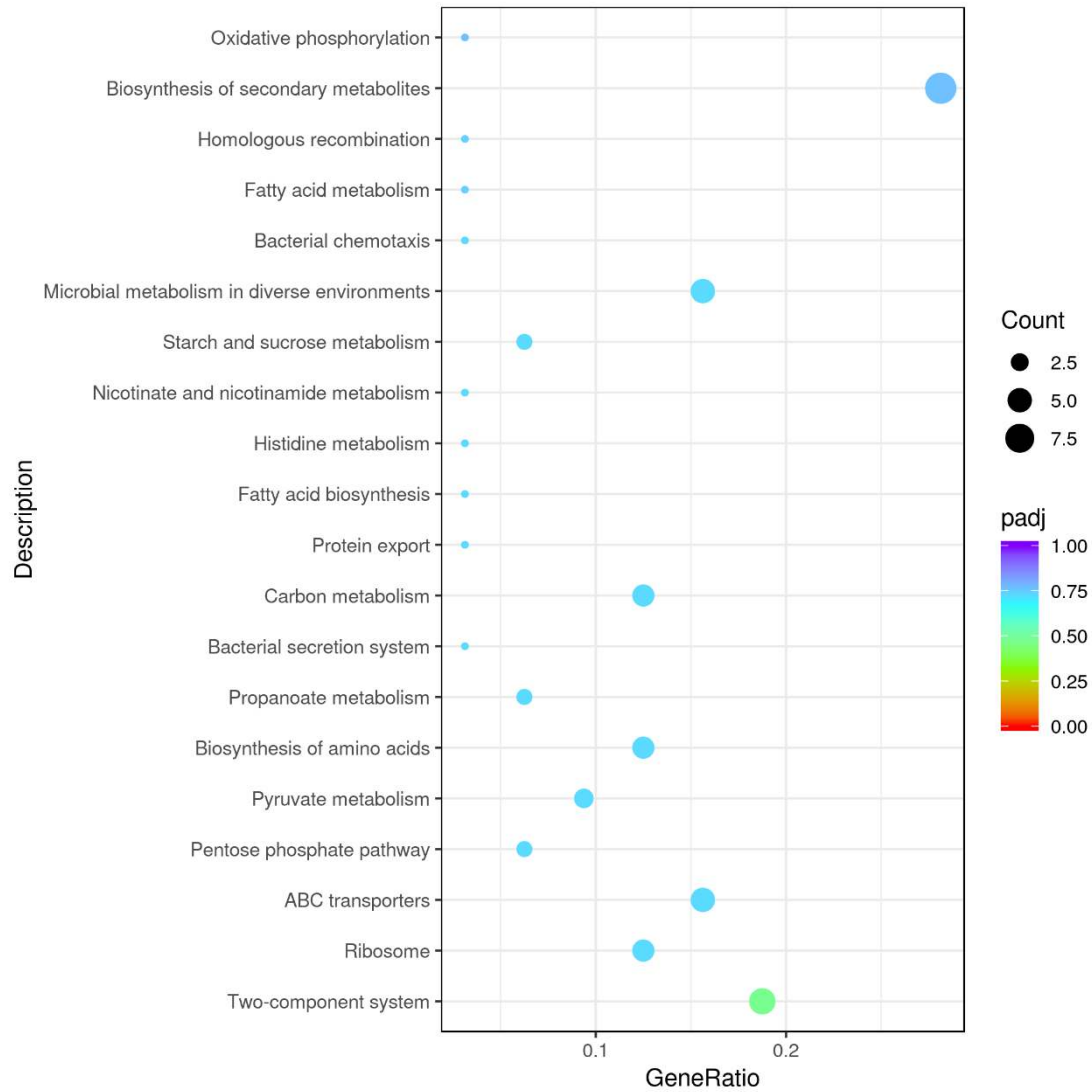
796 **Supplementary Fig. 6. Up-regulation KEGG pathways enrichment (histogram)**

797 **based on the transcriptomic analysis of PET degradation by *Exiguobacterium* sp.**

798 **for 7 d.** The numbers above the column are corresponding genes number related to

799 different pathways.

800

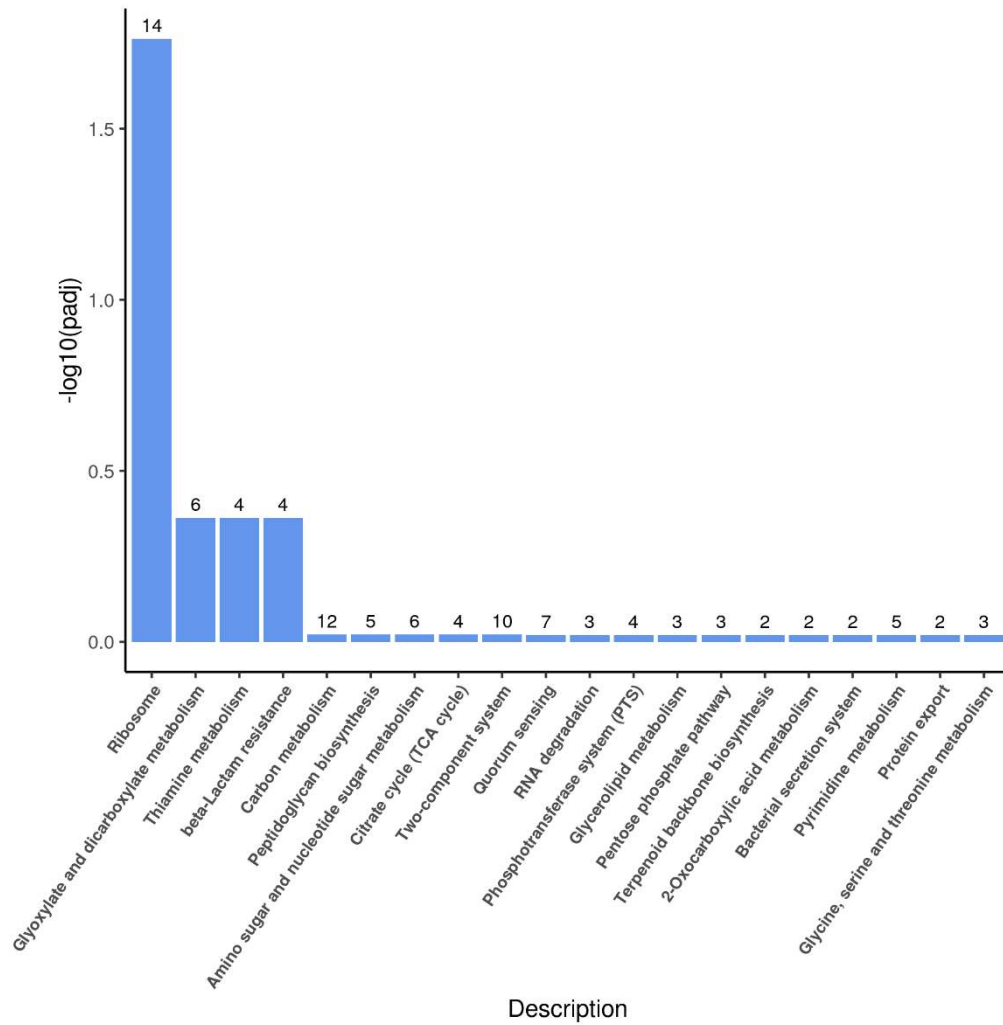


801

802 **Supplementary Fig. 7. Up-regulation KEGG pathways enrichment (scatter plot)**

803 **based on the transcriptomic analysis of PET degradation by *Exiguobacterium* sp.**

804 **for 7 d.**



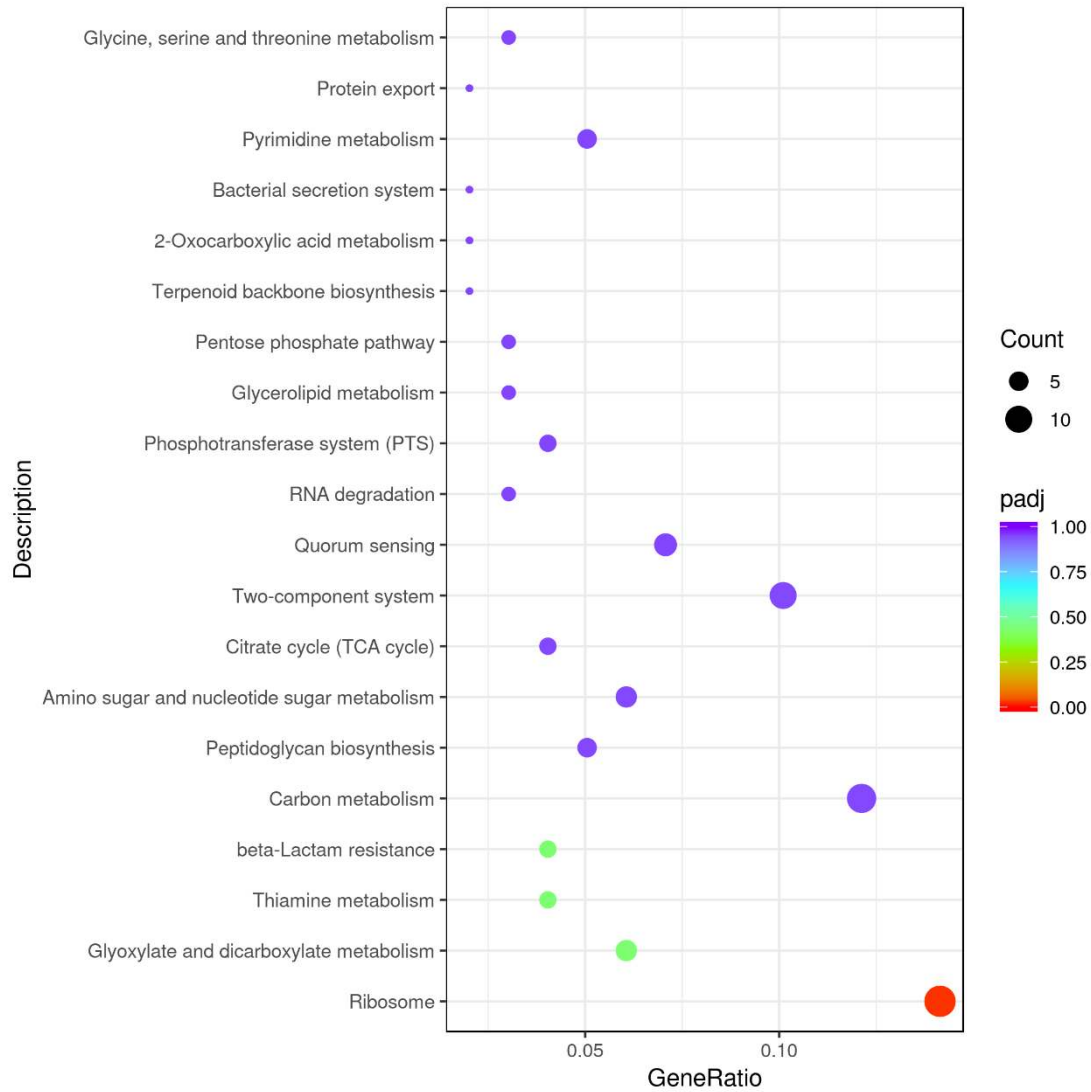
805

806 **Supplementary Fig. 8. Up-regulation KEGG pathways enrichment (histogram)**

807 **based on the transcriptomic analysis of PET degradation by *Exiguobacterium* sp.**

808 **for 14 d.** The numbers above the column are corresponding genes number related to

809 different pathways.



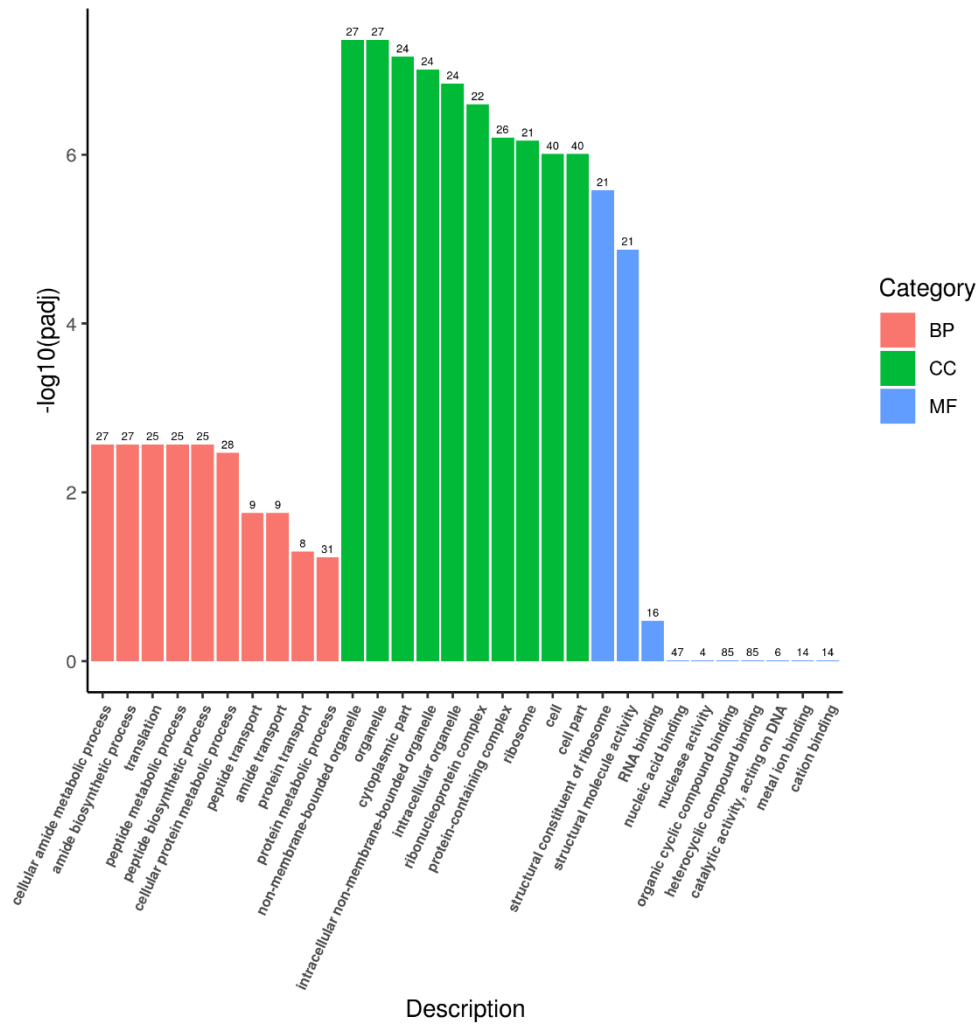
810

811 **Supplementary Fig. 9. Up-regulation KEGG pathways enrichment (scatter plot)**

812 **based on the transcriptomic analysis of PET degradation by *Exiguobacterium* sp.**

813 **for 14 d.**

814



815

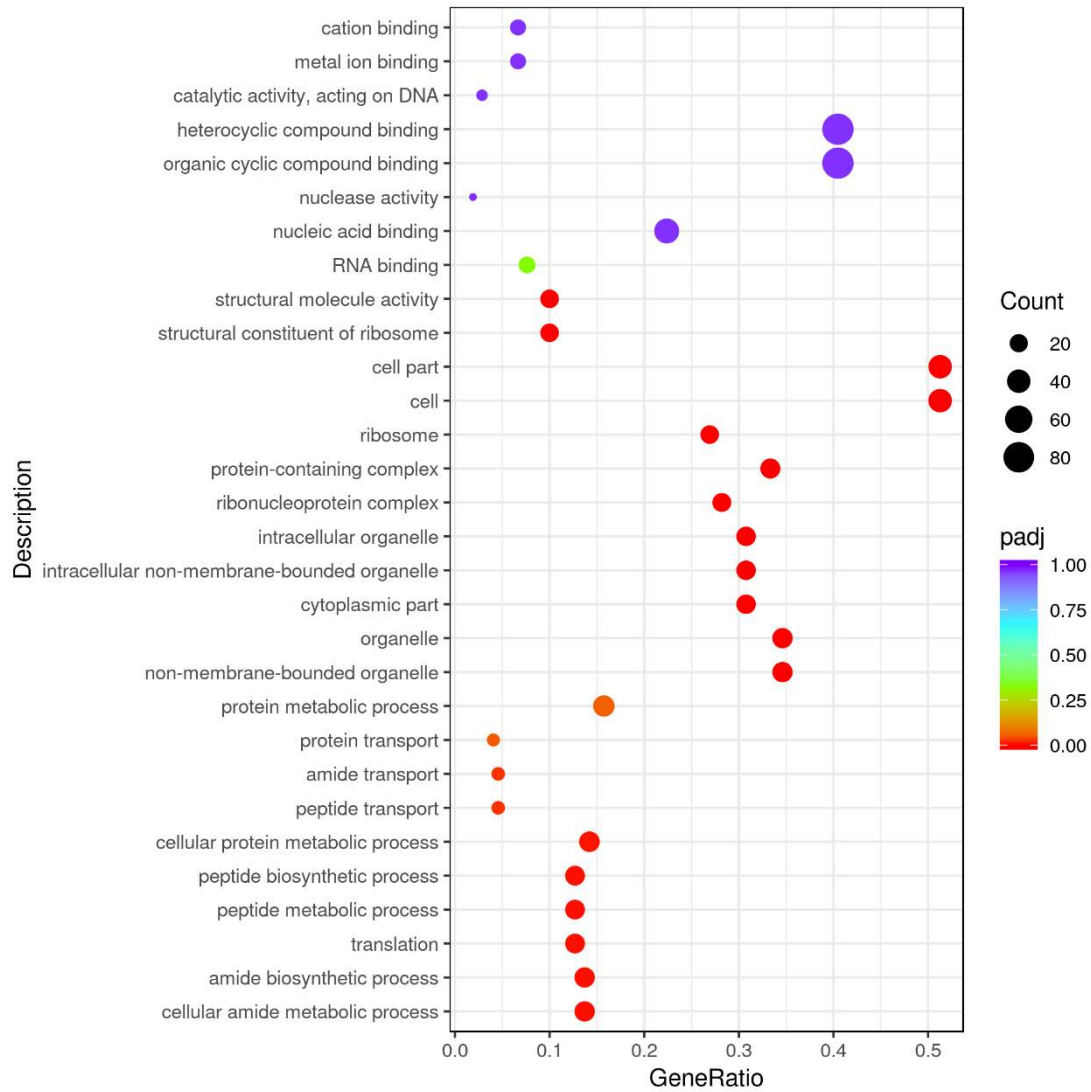
816 **Supplementary Fig. 10. Up-regulation Go enrichment (histogram) based on the**

817 **transcriptomic analysis of PET degradation by *Exiguobacterium* sp. for 8 h. The**

818 numbers above the column are corresponding genes number related to different

819 pathways.

820

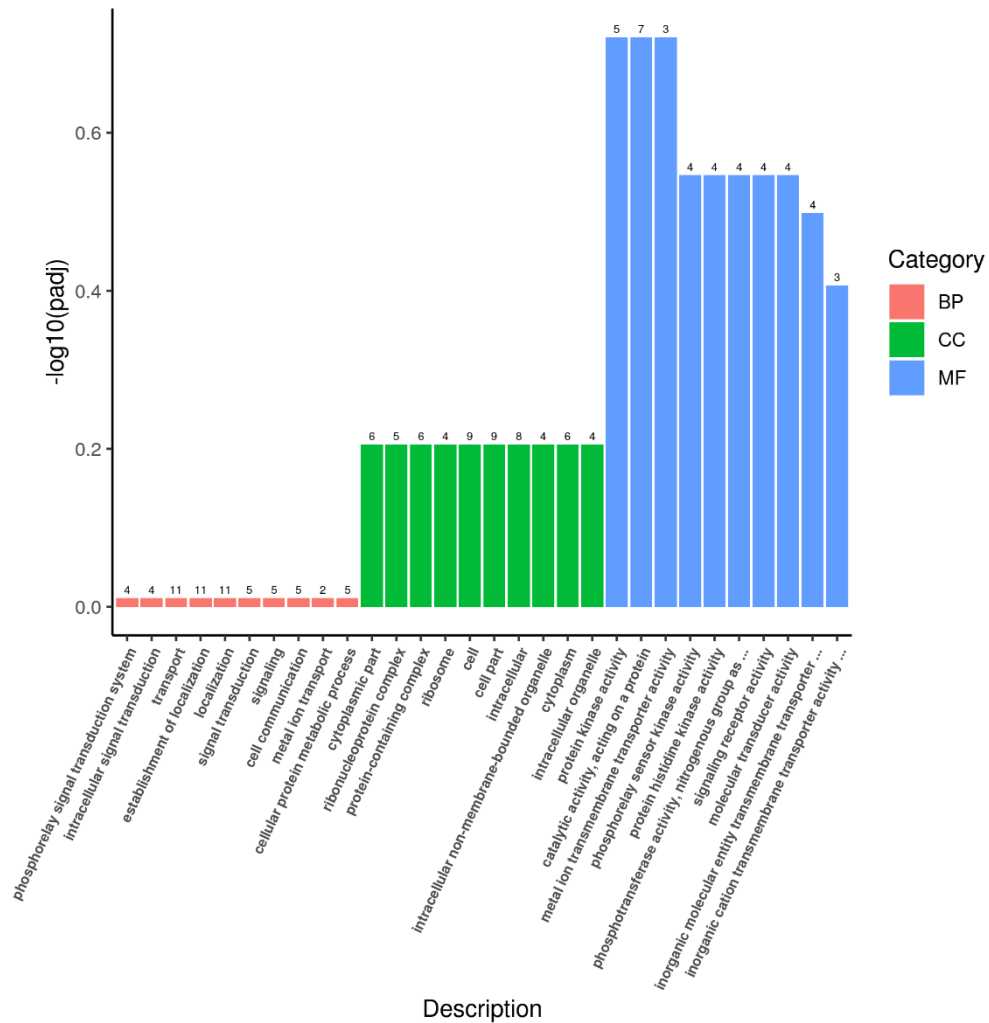


821

822 **Supplementary Fig. 11. Up-regulation GO enrichment (scatter plot) based on the**

823 **transcriptomic analysis of PET degradation by *Exiguobacterium* sp. for 8 h.**

824



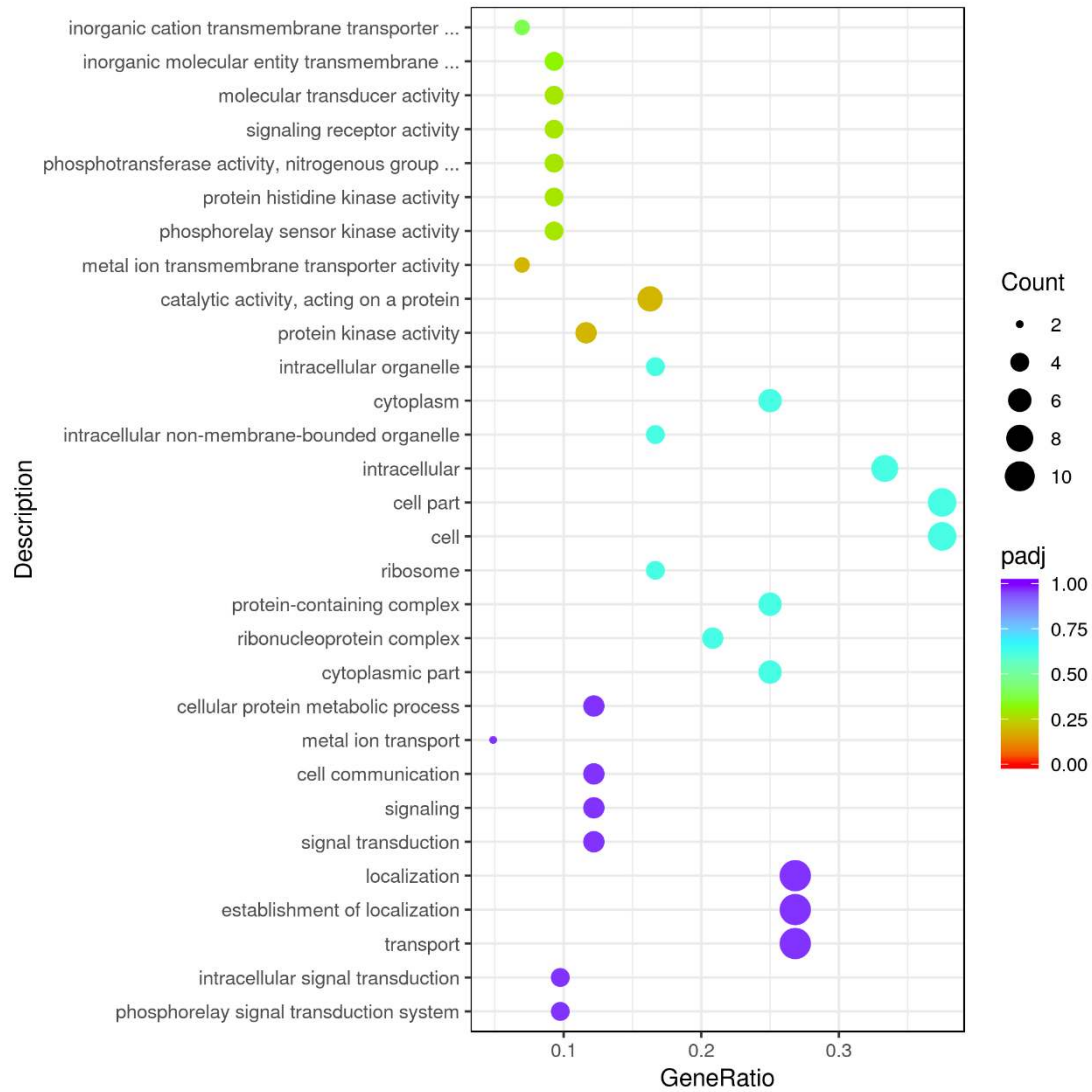
825

826 **Supplementary Fig. 12. Up-regulation Go enrichment (histogram) based on the**

827 **transcriptomic analysis of PET degradation by *Exiguobacterium* sp. for 7 d. The**

828 numbers above the column are corresponding genes number related to different

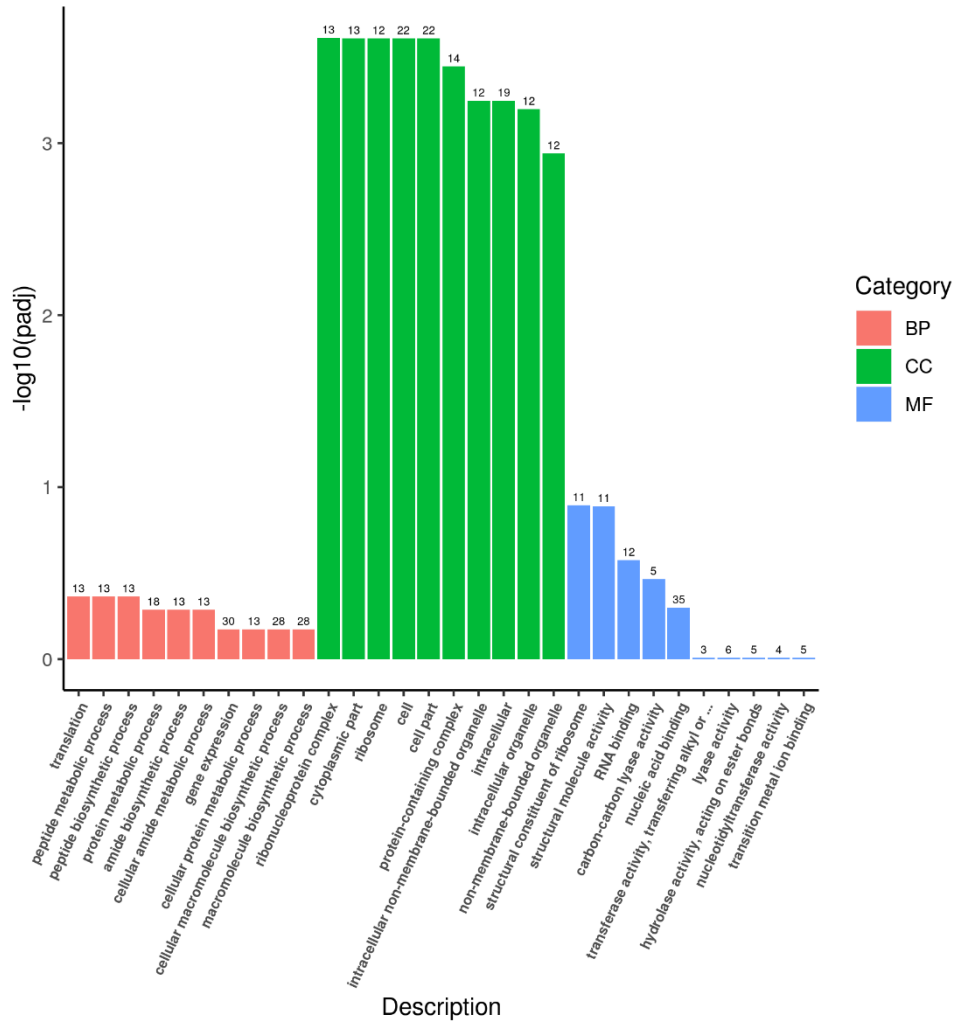
829 pathways.



830

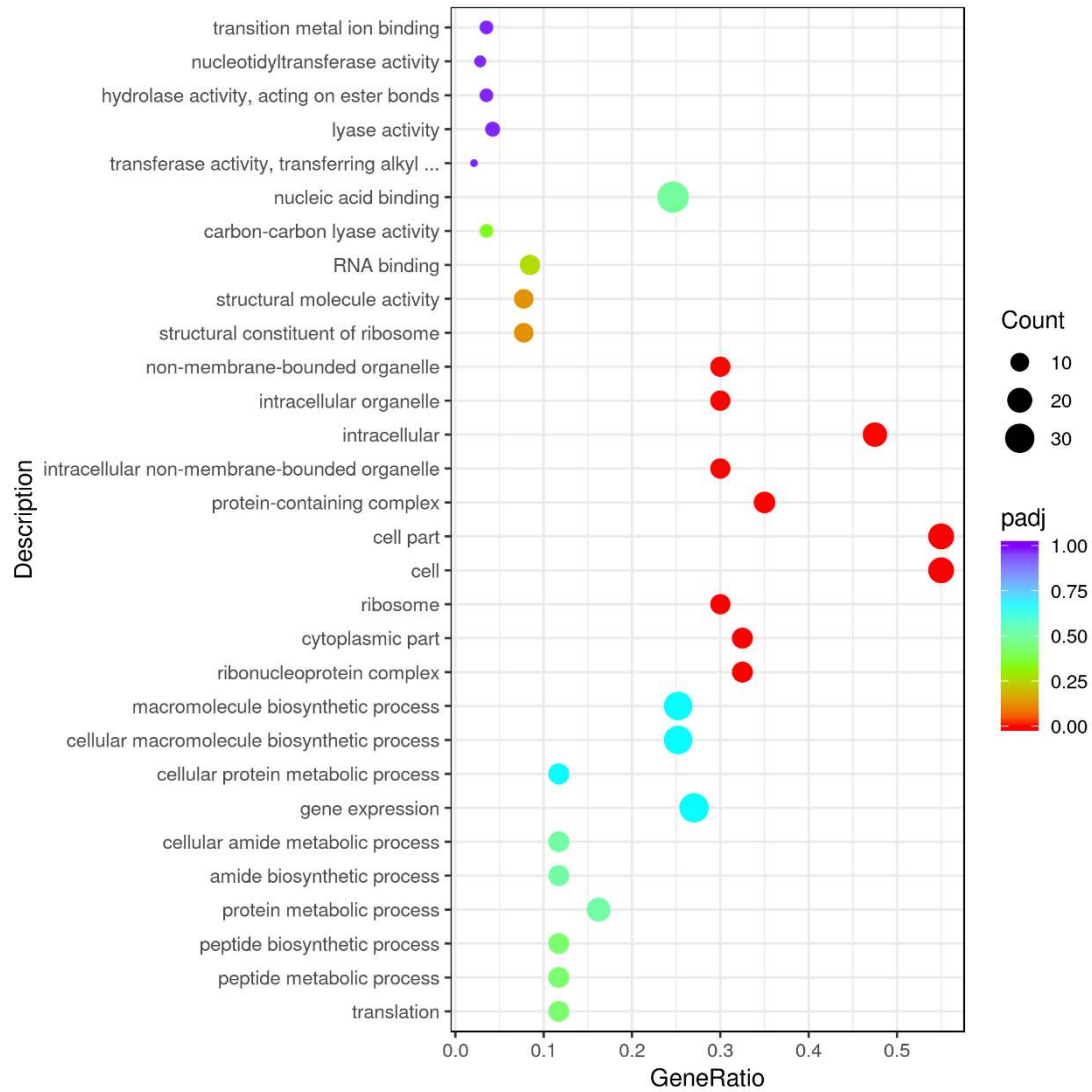
831 **Supplementary Fig. 13. Up-regulation GO enrichment (scatter plot) based on the**

832 **transcriptomic analysis of PET degradation by *Exiguobacterium* sp. for 7 d.**



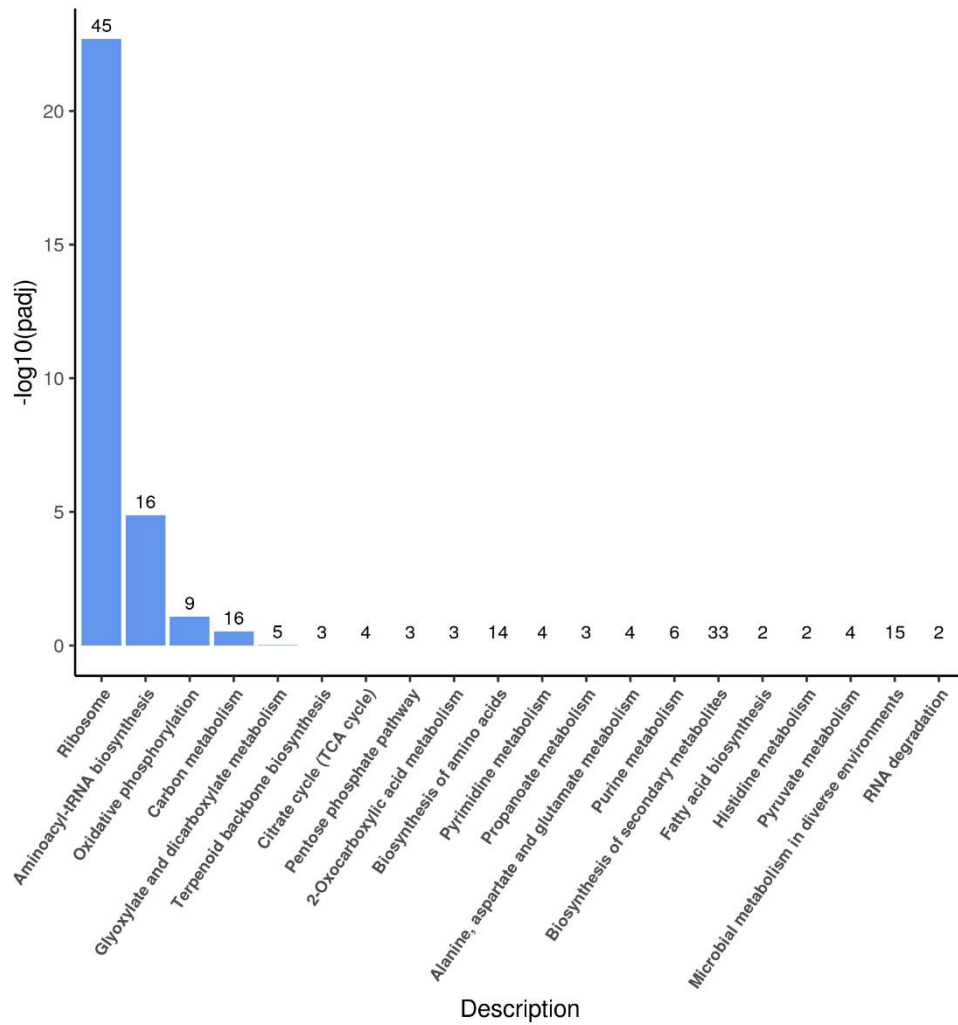
833

834 **Supplementary Fig. 14. Up-regulation Go enrichment (histogram) based on the**
 835 **transcriptomic analysis of PET degradation by *Exiguobacterium* sp. for 14 d. The**
 836 numbers above the column are corresponding genes number related to different
 837 pathways.



838

839 **Supplementary Fig. 15. Up-regulation GO enrichment (scatter plot) based on the**
840 **transcriptomic analysis of PET degradation by *Exiguobacterium* sp. for 14 d.**



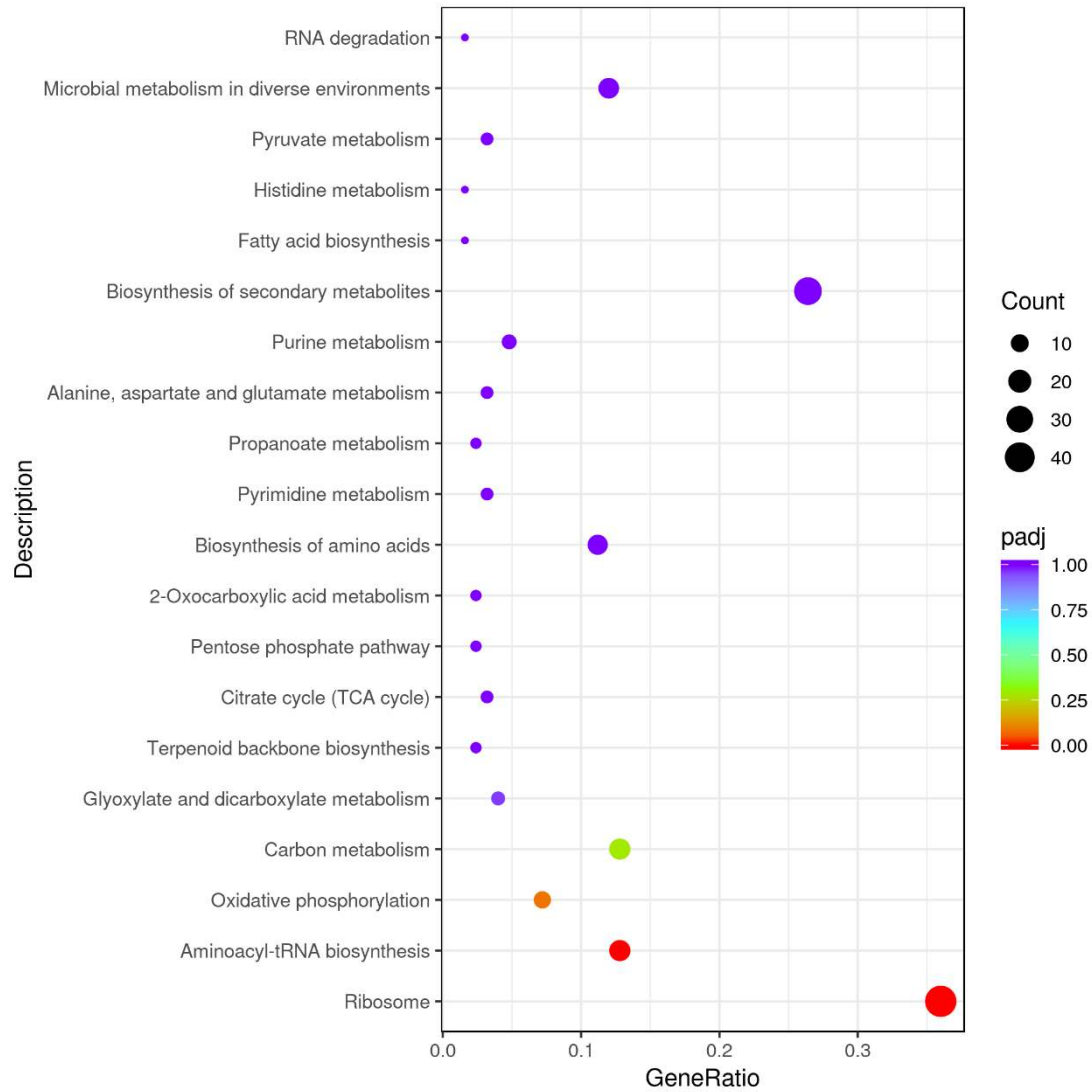
841

842 **Supplementary Fig. 16. Up-regulation KEGG pathways enrichment (histogram)**

843 **based on the transcriptomic analysis of PET degradation by *Halomonas* sp. for 8**

844 **h.** The numbers above the column are corresponding genes number related to different

845 pathways.

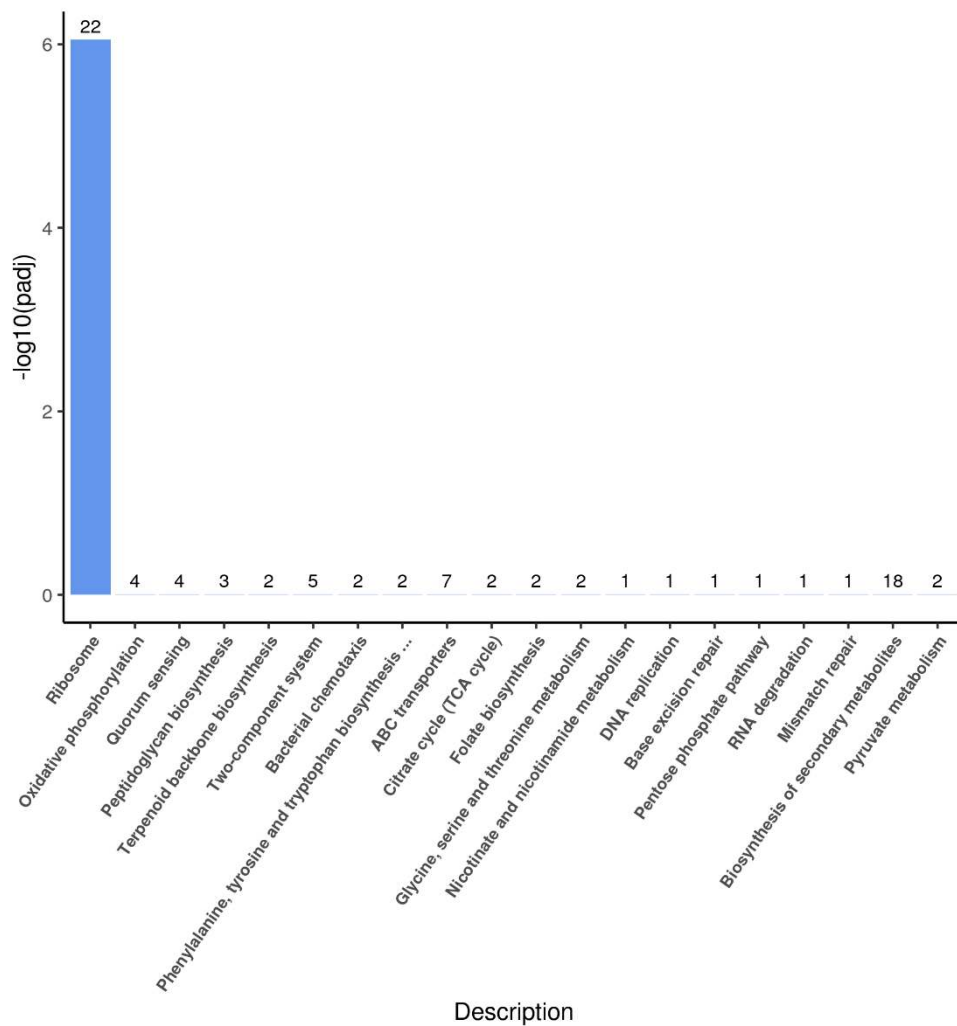


846

847 **Supplementary Fig. 17. Up-regulation KEGG pathways enrichment (scatter plot)**

848 **based on the transcriptomic analysis of PET degradation by *Halomonas* sp. for 8**

849 **h.**



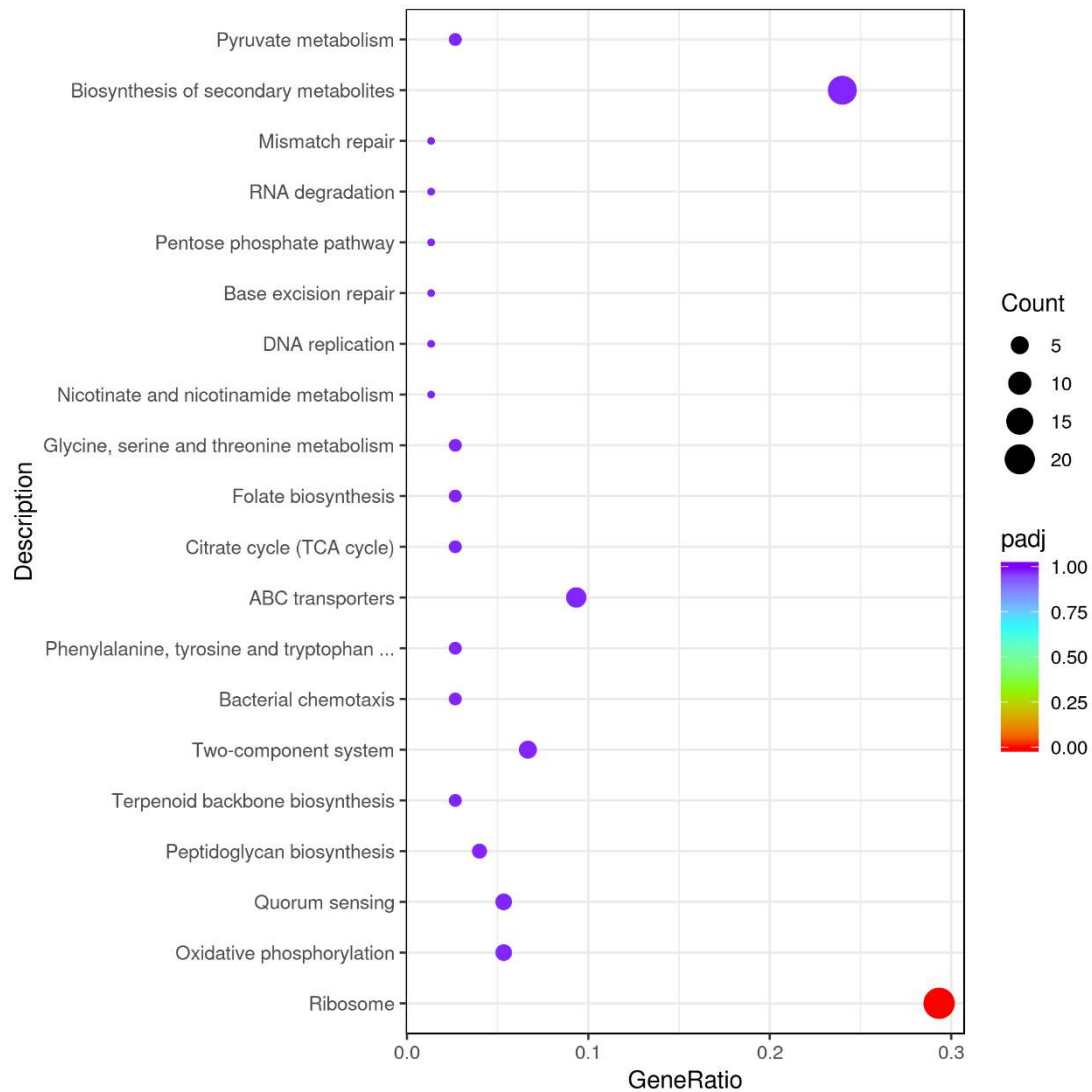
850

851 **Supplementary Fig. 18. Up-regulation KEGG pathways enrichment (histogram)**

852 **based on the transcriptomic analysis of PET degradation by *Halomonas* sp. for 7**

853 **d.** The numbers above the column are corresponding genes number related to different

854 pathways.

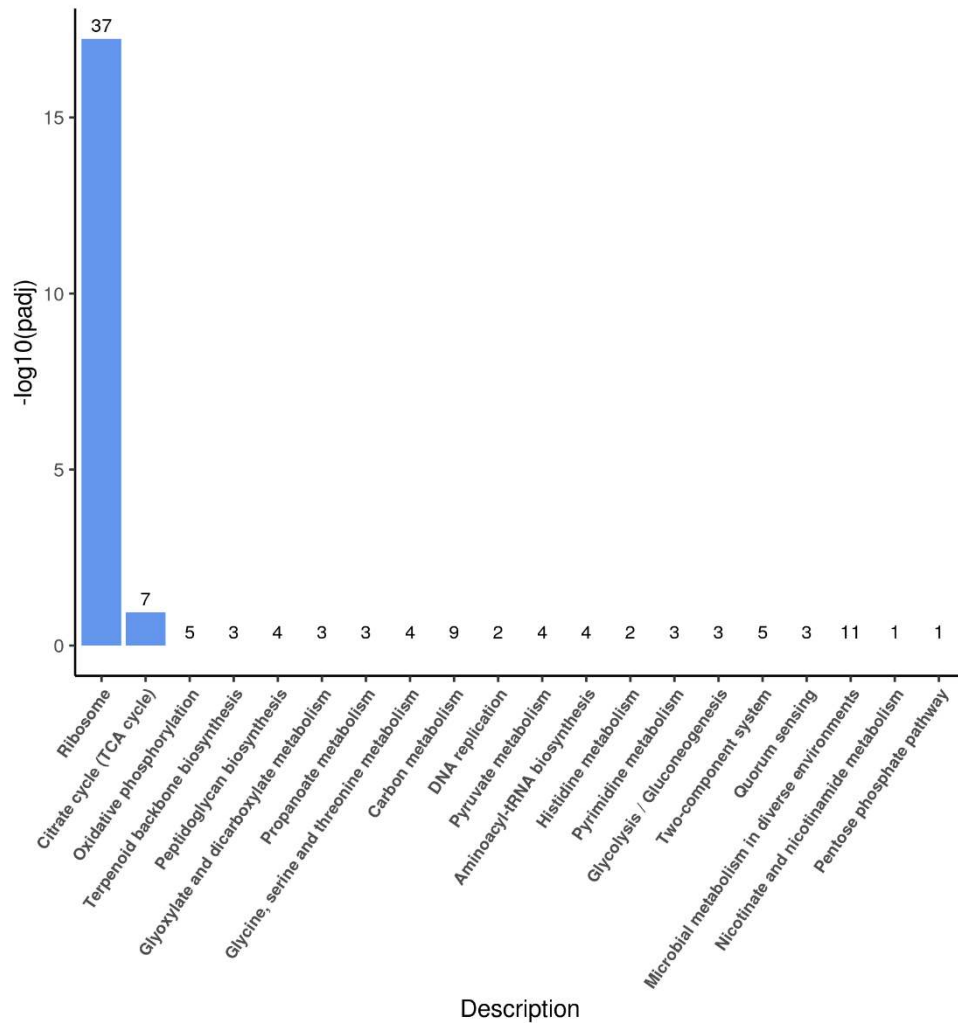


855

856 **Supplementary Fig. 19. Up-regulation KEGG pathways enrichment (scatter plot)**

857 **based on the transcriptomic analysis of PET degradation by *Halomonas* sp. for 7**

858 **d.**



859

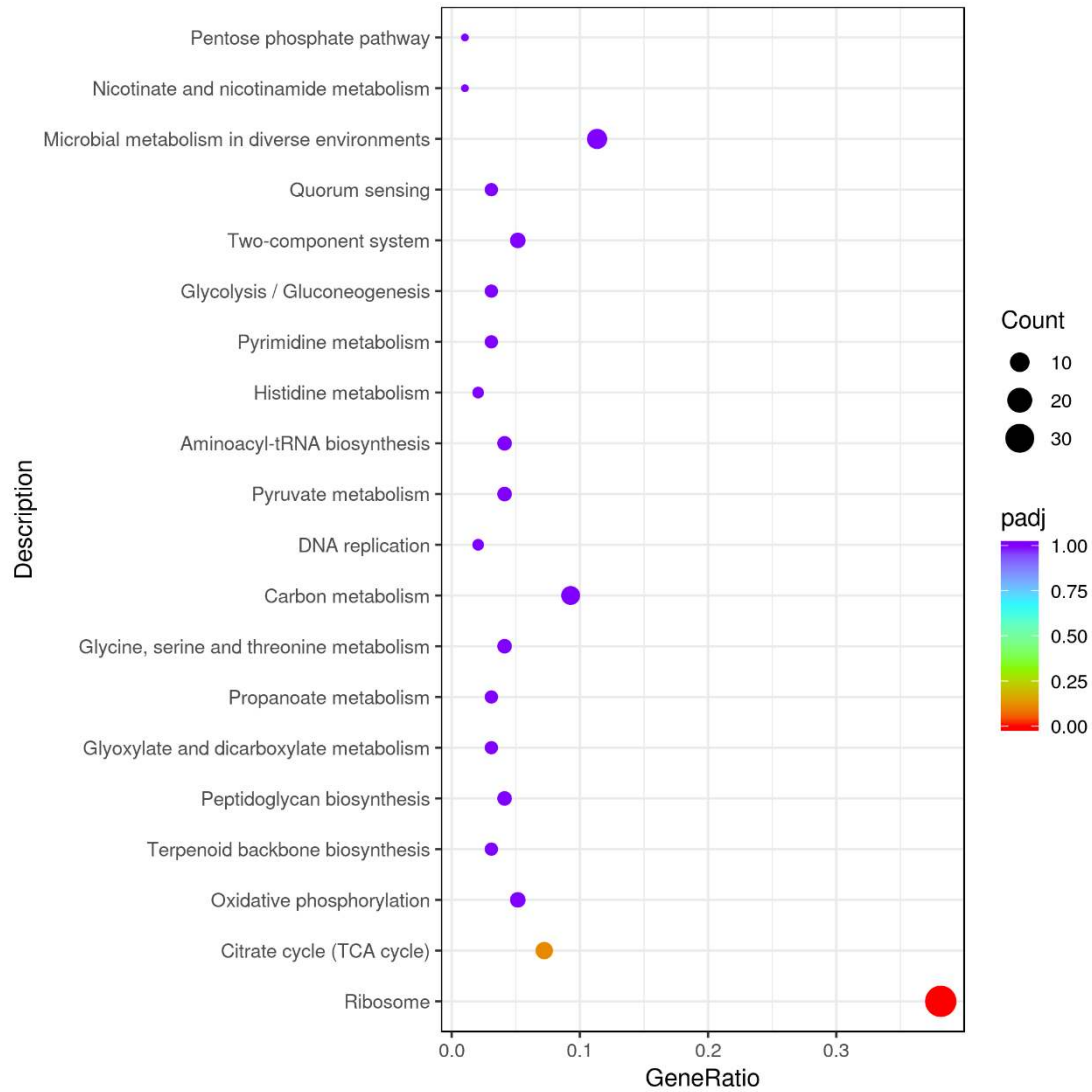
860 **Supplementary Fig. 20. Up-regulation KEGG pathways enrichment (histogram)**

861 **based on the transcriptomic analysis of PET degradation by *Halomonas* sp. for**

862 **14 d.** The numbers above the column are corresponding genes number related to

863 different pathways.

864



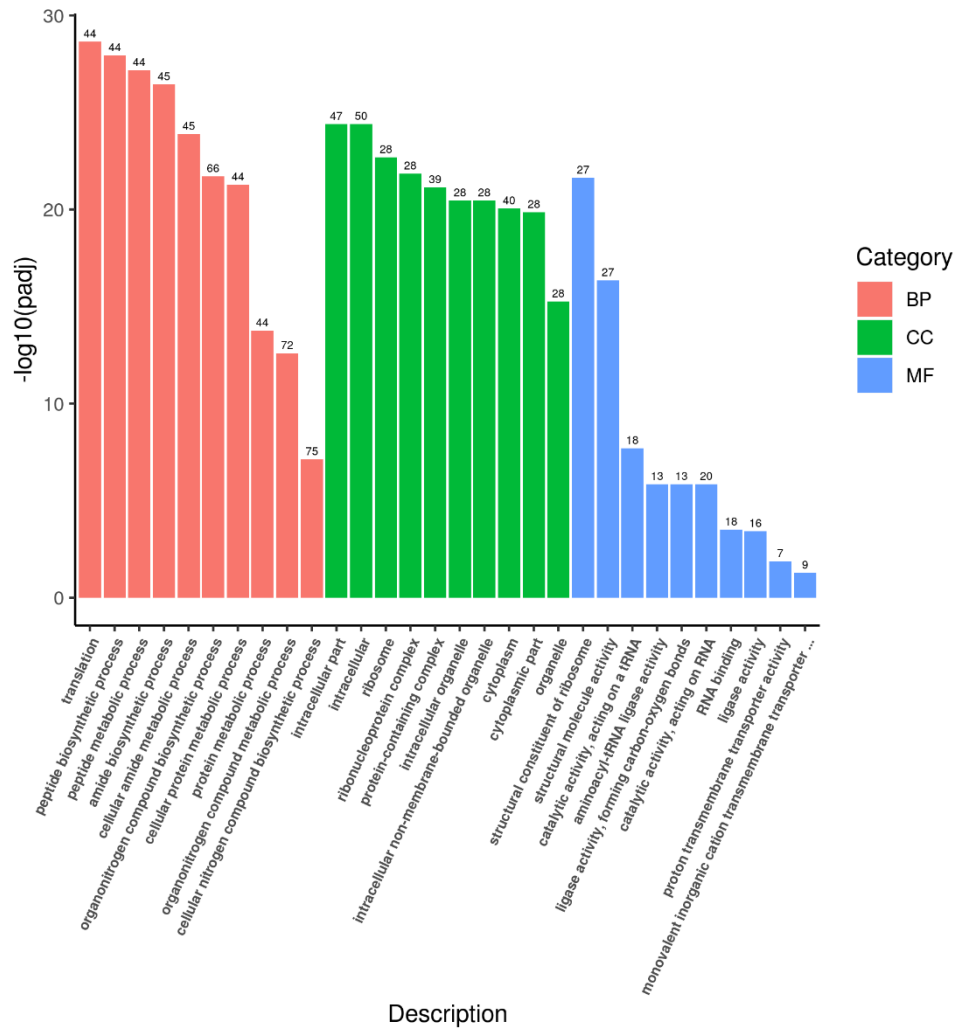
865

866 **Supplementary Fig. 21. Up-regulation KEGG pathways enrichment (scatter plot)**

867 **based on the transcriptomic analysis of PET degradation by *Halomonas* sp. for**

868 **14 d.**

869



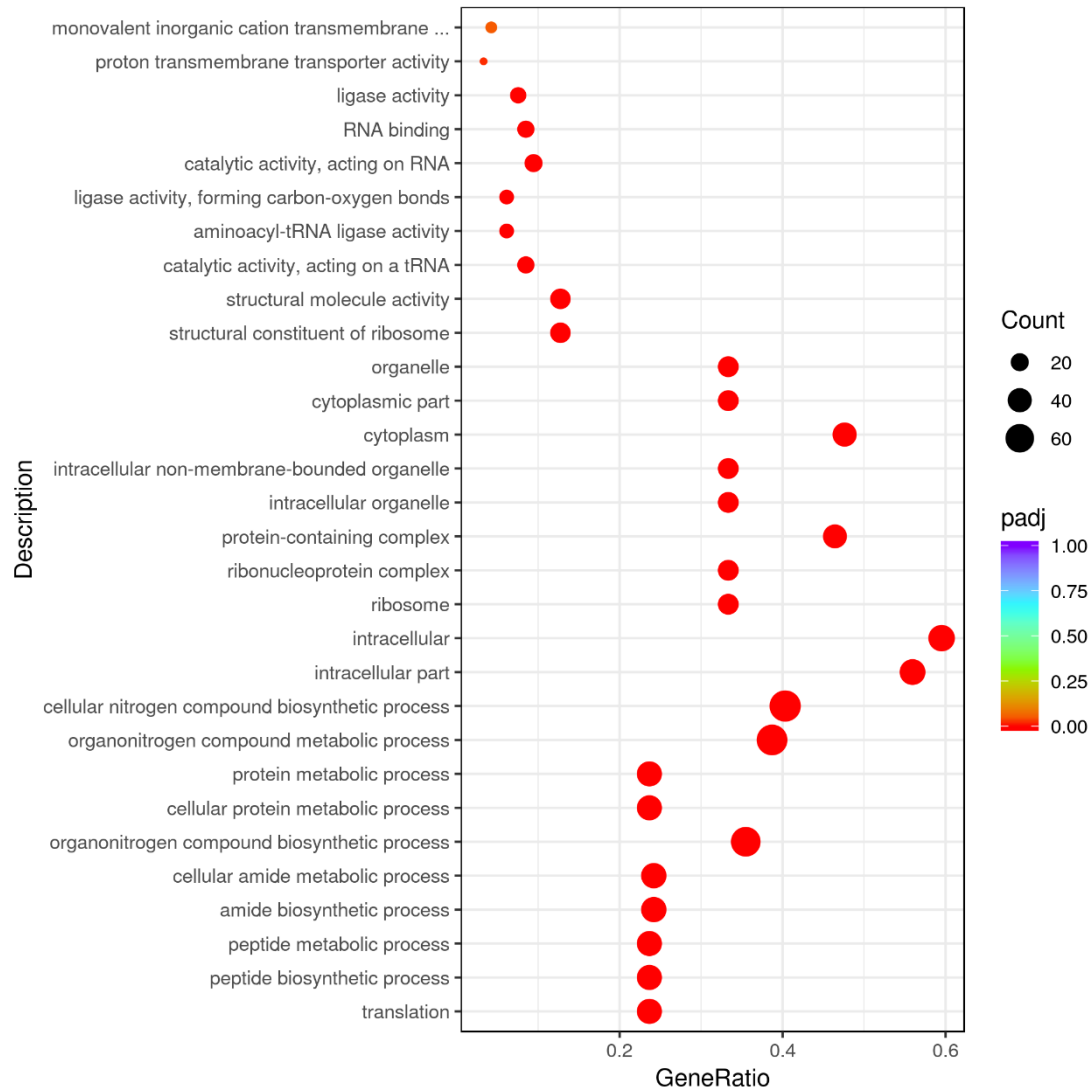
870

871 **Supplementary Fig. 22. Up-regulation Go enrichment (histogram) based on the**

872 **transcriptomic analysis of PET degradation by *Halomonas* sp. for 8 h. The**

873 numbers above the column are corresponding genes number related to different

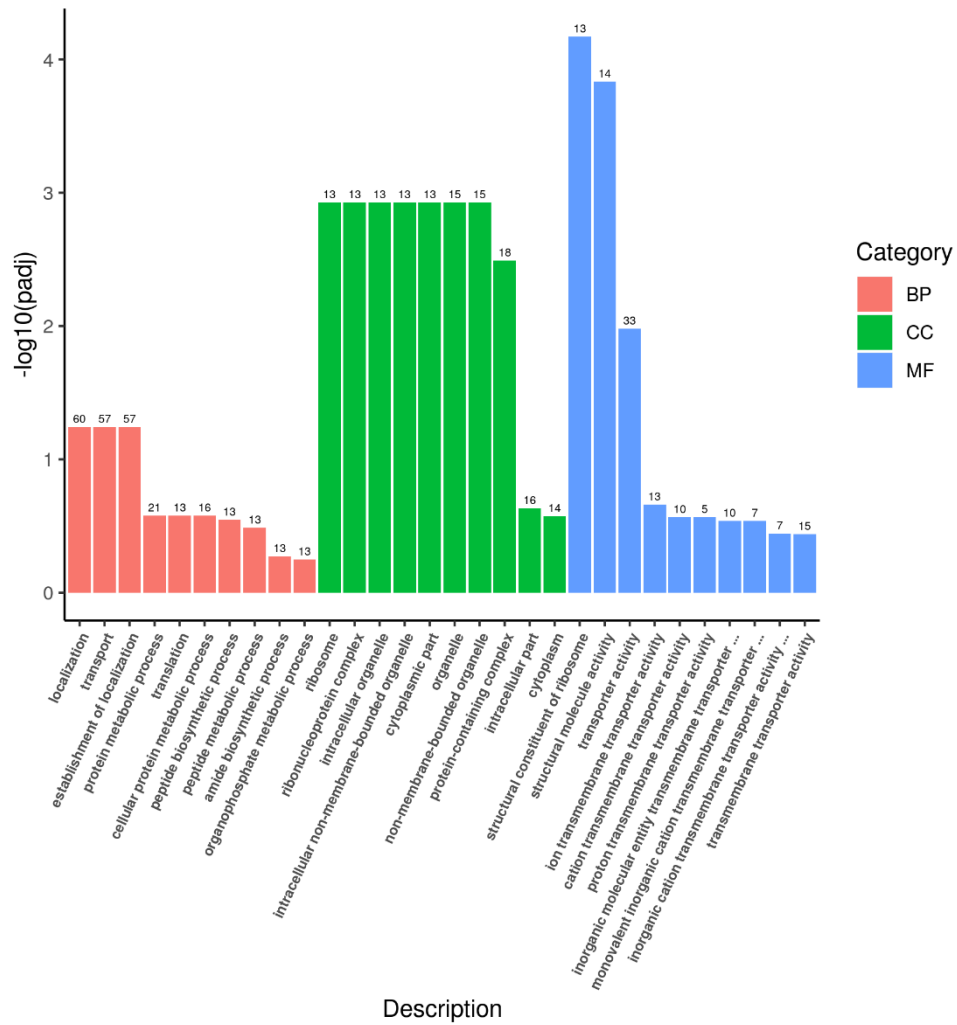
874 pathways.



875

876 **Supplementary Fig. 23. Up-regulation GO enrichment (scatter plot) based on the**

877 **transcriptomic analysis of PET degradation by *Halomonas* sp. for 8 h.**



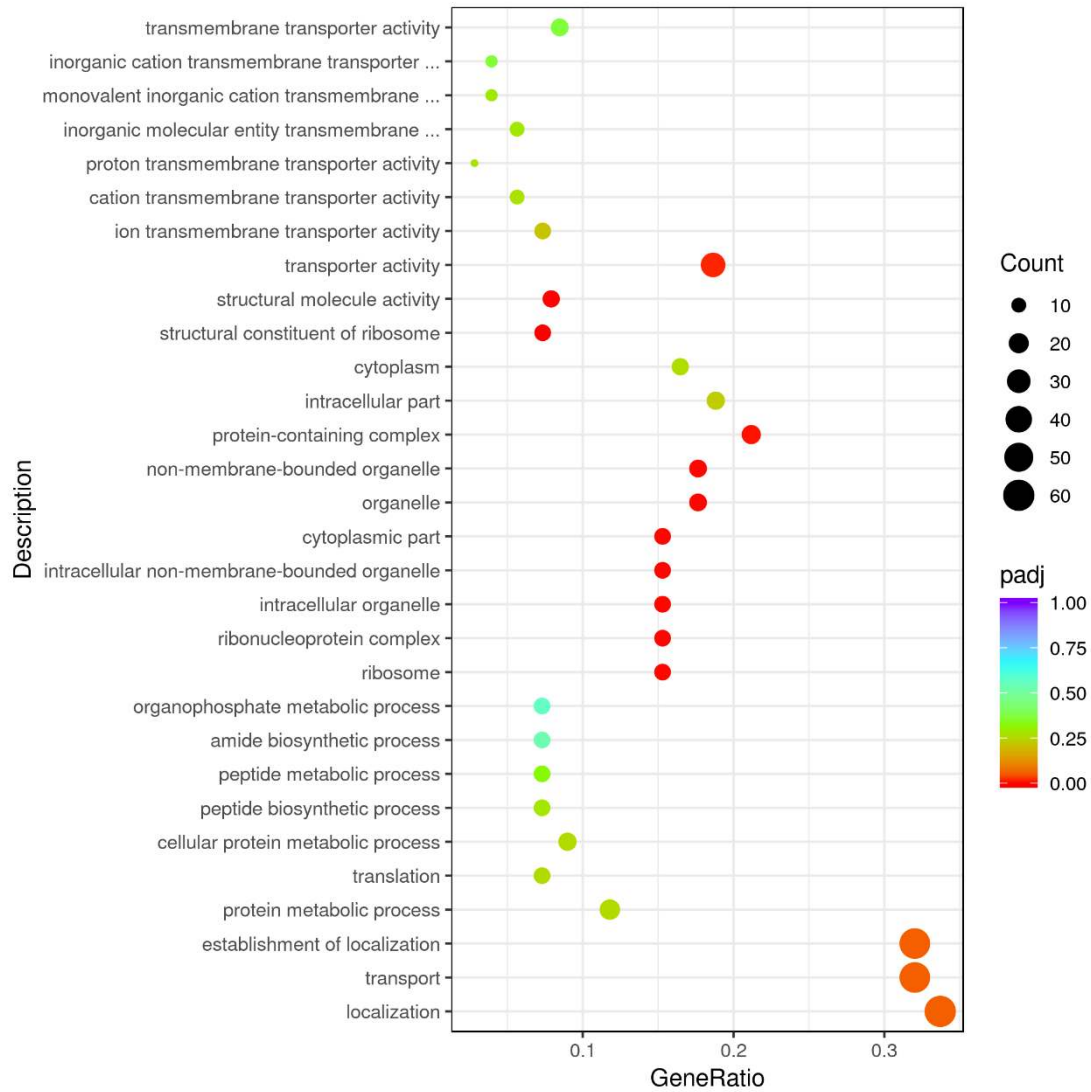
878

879 **Supplementary Fig. 24. Up-regulation Go enrichment (histogram) based on the**

880 **transcriptomic analysis of PET degradation by *Halomonas* sp. for 7 d. The**

881 numbers above the column are corresponding genes number related to different

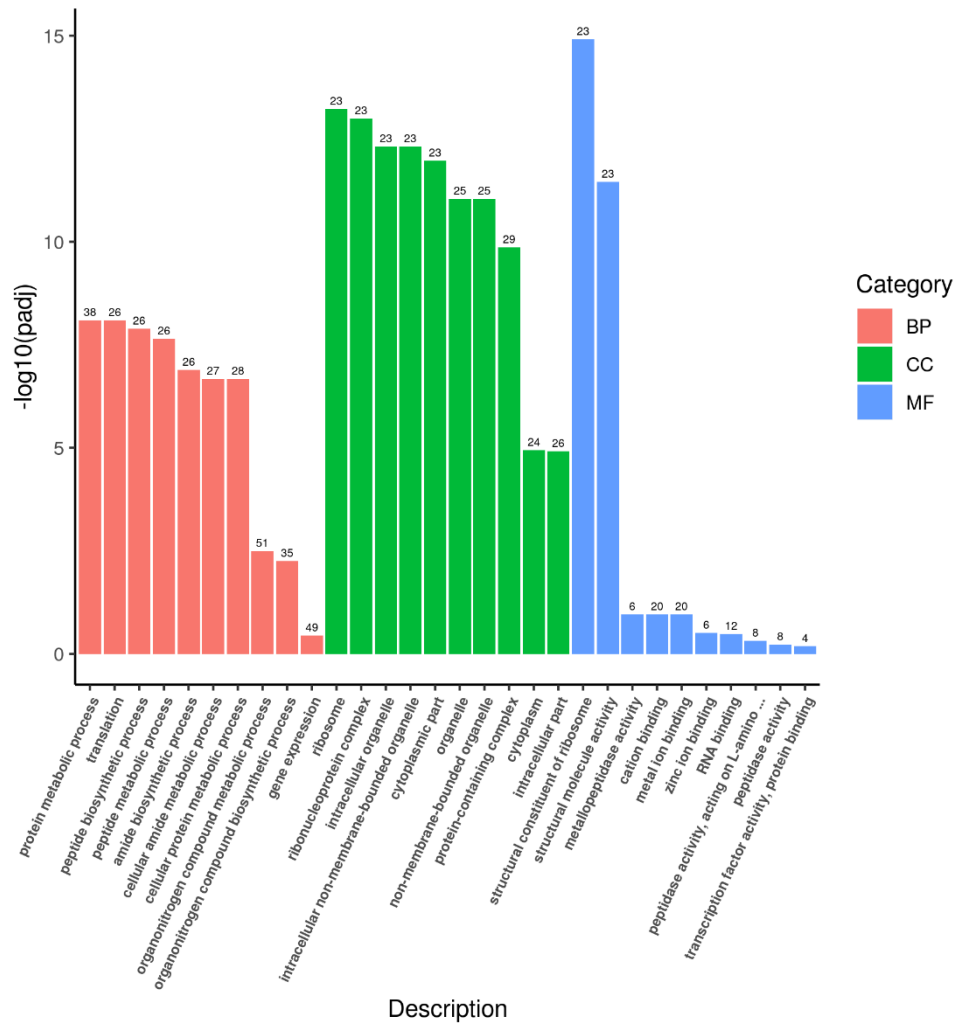
882 pathways.



883

884 **Supplementary Fig. 25. Up-regulation GO enrichment (scatter plot) based on the**

885 **transcriptomic analysis of PET degradation by *Halomonas* sp. for 7 d.**



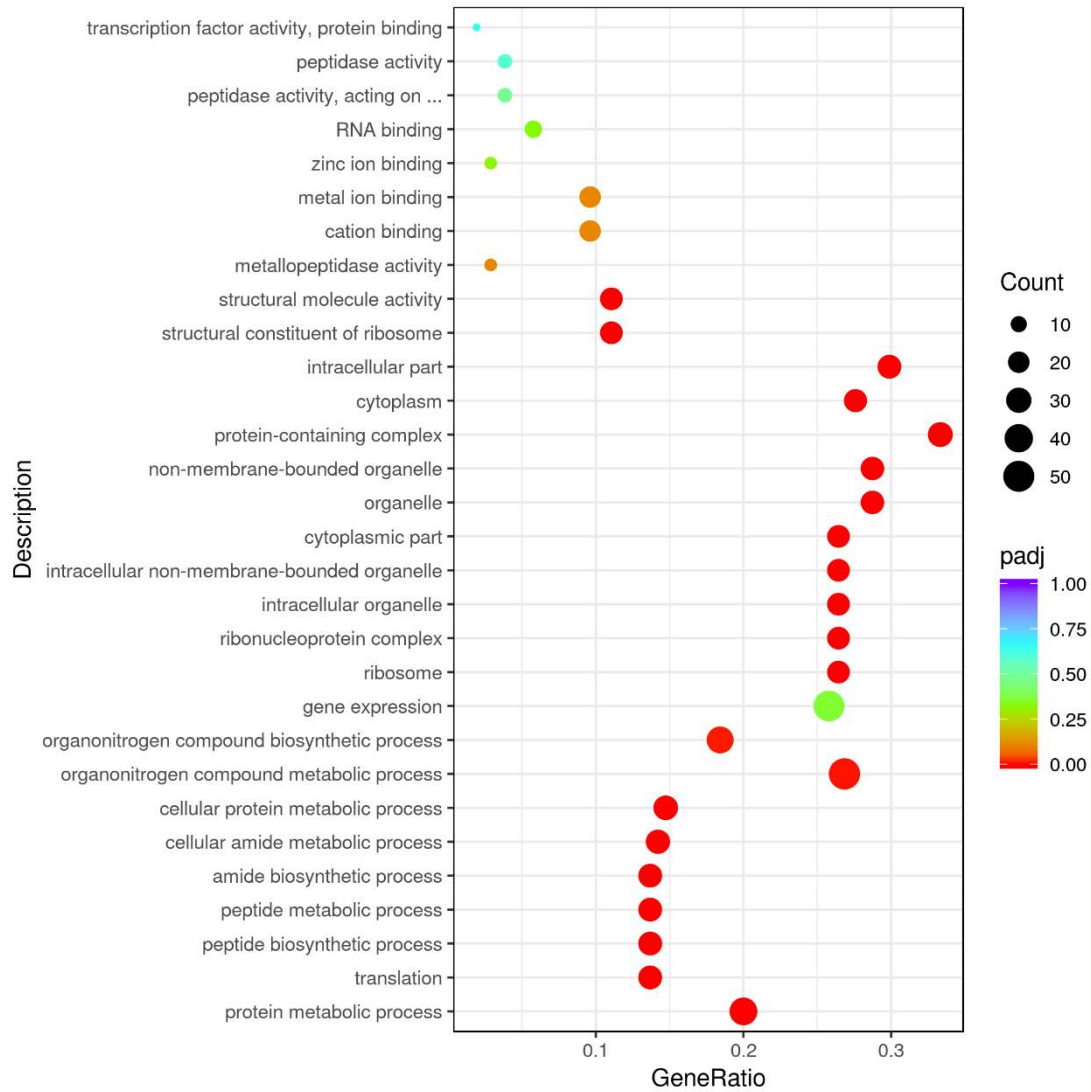
886

887 **Supplementary Fig. 26. Up-regulation Go enrichment (histogram) based on the**

888 **transcriptomic analysis of PET degradation by *Halomonas* sp. for 14 d. The**

889 numbers above the column are corresponding genes number related to different

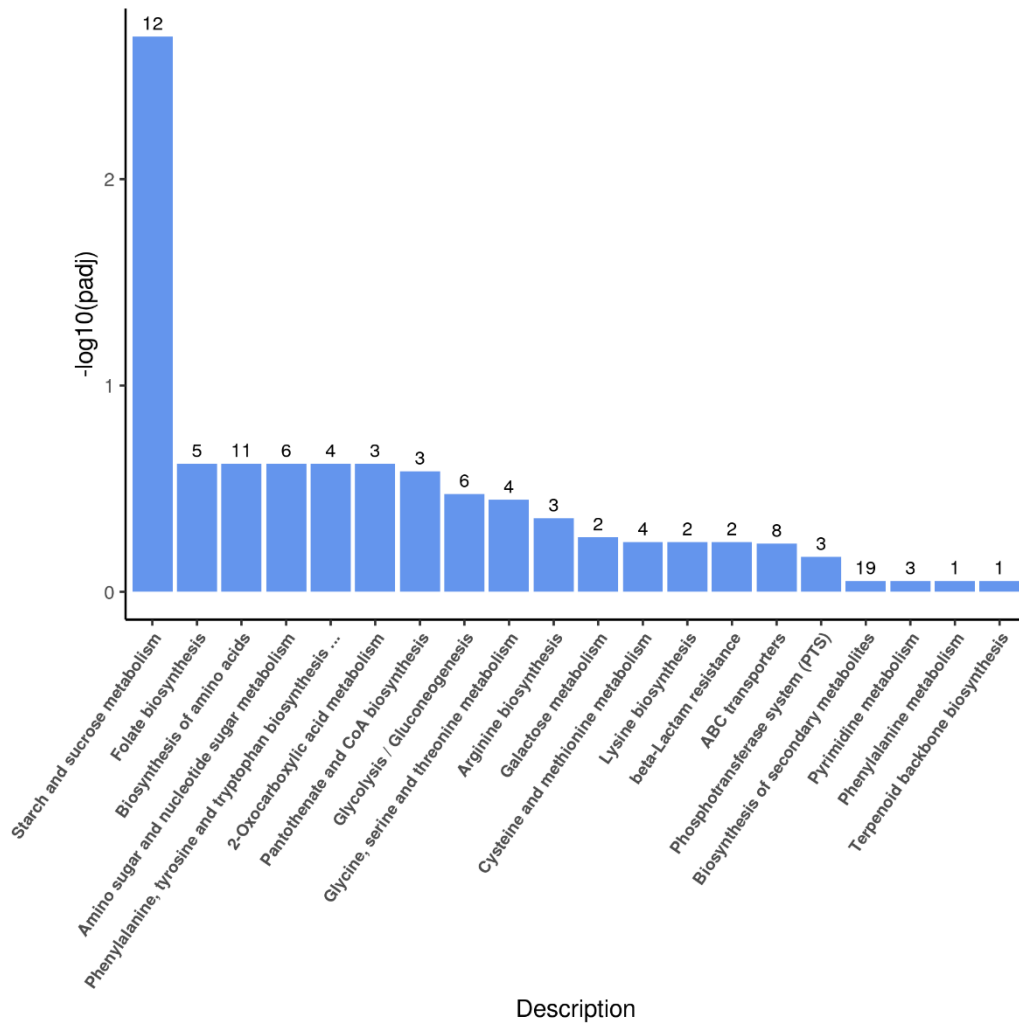
890 pathways.



891

892 **Supplementary Fig. 27. Up-regulation GO enrichment (scatter plot) based on the**

893 **transcriptomic analysis of PET degradation by *Halomonas* sp. for 14 d.**



894

895

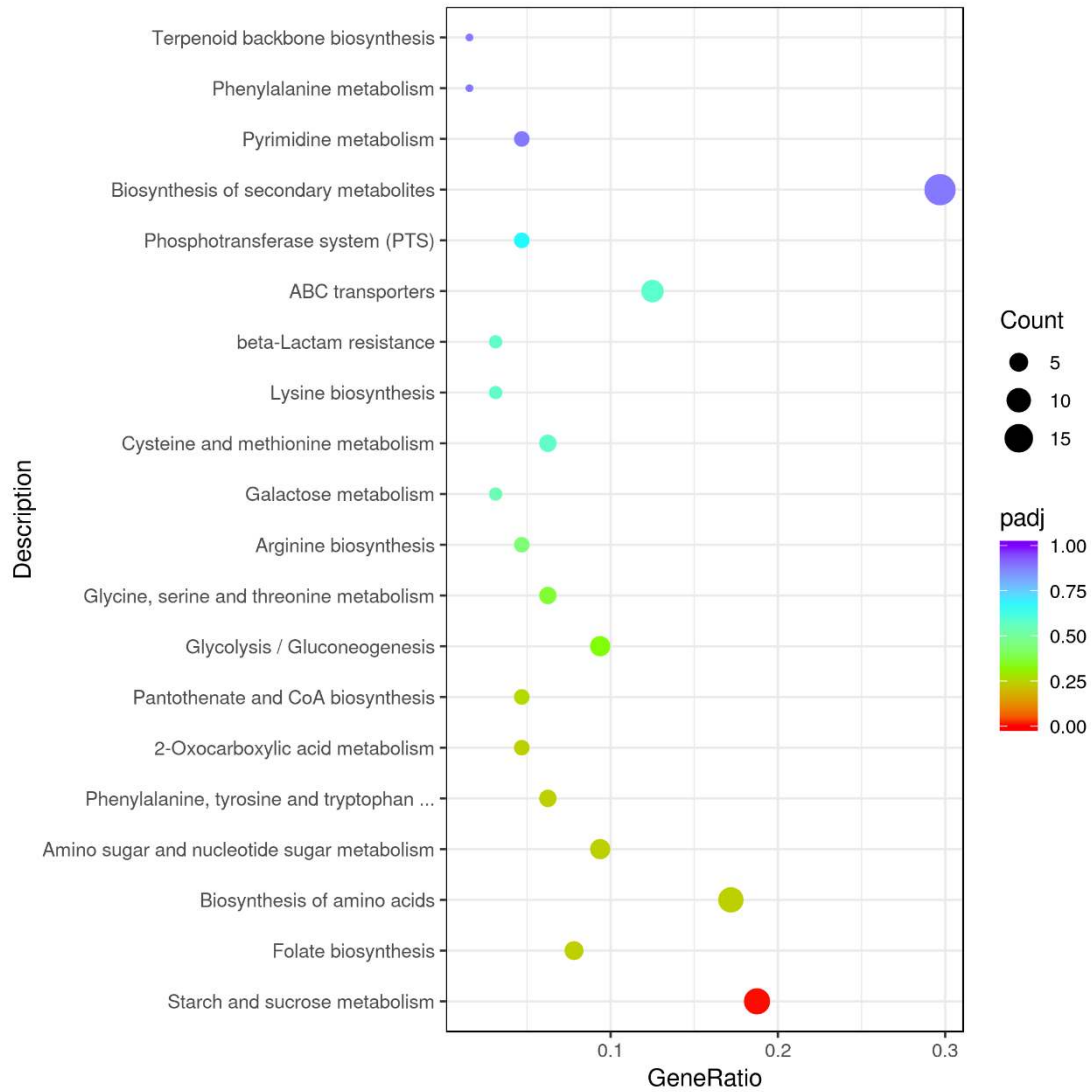
896 **Supplementary Fig. 28. Up-regulation KEGG pathways enrichment (histogram)**

897 **based on the transcriptomic analysis of PE degradation by *Exiguobacterium* sp.**

898 **for 8 h.** The numbers above the column are corresponding genes number related to

899 different pathways.

900

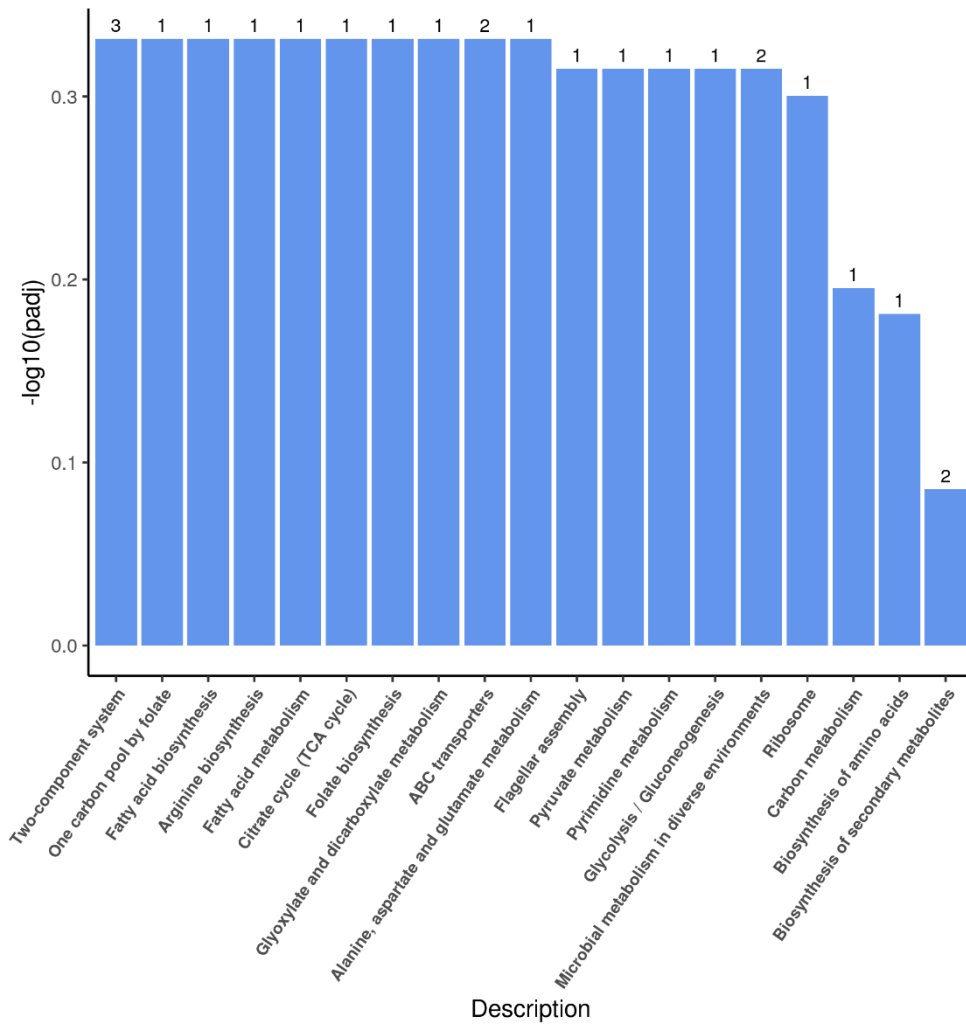


901

902 **Supplementary Fig. 29. Up-regulation KEGG pathways enrichment (scatter plot)**

903 **based on the transcriptomic analysis of PE degradation by *Exiguobacterium* sp.**

904 **for 8 h.**



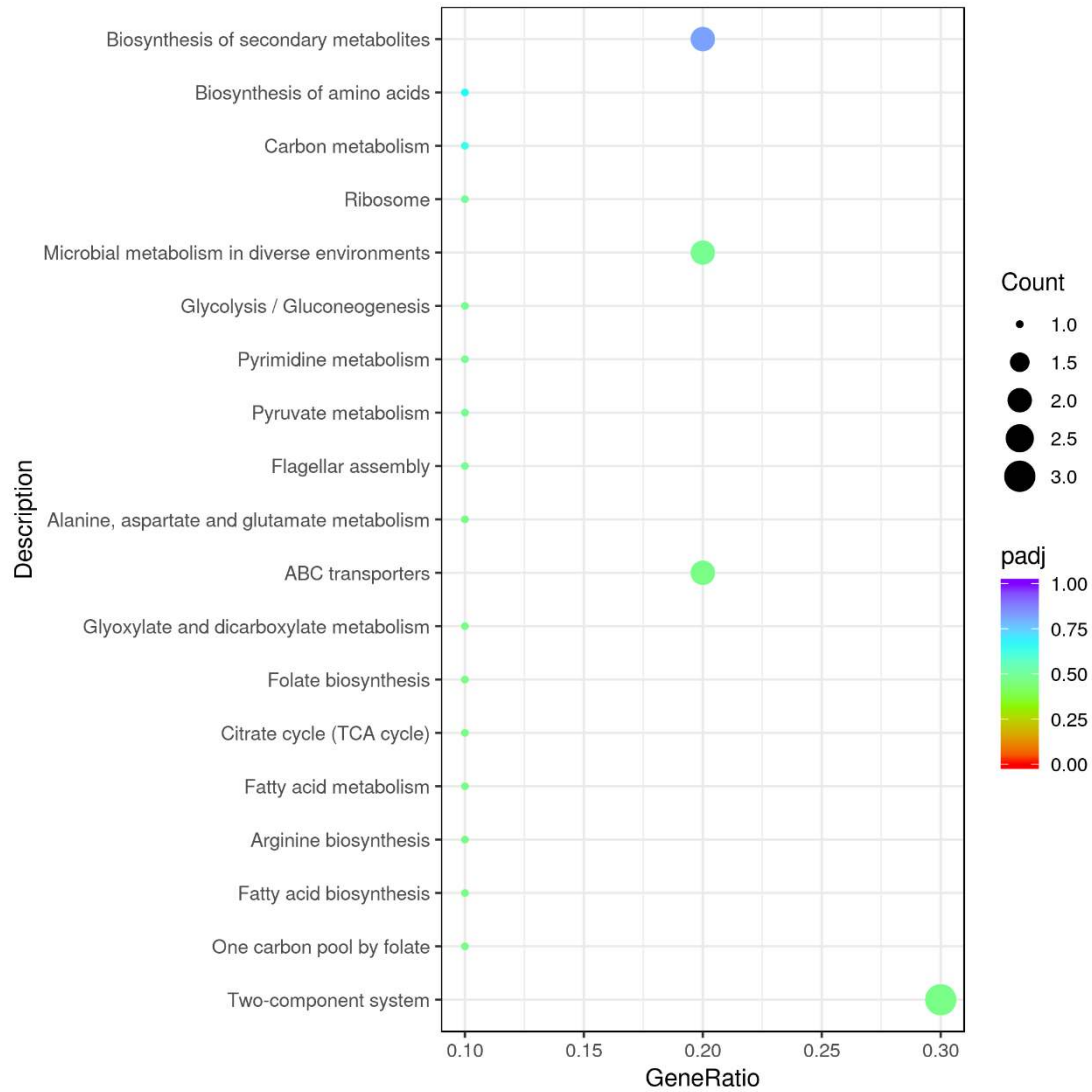
905

906 **Supplementary Fig. 30. Up-regulation KEGG pathways enrichment (histogram)**

907 **based on the transcriptomic analysis of PE degradation by *Exiguobacterium* sp.**

908 **for 7 d.** The numbers above the column are corresponding genes number related to

909 different pathways.



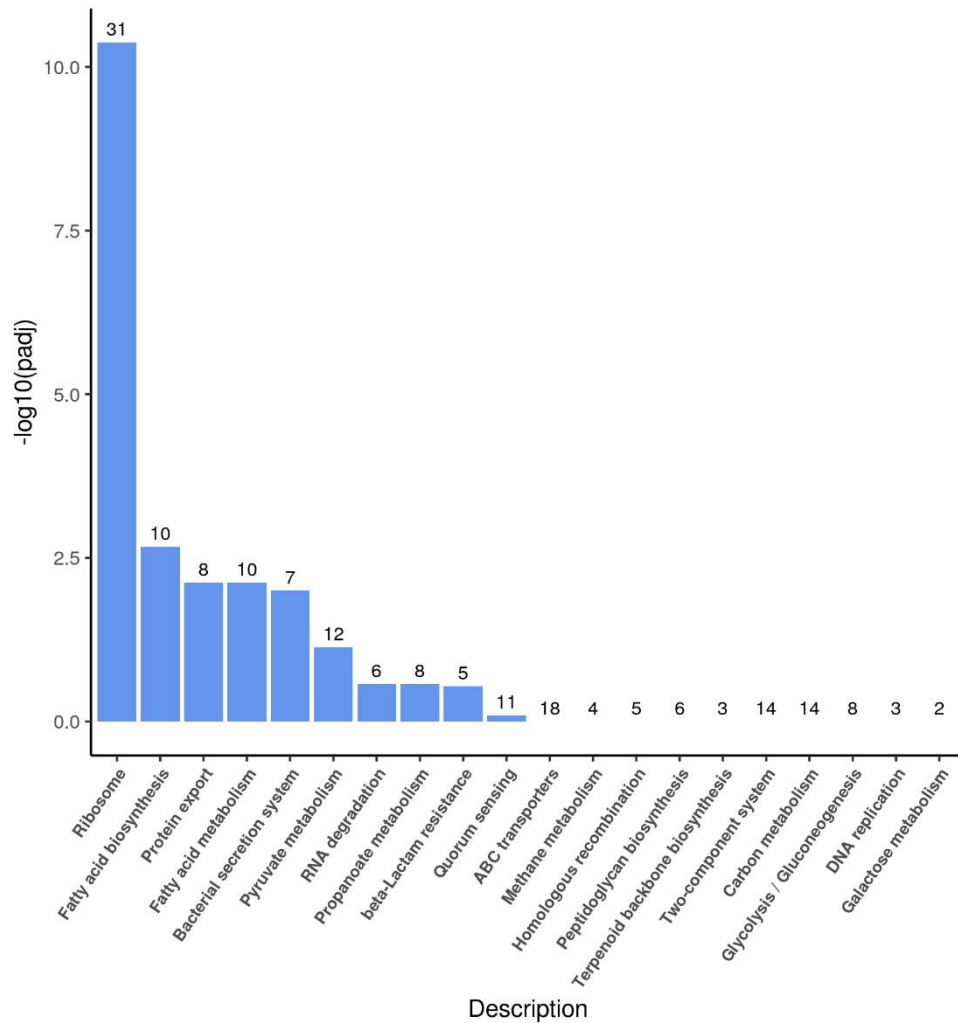
910

911 **Supplementary Fig. 31. Up-regulation KEGG pathways enrichment (scatter plot)**

912 **based on the transcriptomic analysis of PE degradation by *Exiguobacterium* sp.**

913 **for 7 d.**

914



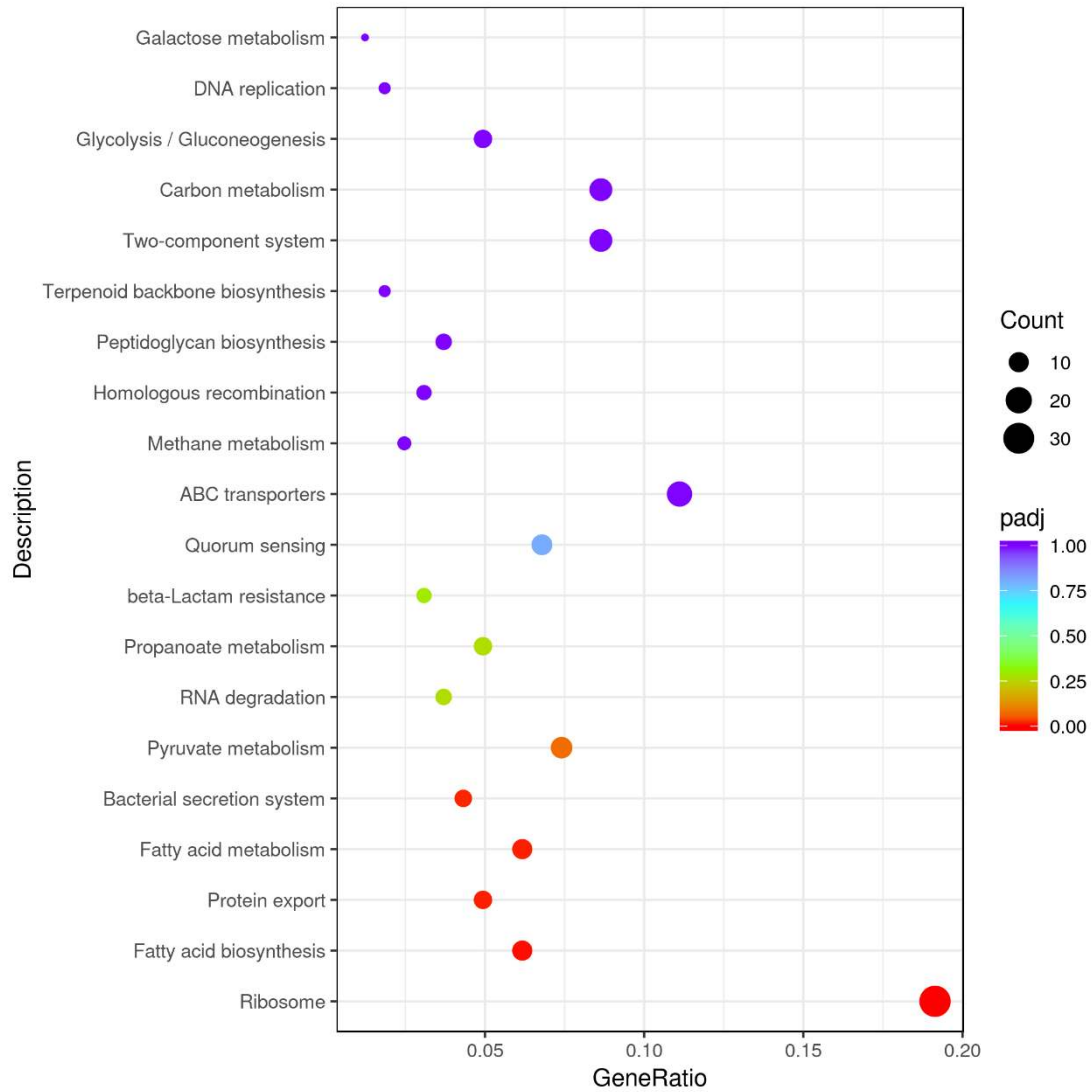
915

916 **Supplementary Fig. 32. Up-regulation KEGG pathways enrichment (histogram)**

917 **based on the transcriptomic analysis of PE degradation by *Exiguobacterium* sp.**

918 **for 14 d.** The numbers above the column are corresponding genes number related to

919 different pathways.

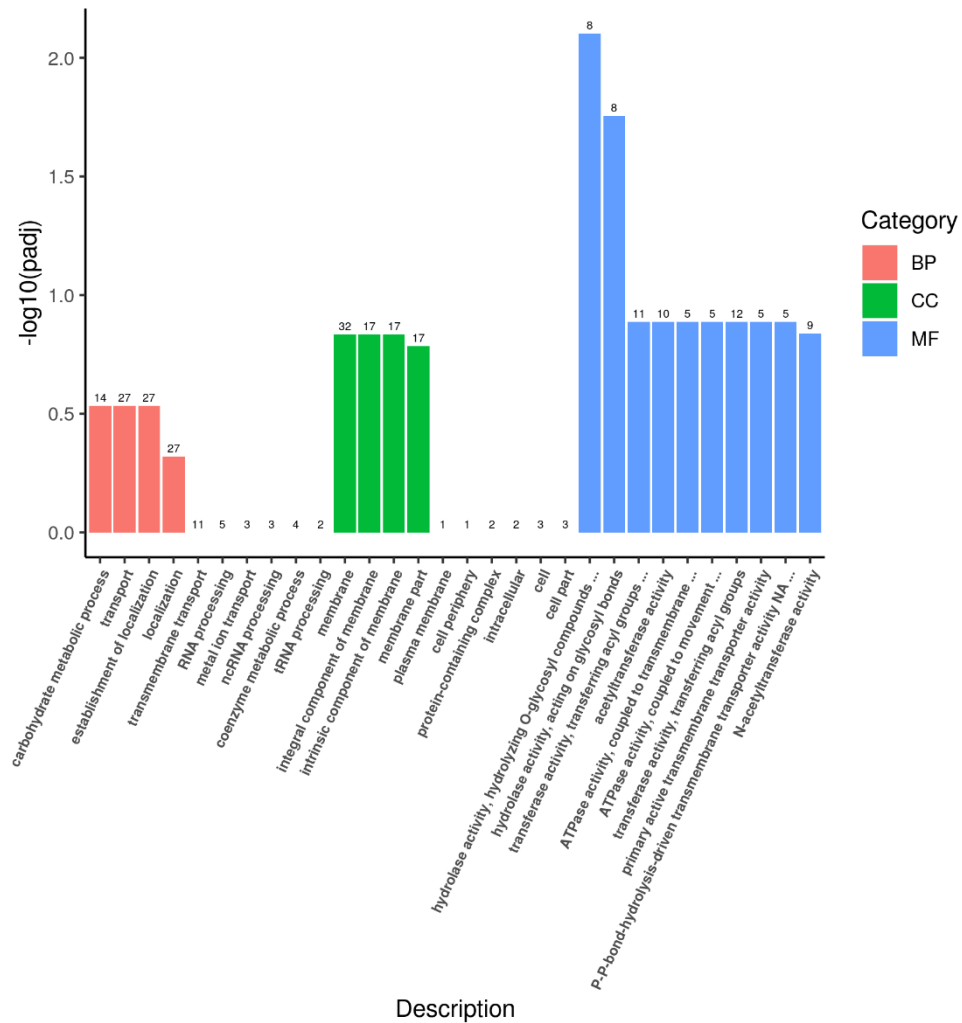


920

921 **Supplementary Fig. 33. Up-regulation KEGG pathways enrichment (scatter plot)**

922 **based on the transcriptomic analysis of PE degradation by *Exiguobacterium* sp.**

923 **for 14 d.**



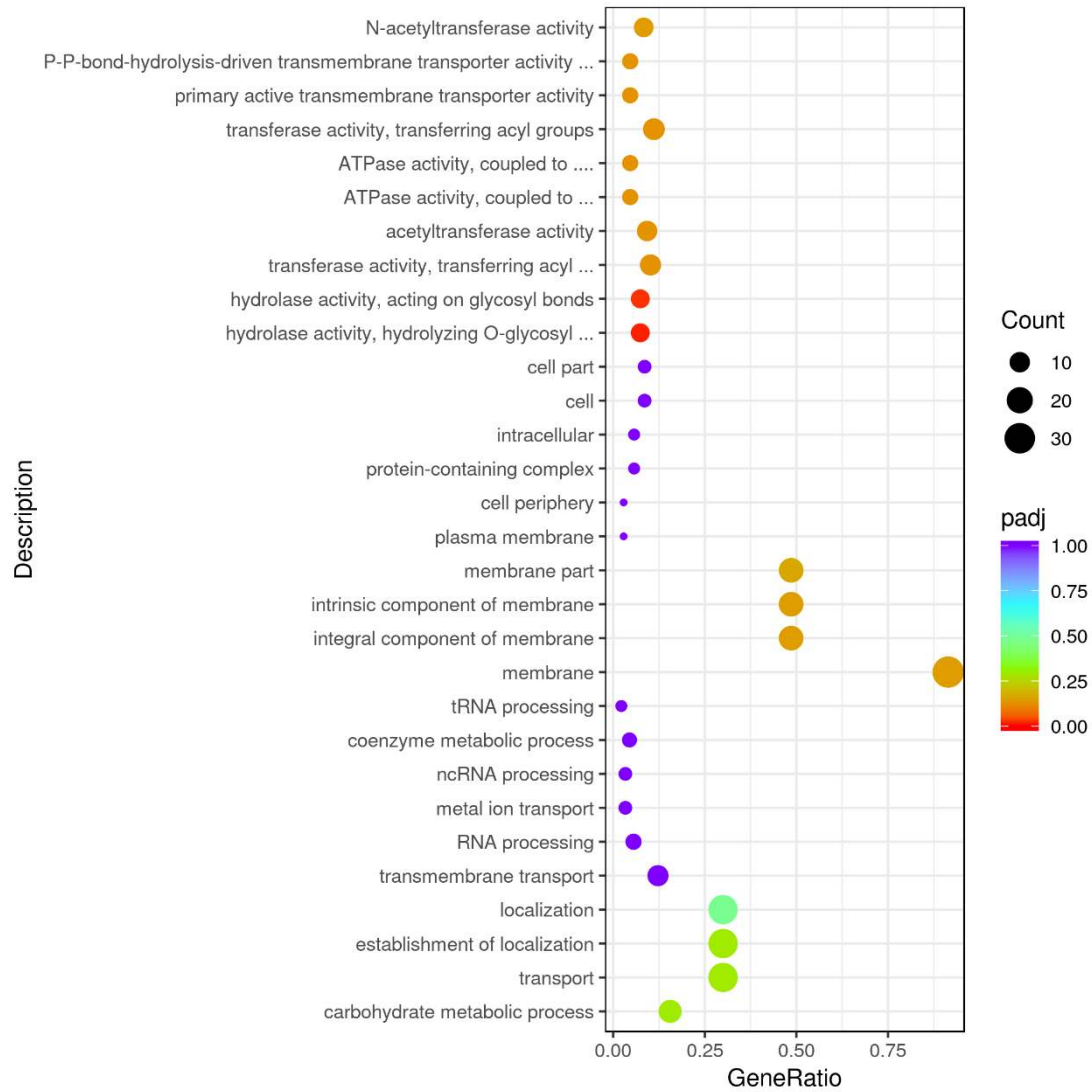
924

925 **Supplementary Fig. 34. Up-regulation Go enrichment (histogram) based on the**

926 **transcriptomic analysis of PE degradation by *Exiguobacterium* sp. for 8 h.** The

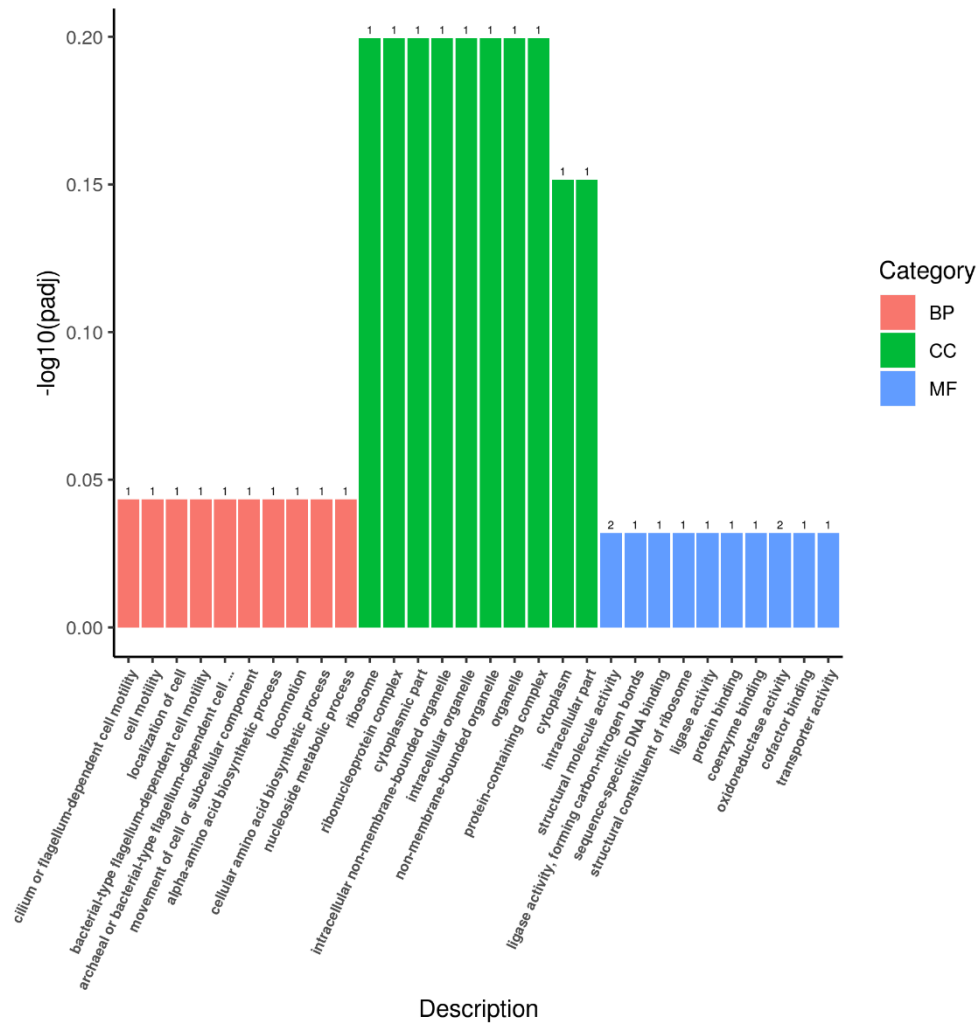
927 numbers above the column are corresponding genes number related to different

928 pathways.



929

930 **Supplementary Fig. 35. Up-regulation GO enrichment (scatter plot) based on the**
 931 **transcriptomic analysis of PE degradation by *Exiguobacterium* sp. for 8 h.**



932

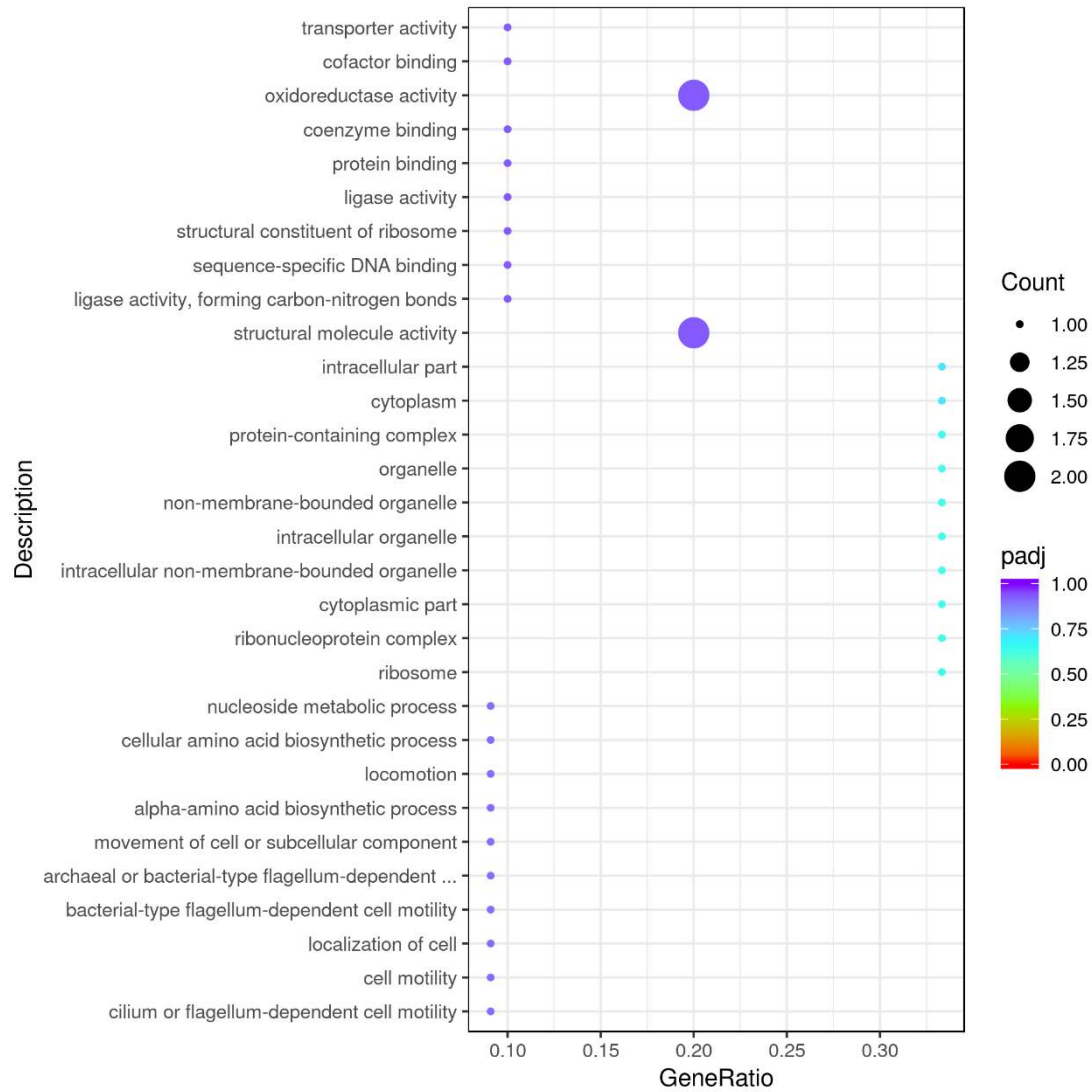
933 **Supplementary Fig. 36. Up-regulation Go enrichment (histogram) based on the**

934 **transcriptomic analysis of PE degradation by *Exiguobacterium* sp. for 7 d. The**

935 numbers above the column are corresponding genes number related to different

936 pathways.

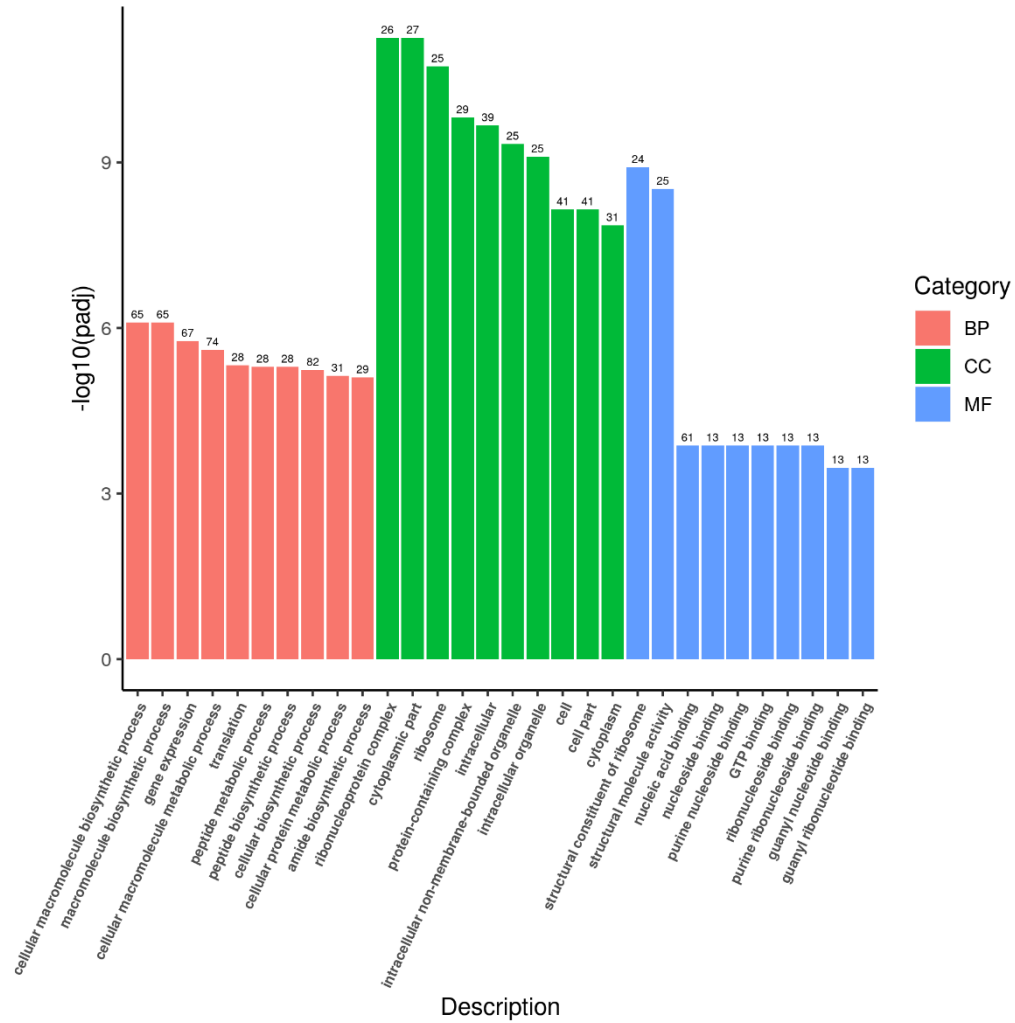
937



938

939 **Supplementary Fig. 37. Up-regulation GO enrichment (scatter plot) based on the**

940 **transcriptomic analysis of PE degradation by *Exiguobacterium* sp. for 7 d.**



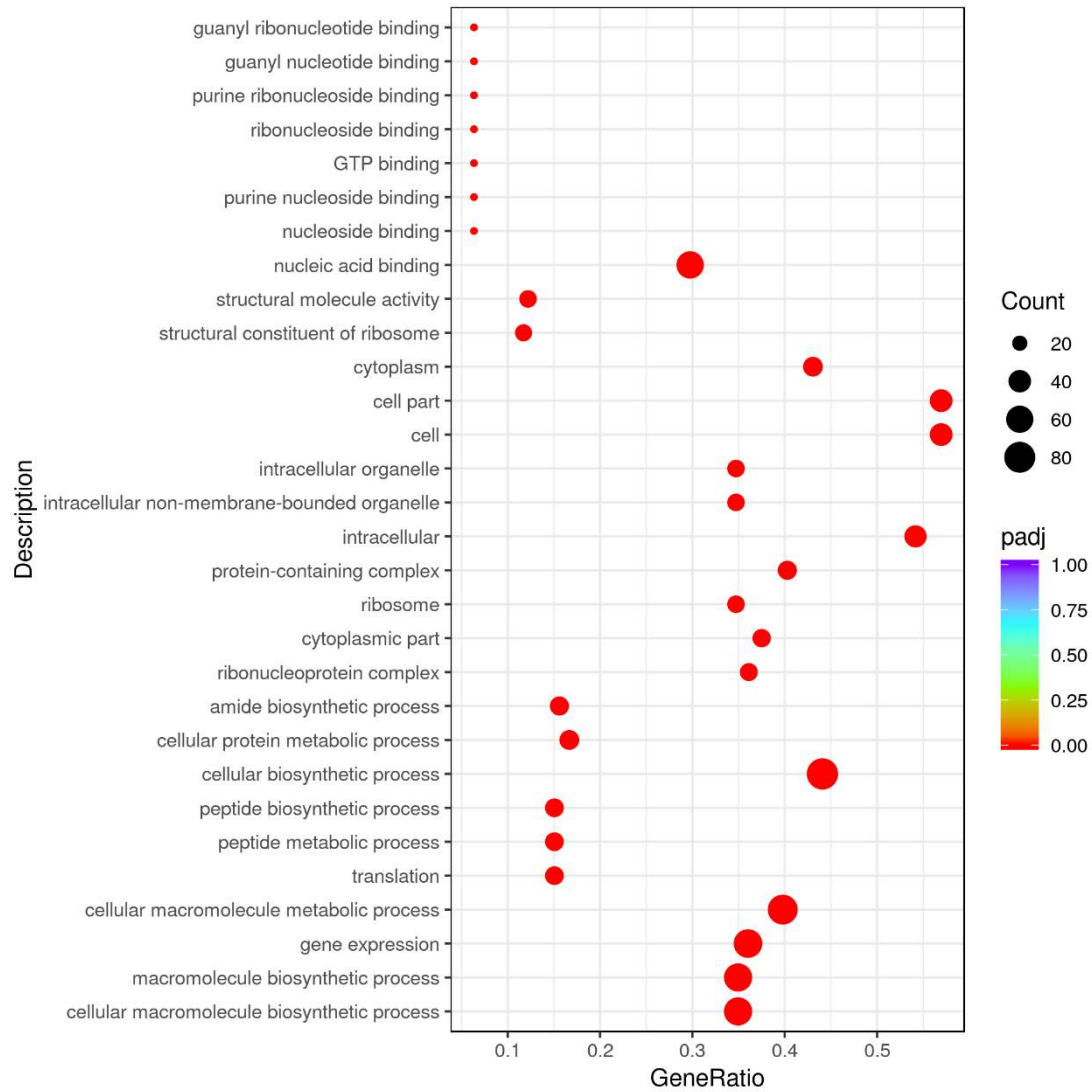
941

942 **Supplementary Fig. 38. Up-regulation Go enrichment (histogram) based on the**

943 **transcriptomic analysis of PE degradation by *Exiguobacterium* sp. for 14 d. The**

944 numbers above the column are corresponding genes number related to different

945 pathways.

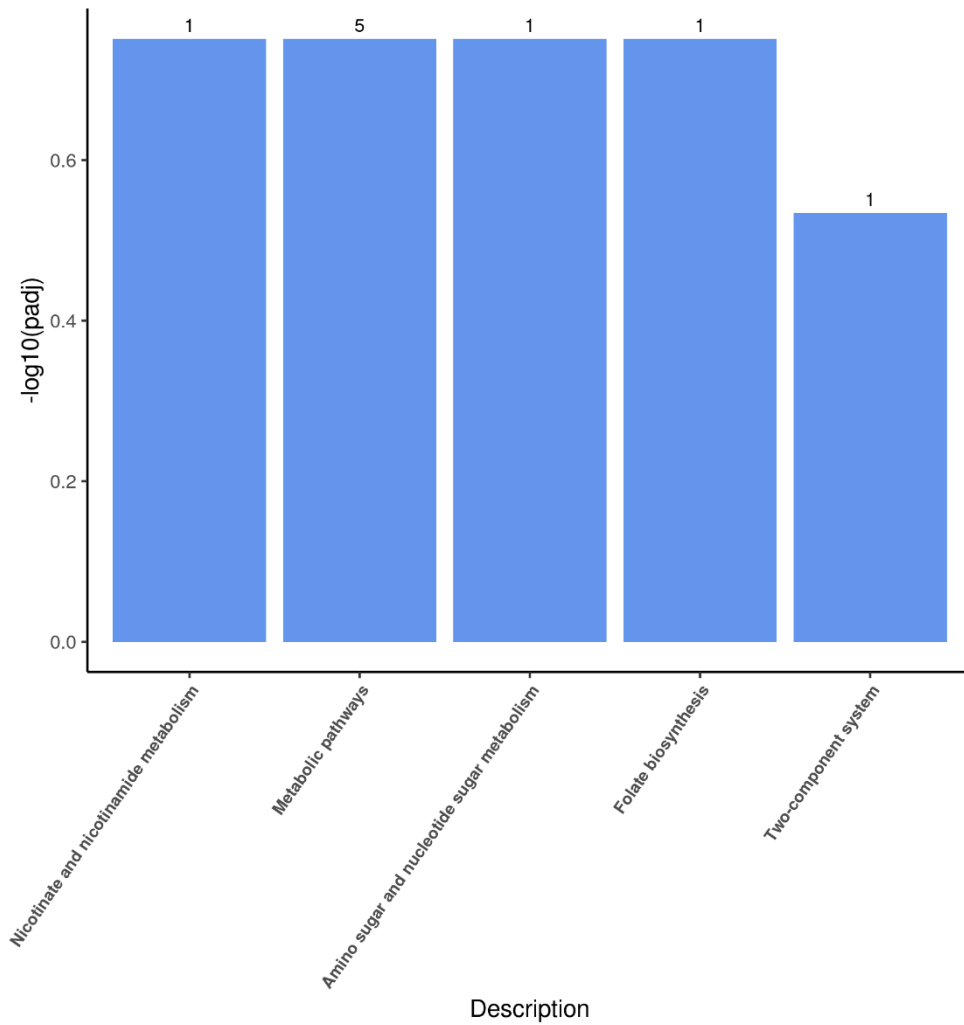


946

947 **Supplementary Fig. 39. Up-regulation GO enrichment (scatter plot) based on the**

948 **transcriptomic analysis of PE degradation by *Exiguobacterium* sp. for 14 d.**

949



950

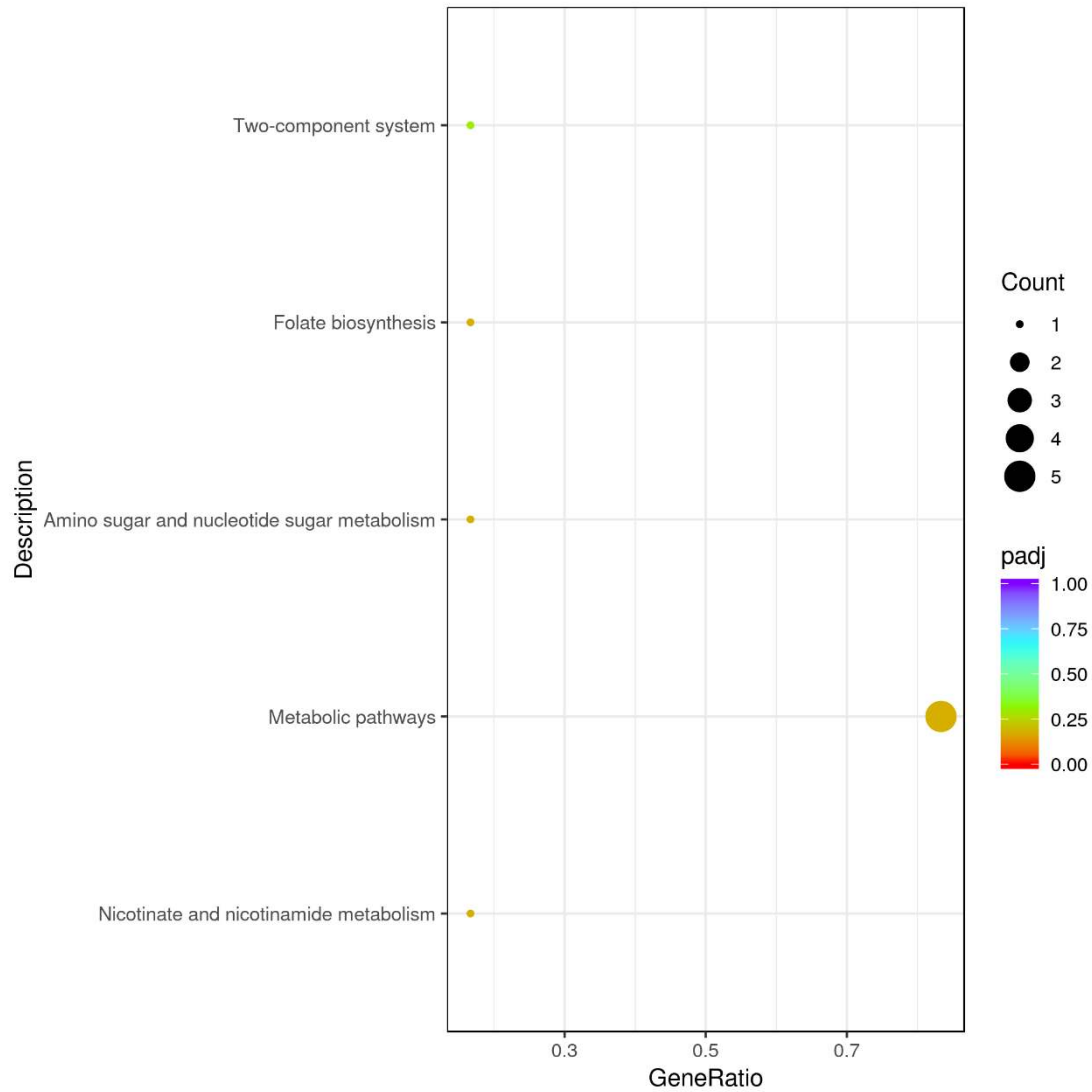
951 **Supplementary Fig. 40. Up-regulation KEGG pathways enrichment (histogram)**

952 **based on the transcriptomic analysis of PE degradation by *Halomonas* sp. for 8 h.**

953 The numbers above the column are corresponding genes number related to different

954 pathways.

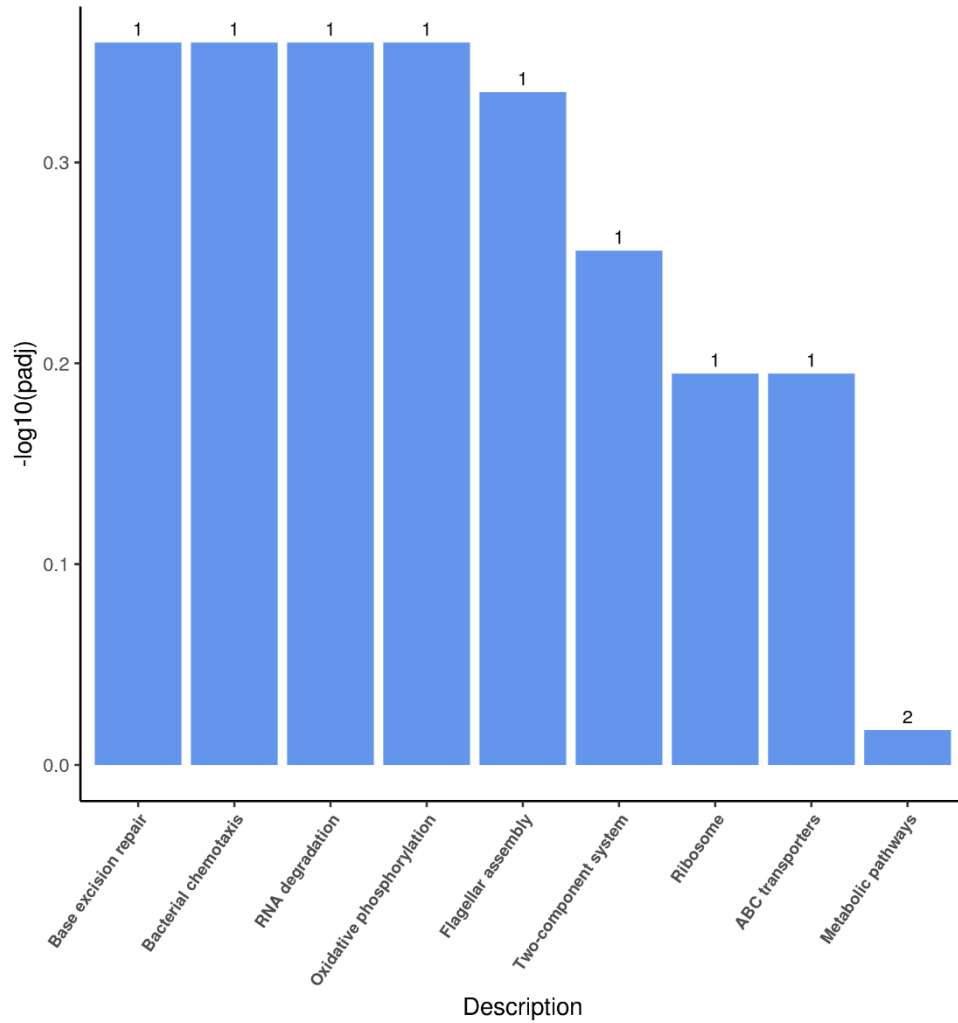
955



956

957 **Supplementary Fig. 41. Up-regulation KEGG pathways enrichment (scatter plot)**

958 **based on the transcriptomic analysis of PE degradation by *Halomonas* sp. for 8 h.**



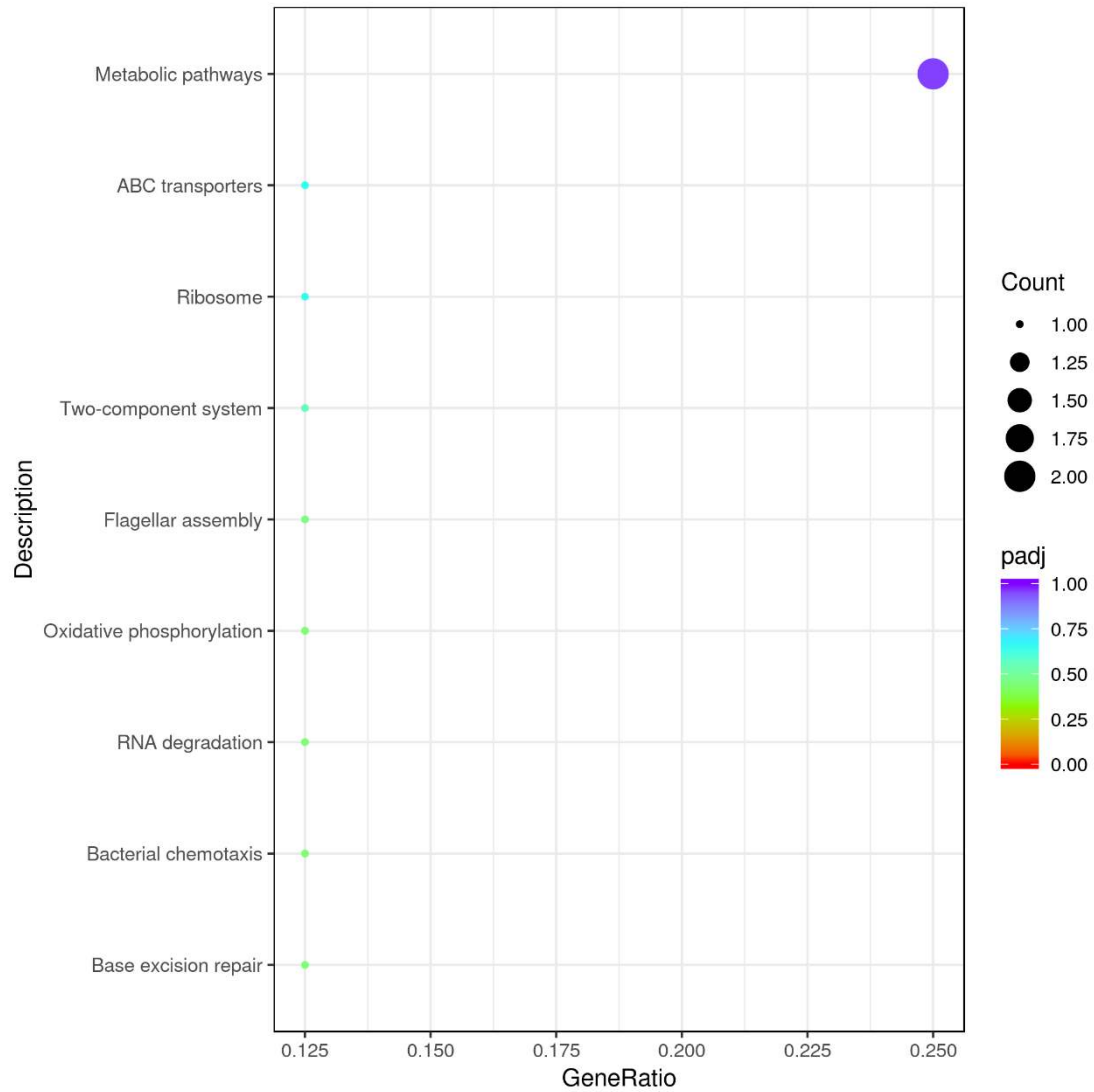
959

960 **Supplementary Fig. 42. Up-regulation KEGG pathways enrichment (histogram)**

961 **based on the transcriptomic analysis of PE degradation by *Halomonas* sp. for 7 d.**

962 The numbers above the column are corresponding genes number related to different

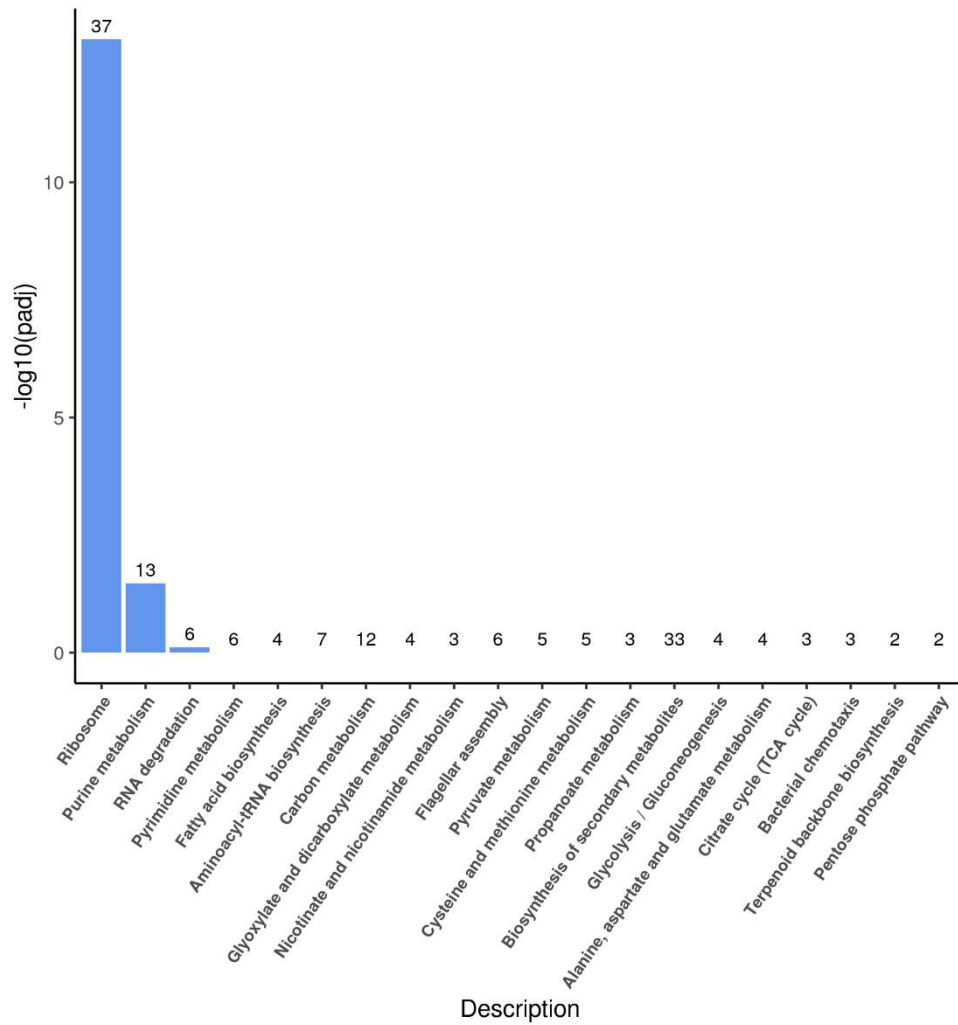
963 pathways.



964

965 **Supplementary Fig. 43. Up-regulation KEGG pathways enrichment (scatter plot)**

966 **based on the transcriptomic analysis of PE degradation by *Halomonas* sp. for 7 d.**



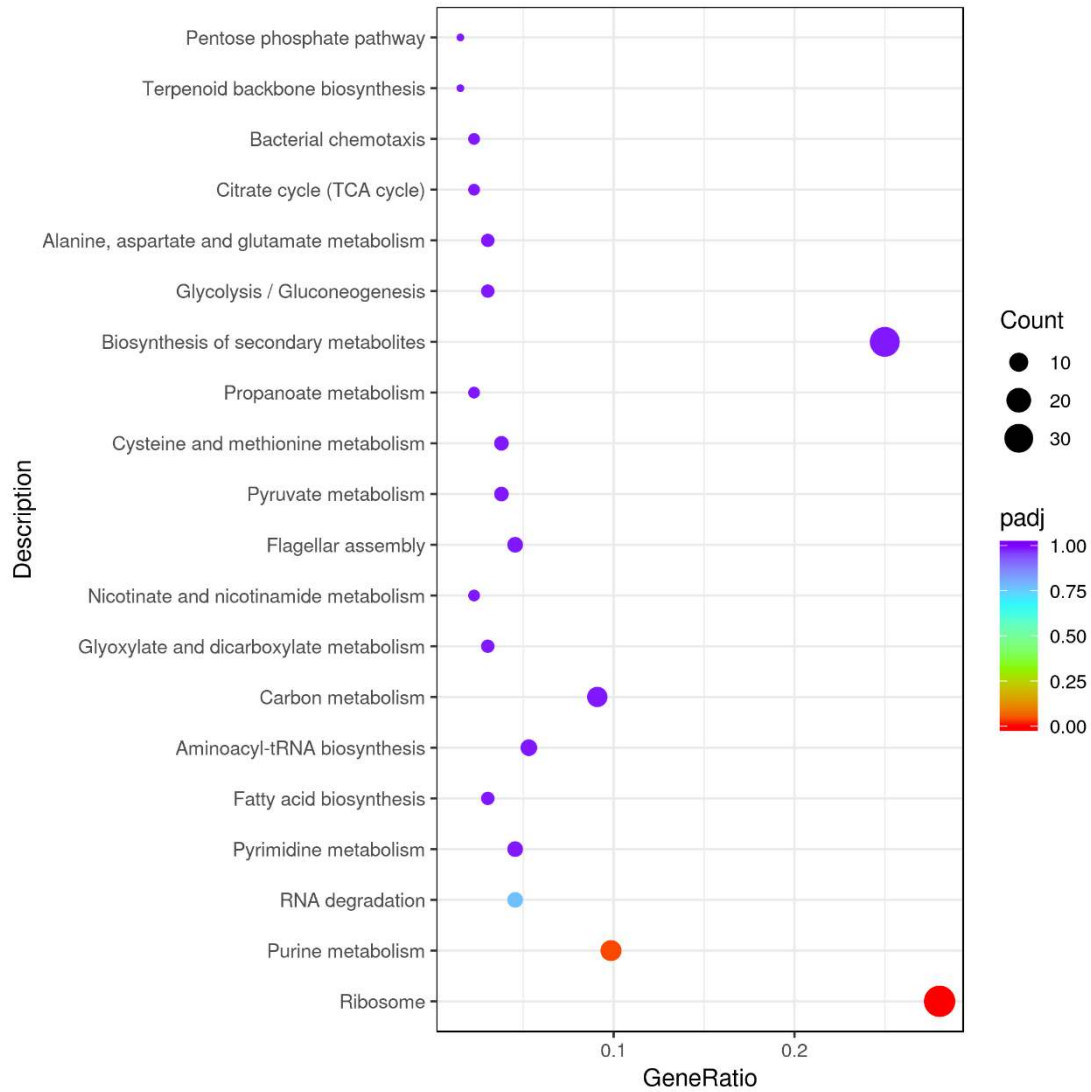
967

968 **Supplementary Fig. 44. Up-regulation KEGG pathways enrichment (histogram)**

969 **based on the transcriptomic analysis of PE degradation by *Halomonas* sp. for 14**

970 **d.** The numbers above the column are corresponding genes number related to different

971 pathways.



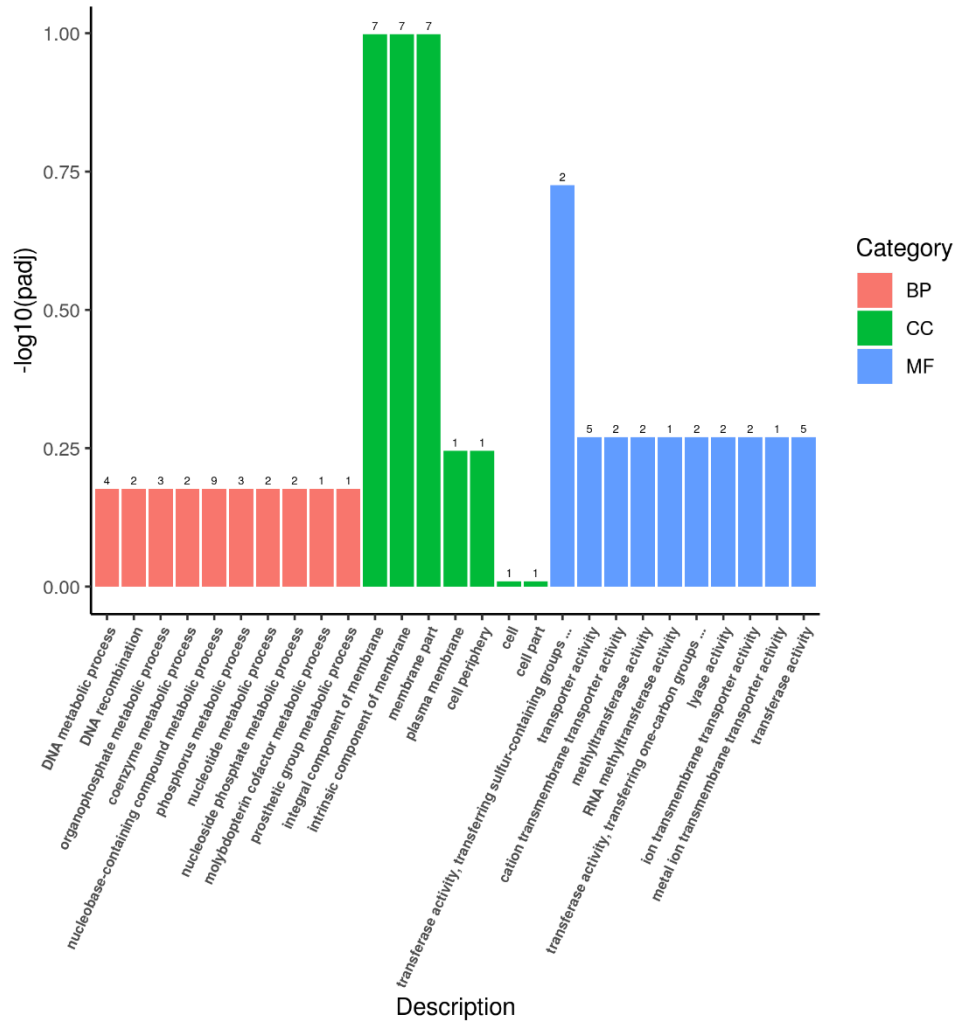
972

973 **Supplementary Fig. 45. Up-regulation KEGG pathways enrichment (scatter plot)**

974 **based on the transcriptomic analysis of PE degradation by *Halomonas* sp. for 14**

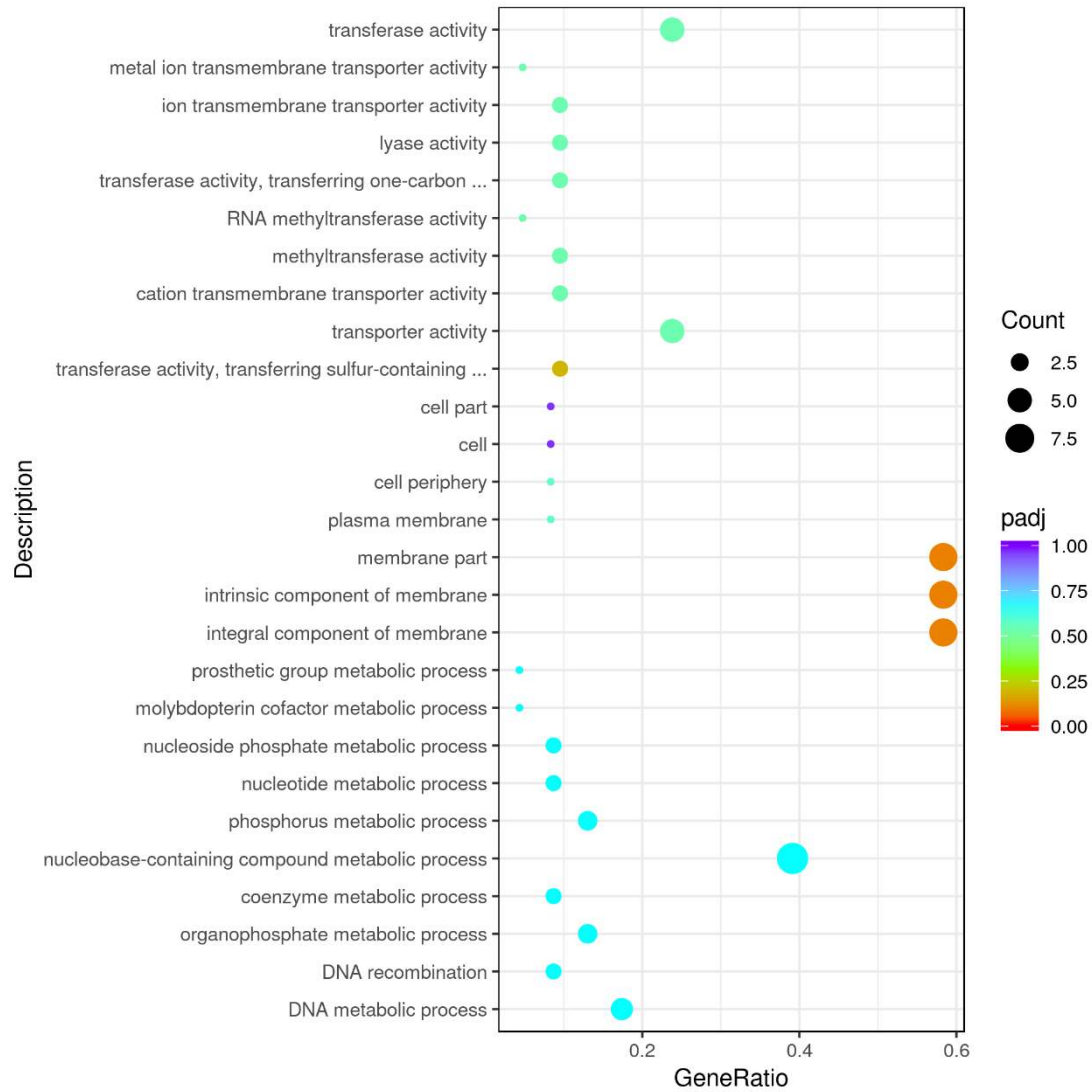
975 **d.**

976



977

978 **Supplementary Fig. 46. Up-regulation Go enrichment (histogram) based on the**
 979 **transcriptomic analysis of PE degradation by *Halomonas* sp. for 8 h.** The numbers
 980 above the column are corresponding genes number related to different pathways.



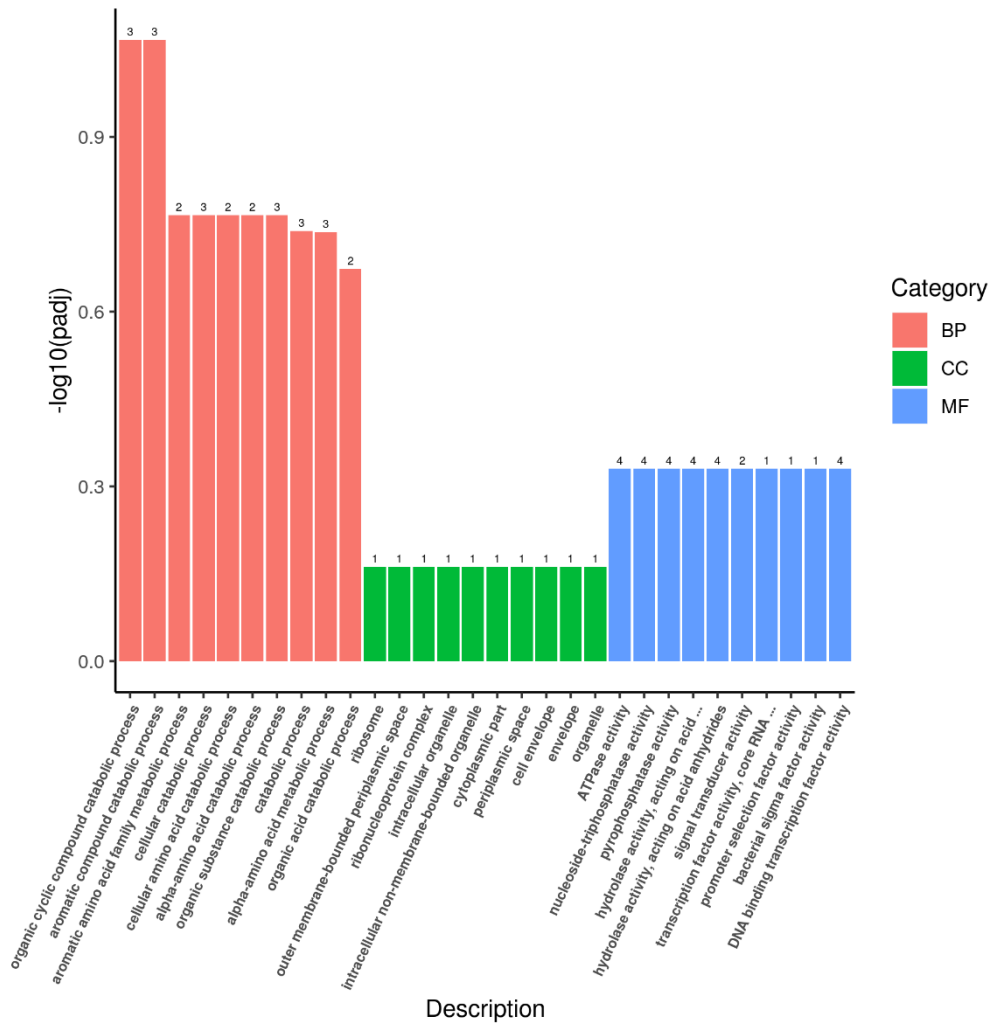
981

982 **Supplementary Fig. 47. Up-regulation GO enrichment (scatter plot) based on the**

983 **transcriptomic analysis of PE degradation by *Halomonas* sp. for 8 h.**

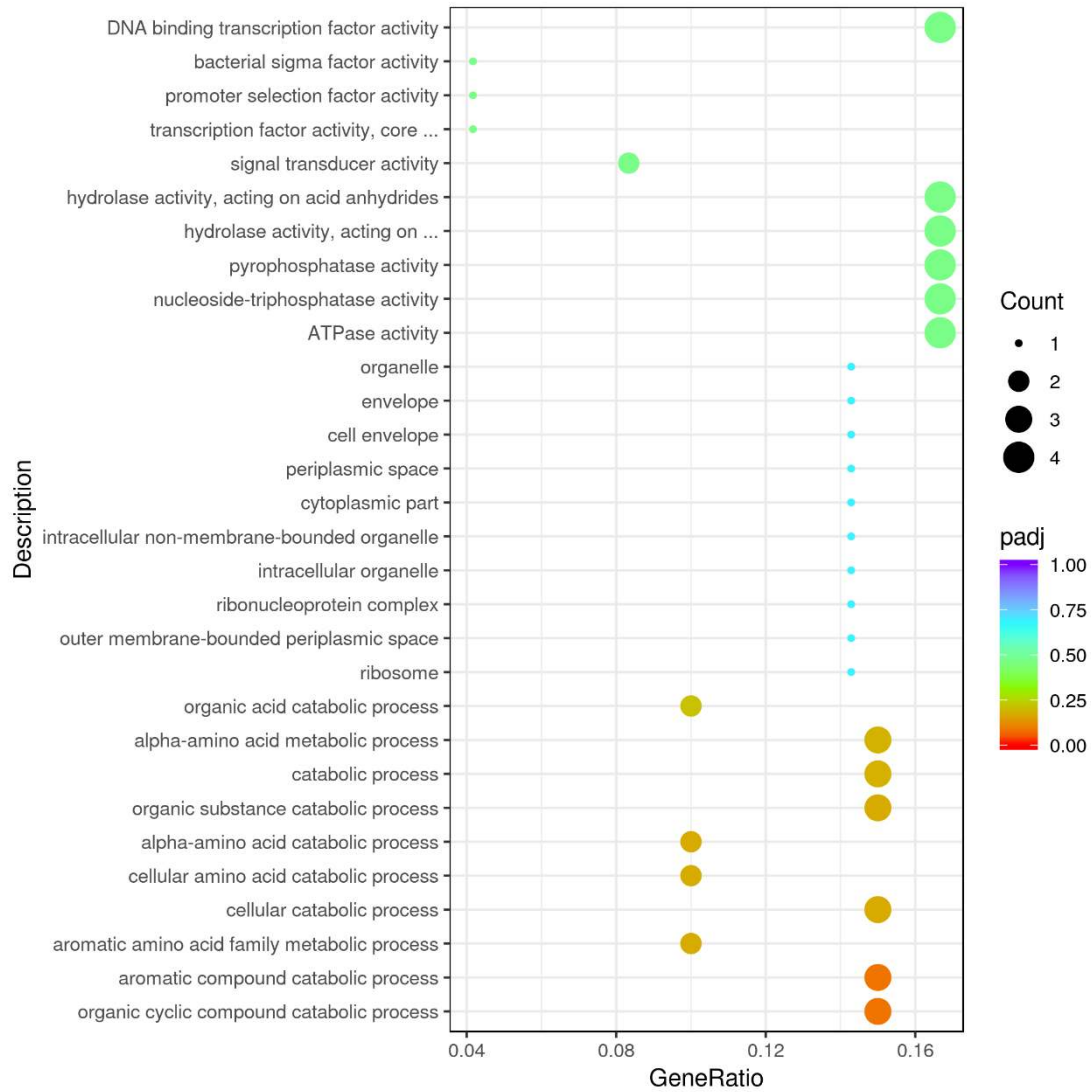
984

985



986

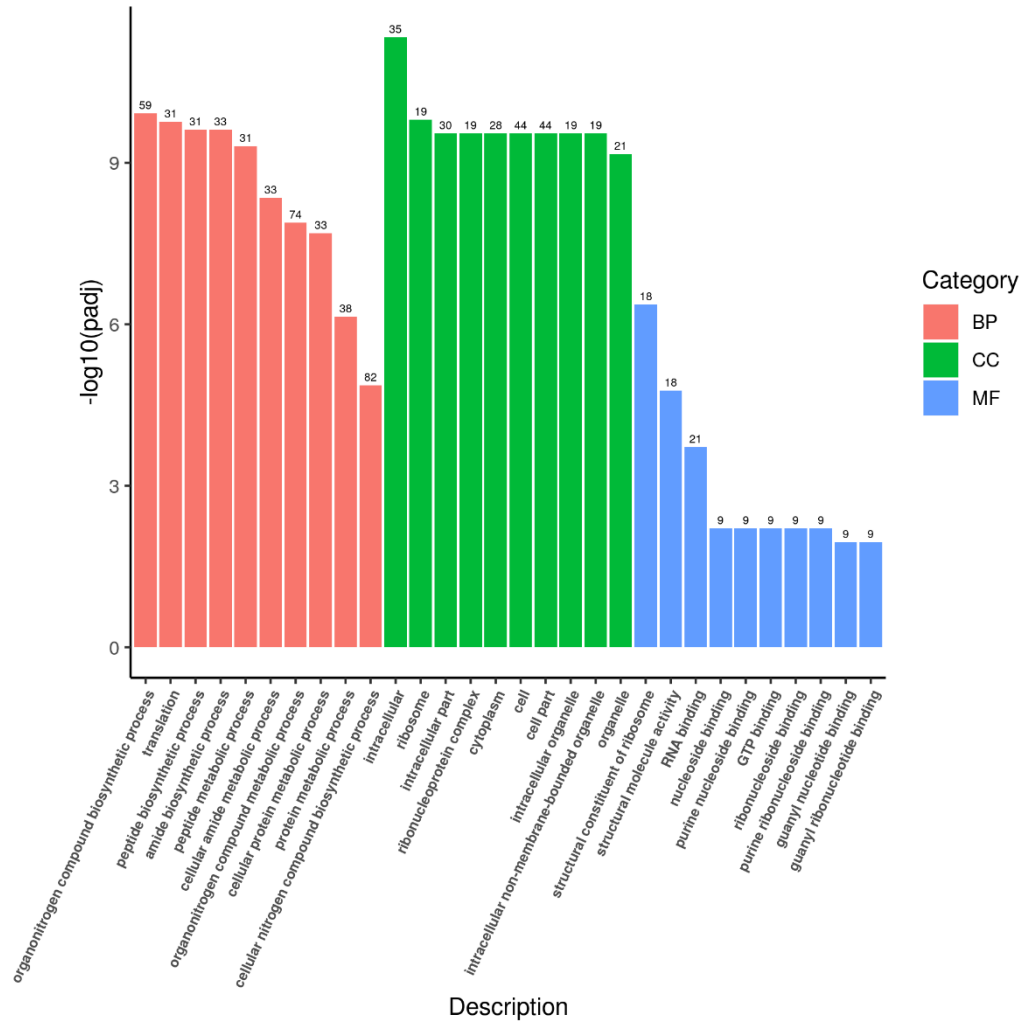
987 **Supplementary Fig. 48. Up-regulation Go enrichment (histogram) based on the**
 988 **transcriptomic analysis of PE degradation by *Halomonas* sp. for 7 d.** The numbers
 989 above the column are corresponding genes number related to different pathways.



990

991 **Supplementary Fig. 49. Up-regulation GO enrichment (scatter plot) based on the**

992 **transcriptomic analysis of PE degradation by *Halomonas* sp. for 7 d.**



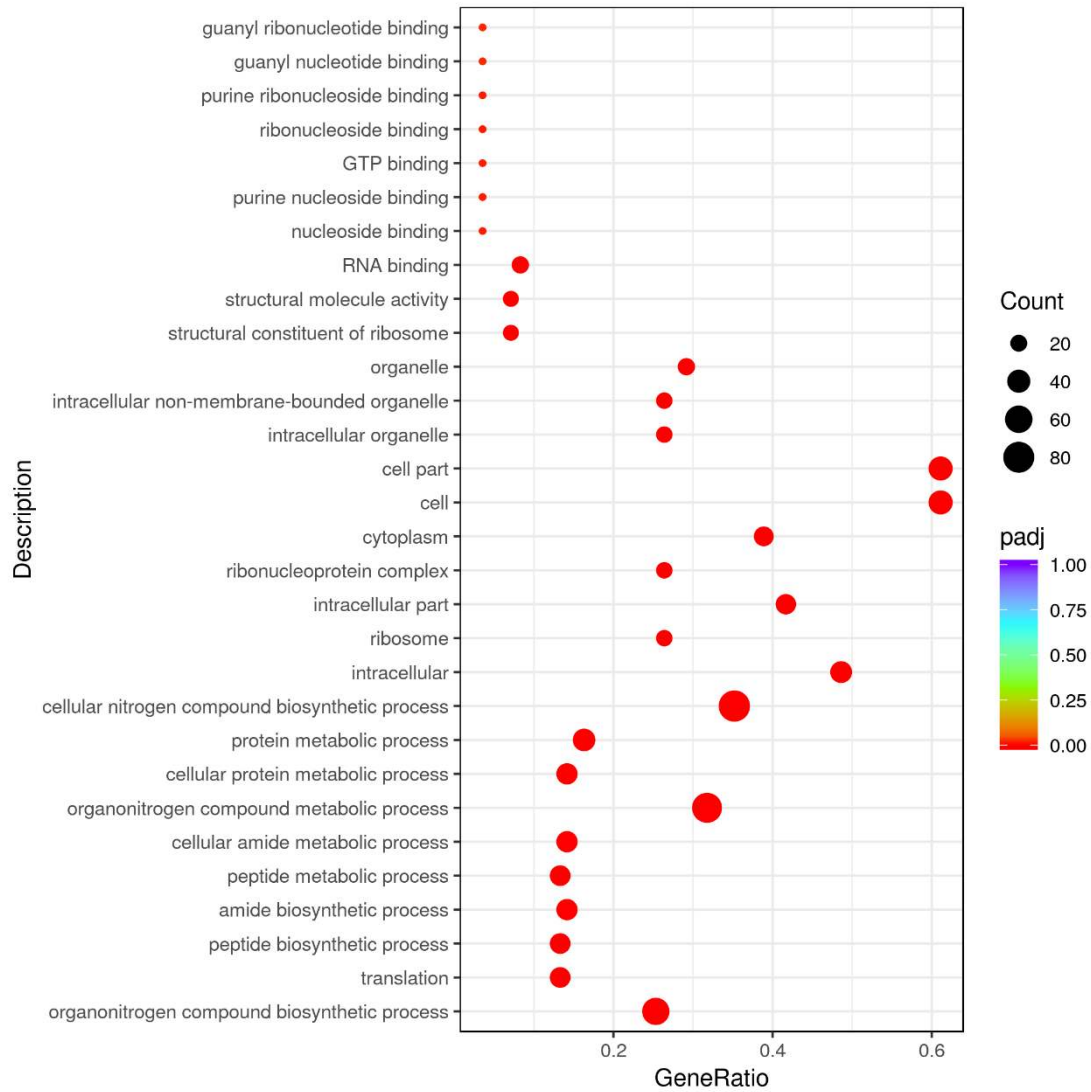
993

994 **Supplementary Fig. 50. Up-regulation Go enrichment (histogram) based on the**

995 **transcriptomic analysis of PE degradation by *Halomonas* sp. for 14 d. The**

996 numbers above the column are corresponding genes number related to different

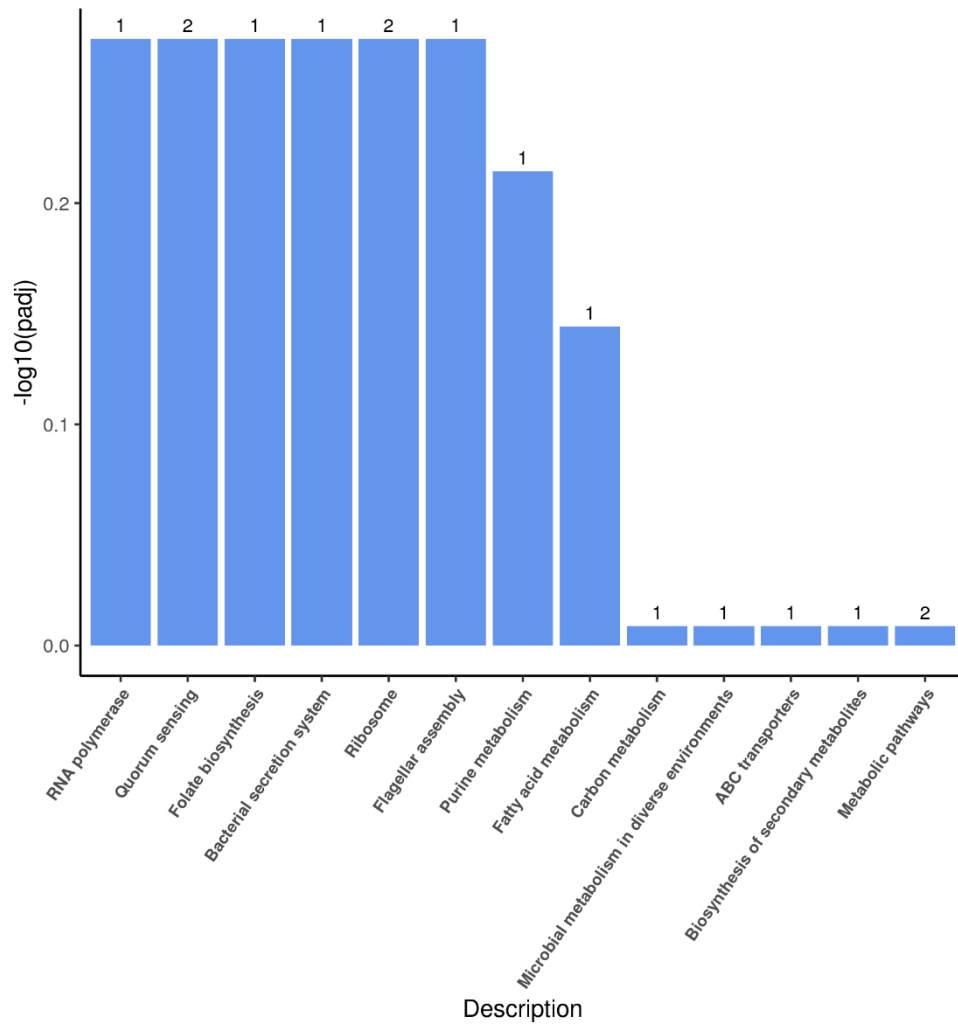
997 pathways.



998

999 **Supplementary Fig. 51. Up-regulation GO enrichment (scatter plot) based on the**

1000 **transcriptomic analysis of PE degradation by *Halomonas* sp. for 14 d.**



1001

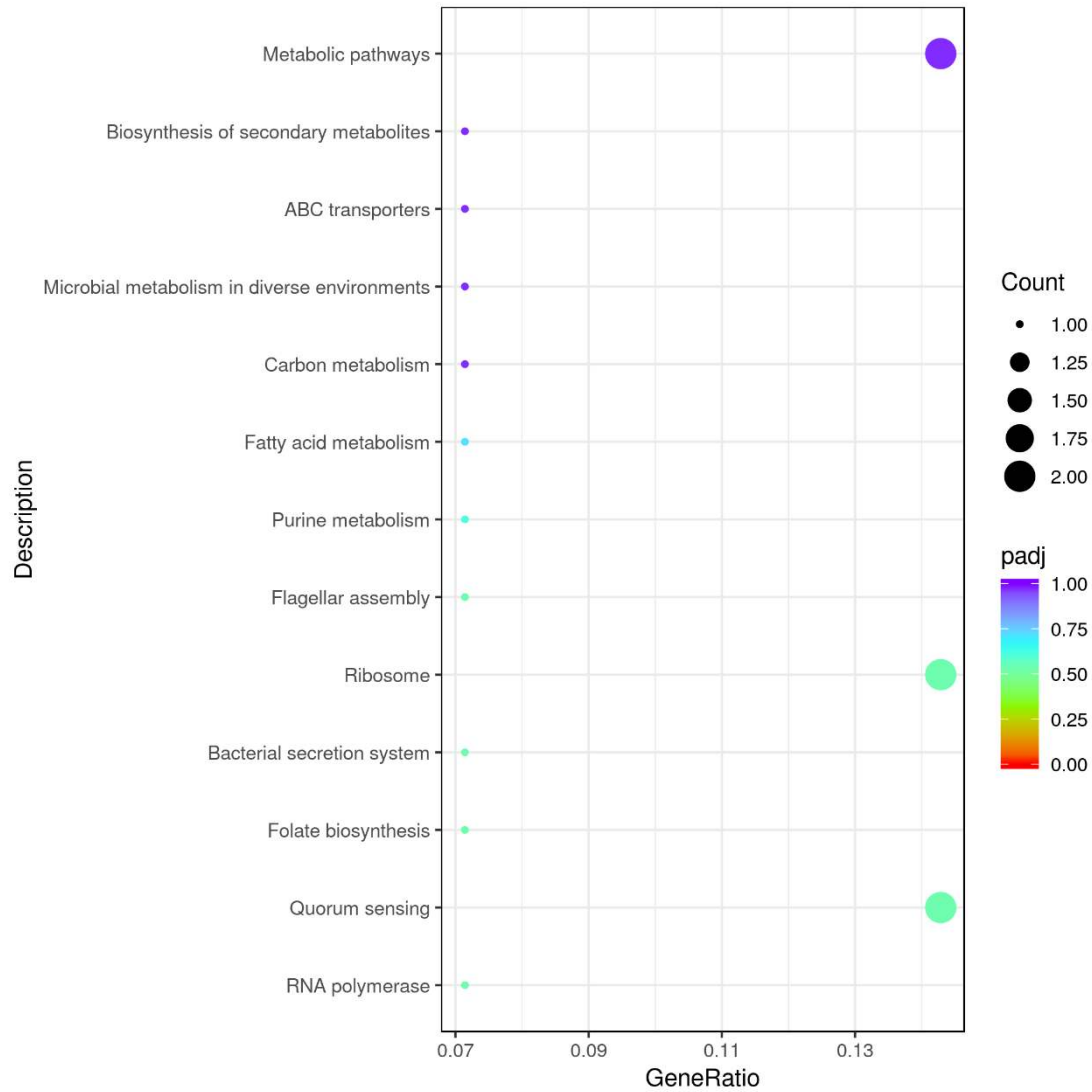
1002 **Supplementary Fig. 52. Up-regulation KEGG pathways enrichment (histogram)**

1003 **based on the transcriptomic analysis of PE degradation by *Ochrobactrum* sp. for**

1004 **8 h.** The numbers above the column are corresponding genes number related to

1005 different pathways.

1006

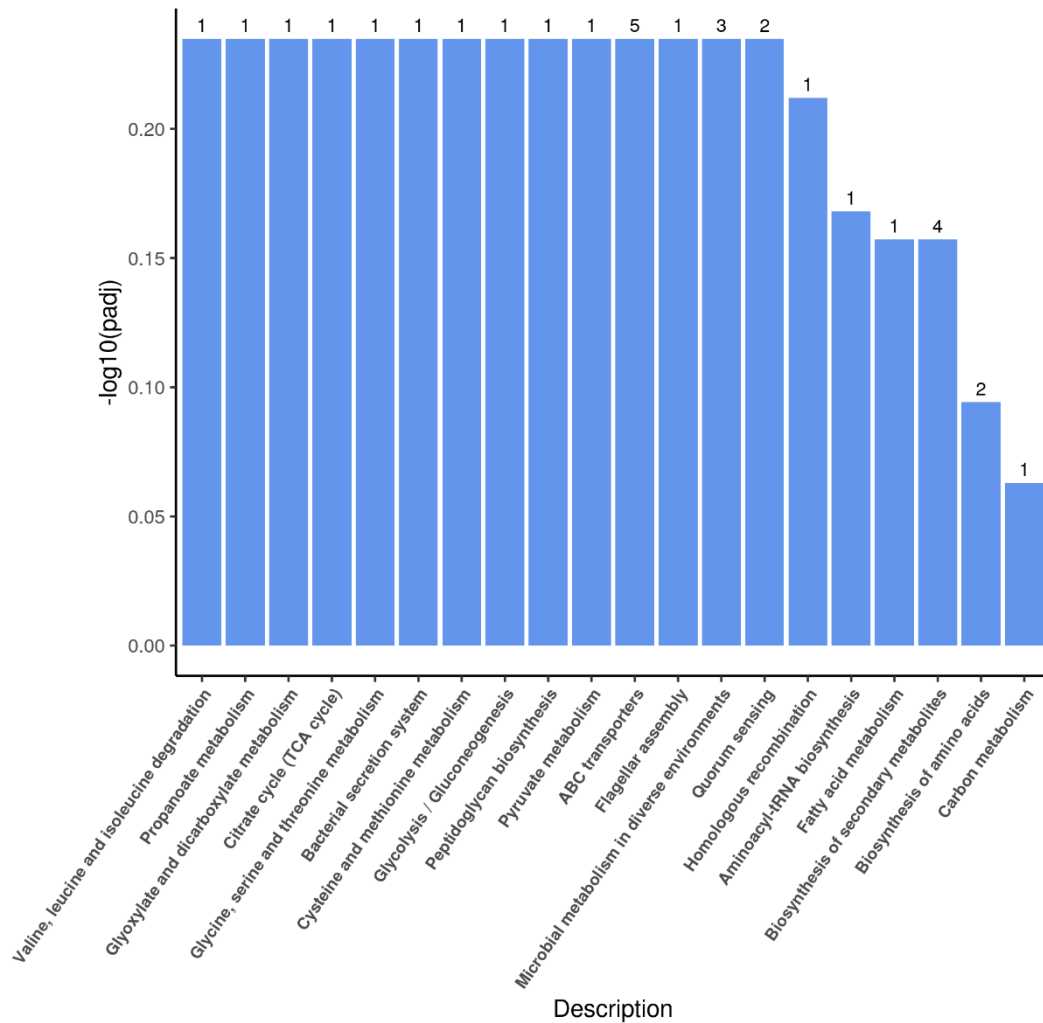


1007

1008 **Supplementary Fig. 53. Up-regulation KEGG pathways enrichment (scatter plot)**

1009 **based on the transcriptomic analysis of PE degradation by *Ochrobactrum* sp. for**

1010 **8 h.**



1011

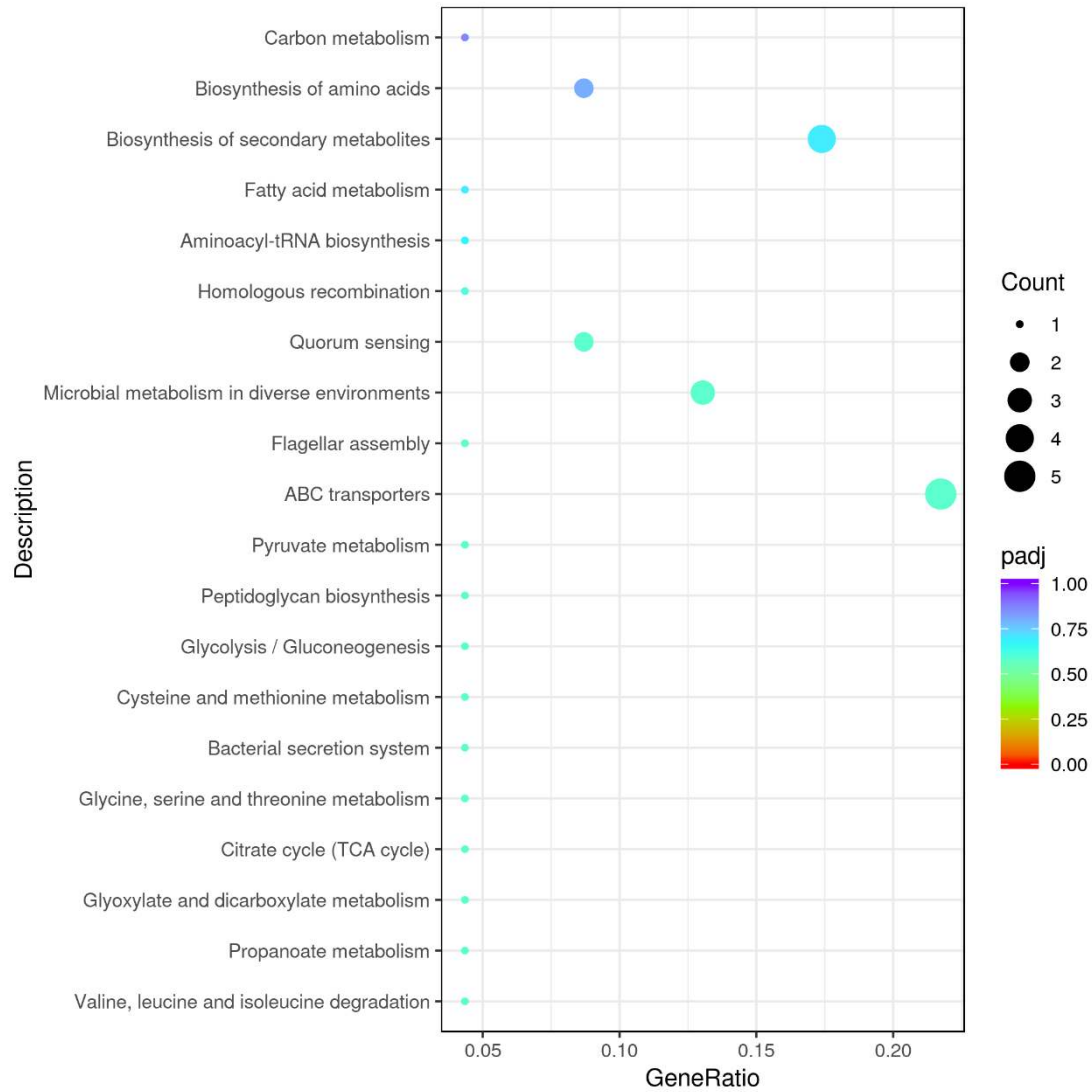
1012 **Supplementary Fig. 54. Up-regulation KEGG pathways enrichment (histogram)**

1013 **based on the transcriptomic analysis of PE degradation by *Ochrobactrum* sp. for**

1014 **7 d.** The numbers above the column are corresponding genes number related to

1015 different pathways.

1016



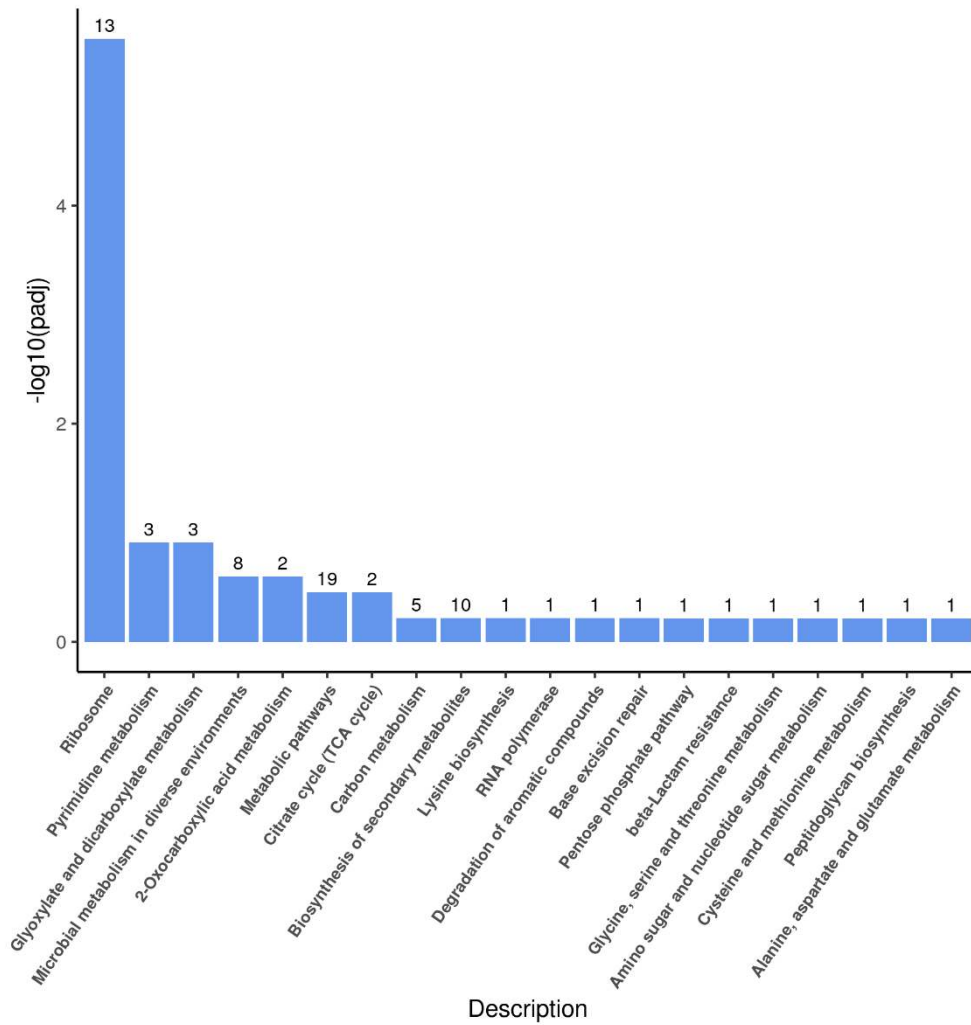
1017

1018 **Supplementary Fig. 55. Up-regulation KEGG pathways enrichment (scatter plot)**

1019 **based on the transcriptomic analysis of PE degradation by *Ochrobactrum* sp. for**

1020 **7 d.**

1021



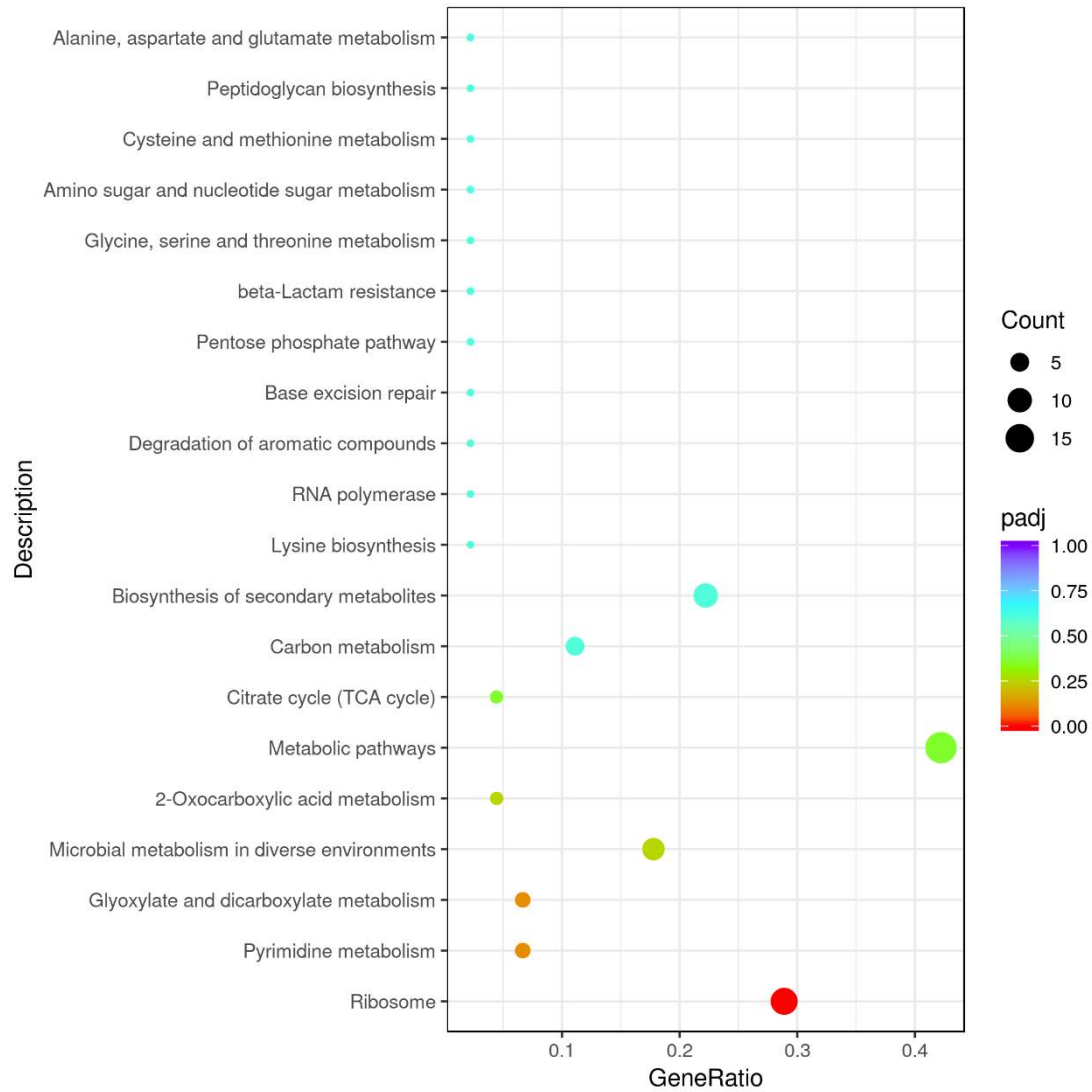
1022

1023 **Supplementary Fig. 56. Up-regulation KEGG pathways enrichment (histogram)**

1024 **based on the transcriptomic analysis of PE degradation by *Ochrobactrum* sp. for**

1025 **14 d.** The numbers above the column are corresponding genes number related to

1026 different pathways.



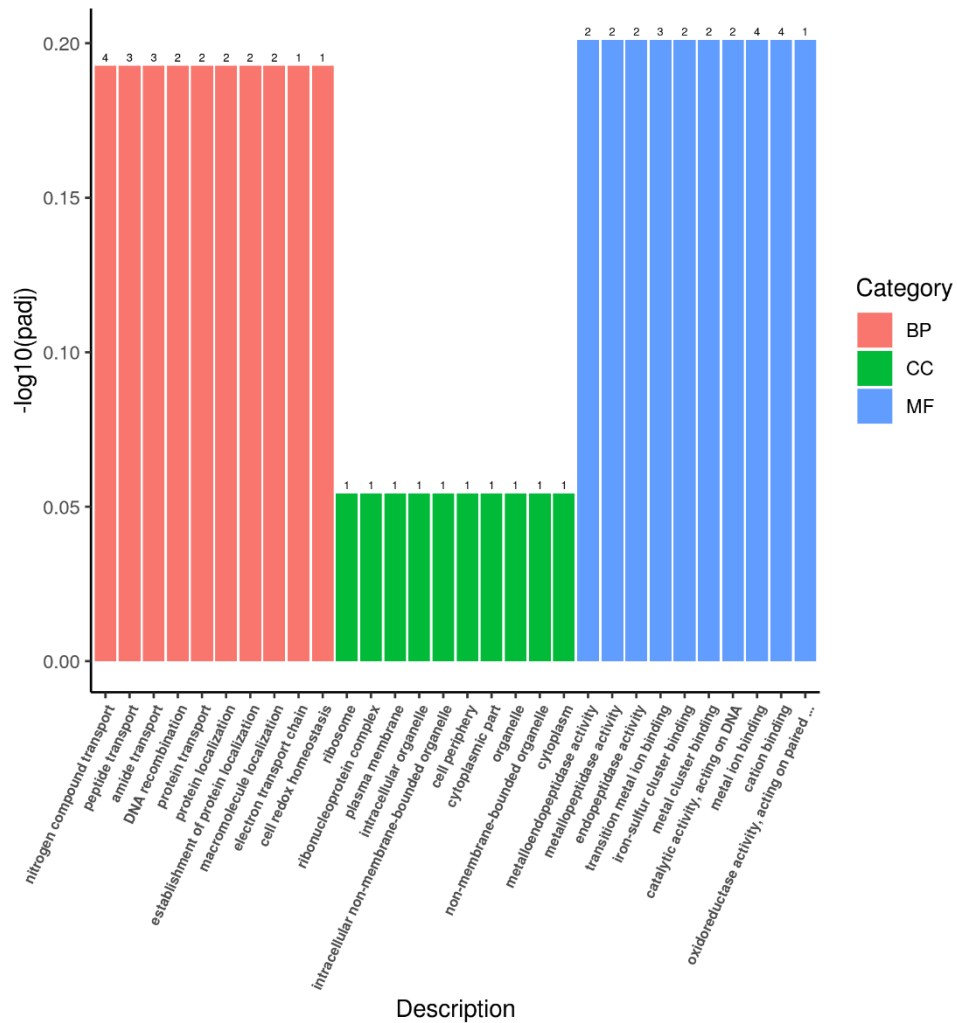
1027

1028 **Supplementary Fig. 57. Up-regulation KEGG pathways enrichment (scatter plot)**

1029 **based on the transcriptomic analysis of PE degradation by *Ochrobactrum* sp. for**

1030 **14 d.**

1031



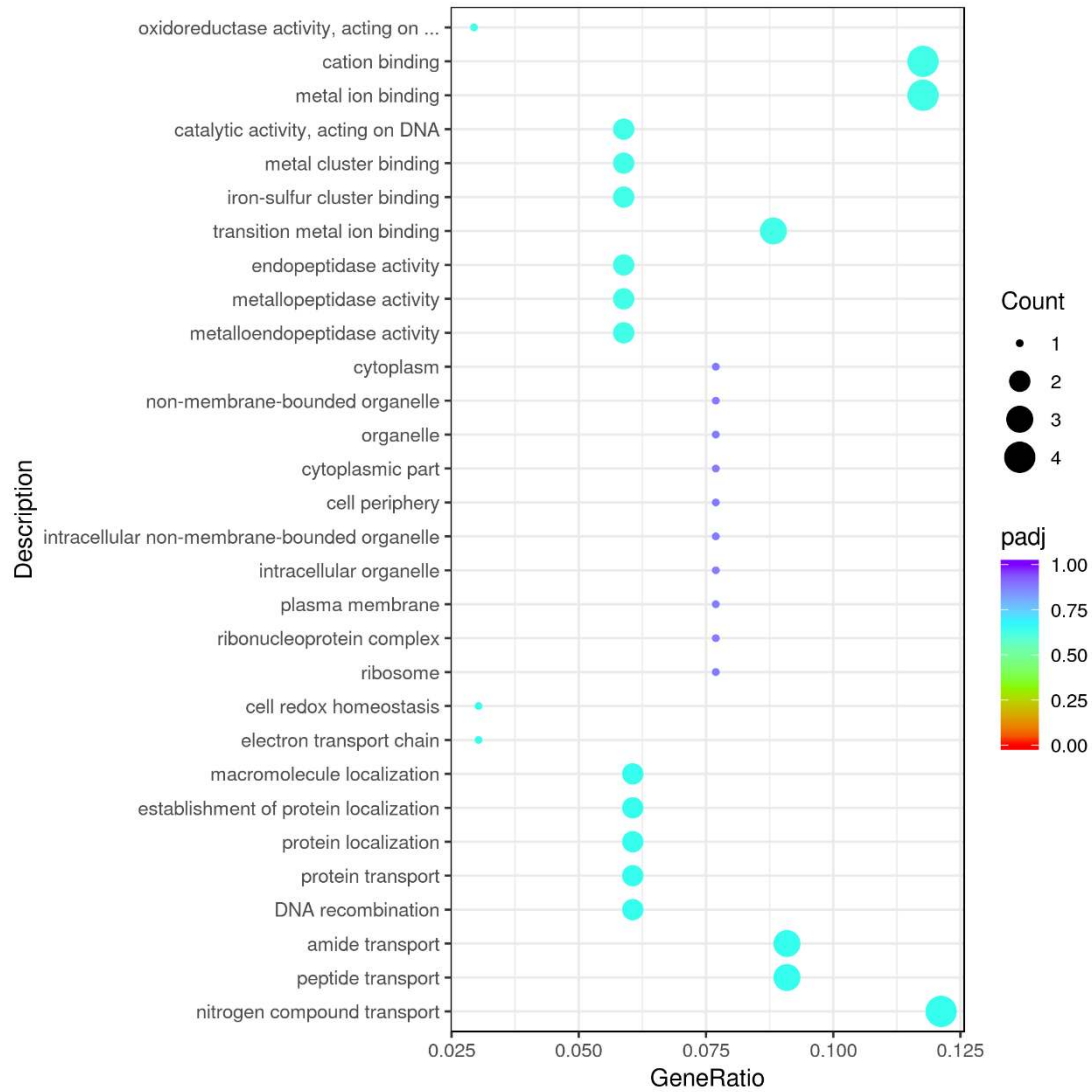
1032

1033 **Supplementary Fig. 58. Up-regulation Go enrichment (histogram) based on the**

1034 **transcriptomic analysis of PE degradation by *Ochrobactrum* sp. for 8 h. The**

1035 numbers above the column are corresponding genes number related to different

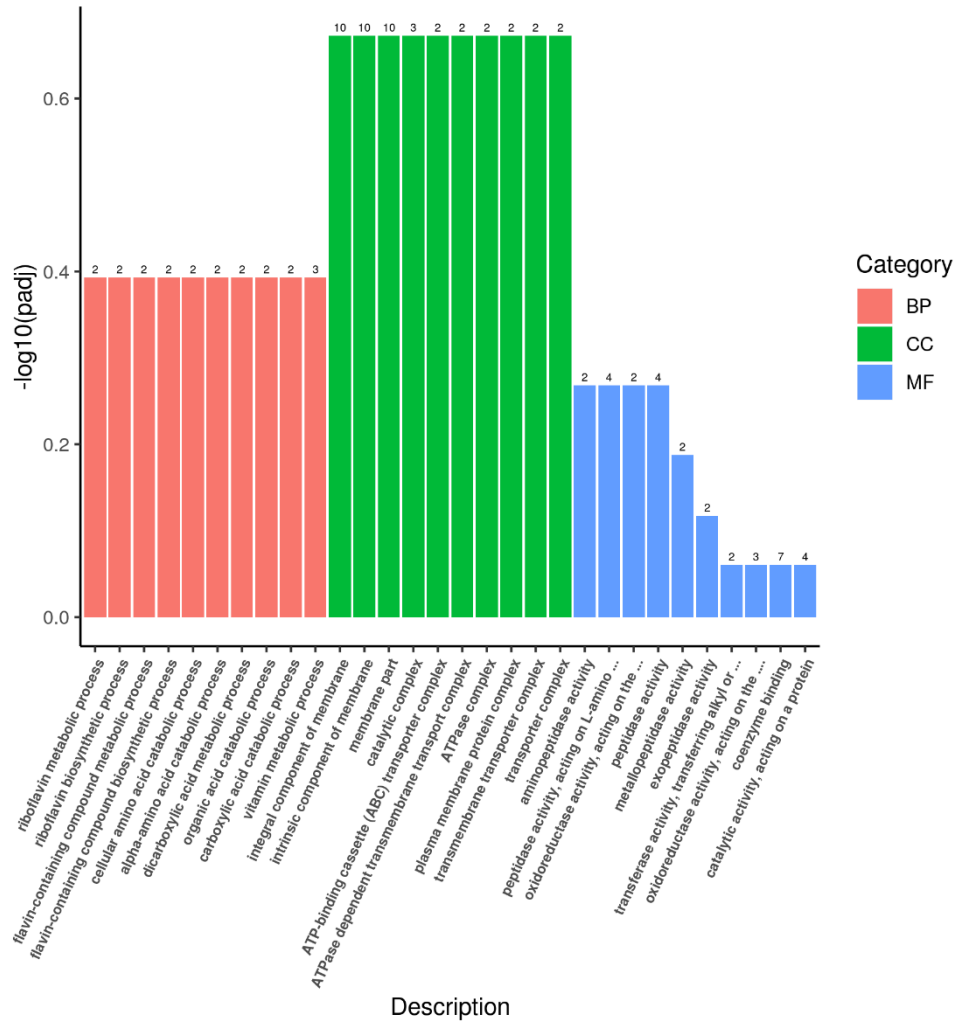
1036 pathways.



1037

1038 **Supplementary Fig. 59. Up-regulation GO enrichment (scatter plot) based on the**

1039 **transcriptomic analysis of PE degradation by *Ochrobactrum* sp. for 8 h.**



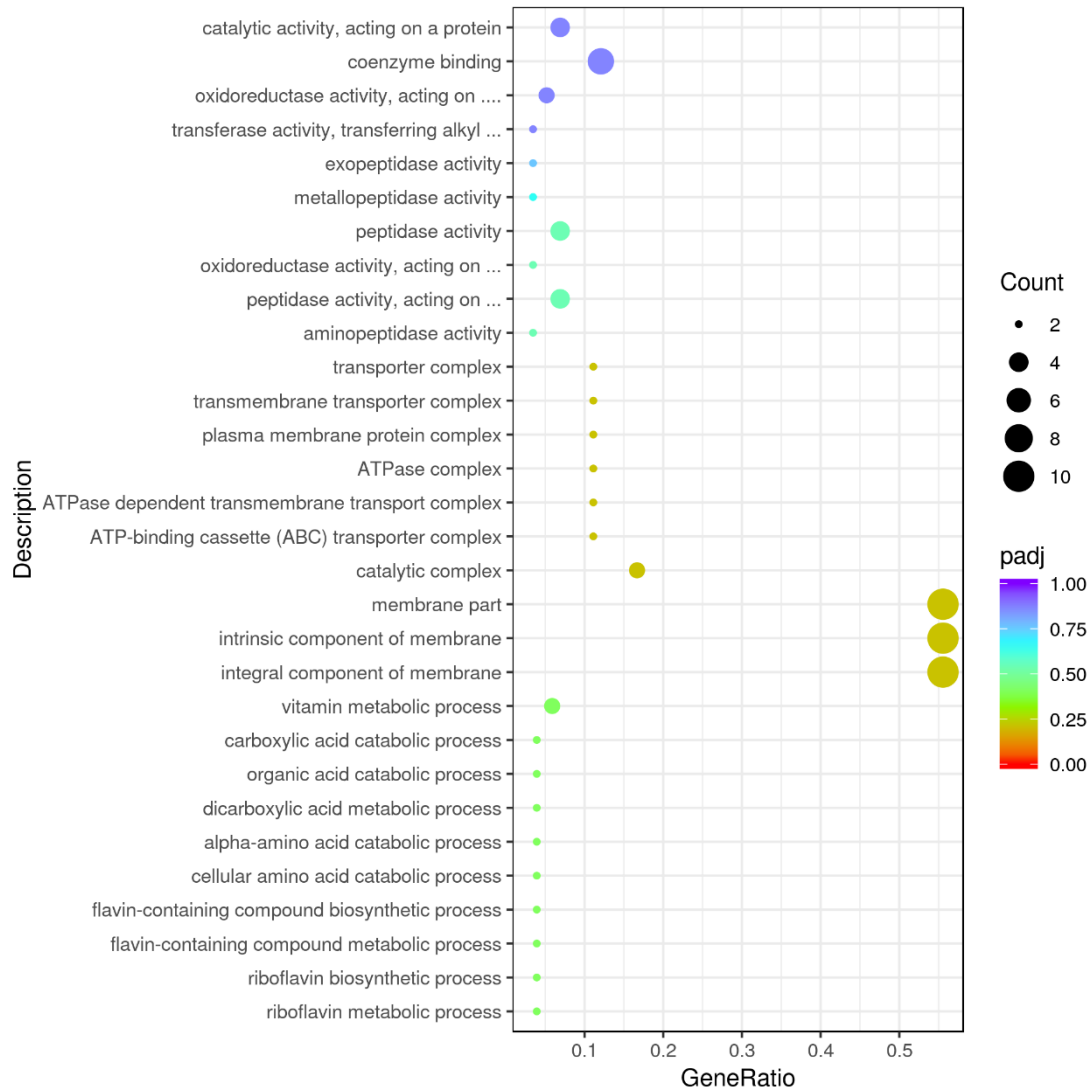
1040

1041 **Supplementary Fig. 60. Up-regulation Go enrichment (histogram) based on the**

1042 **transcriptomic analysis of PE degradation by *Ochrobactrum* sp. for 7 d. The**

1043 numbers above the column are corresponding genes number related to different

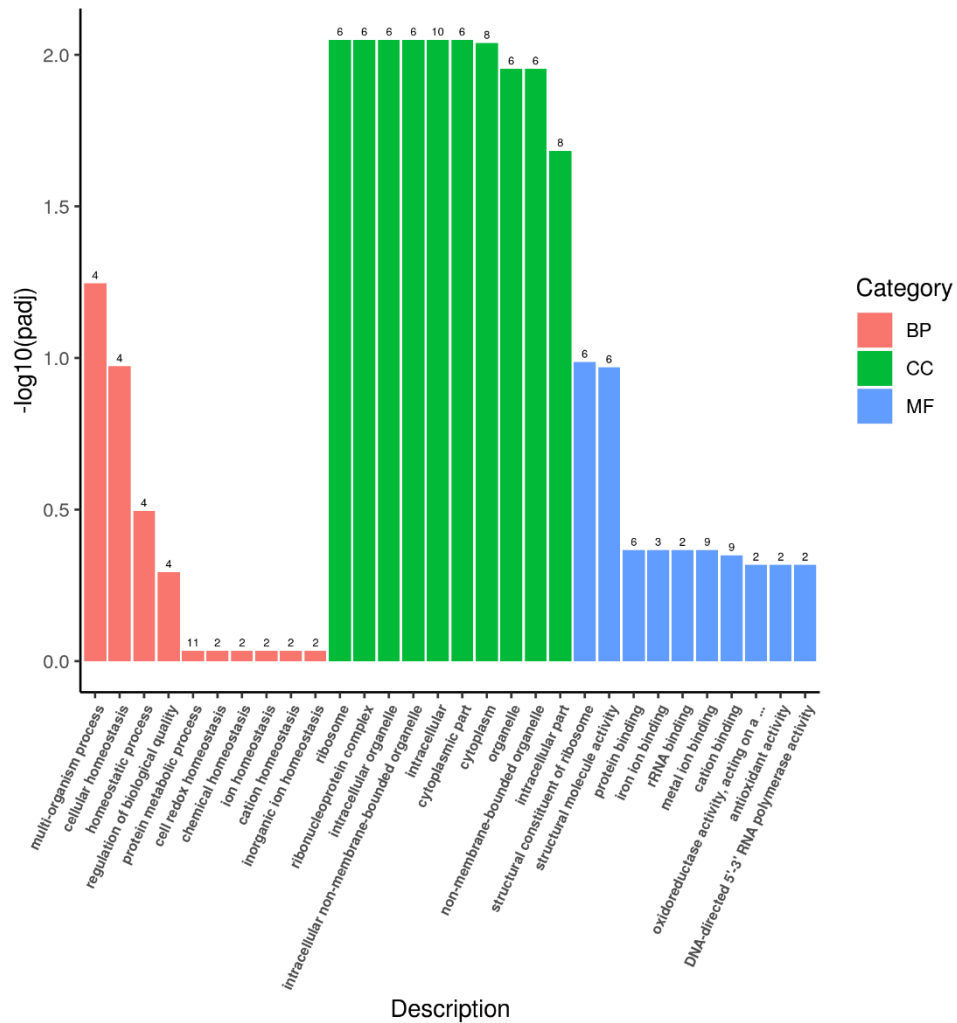
1044 pathways.



1045

1046 **Supplementary Fig. 61. Up-regulation GO enrichment (scatter plot) based on the**

1047 **transcriptomic analysis of PE degradation by *Ochrobactrum* sp. for 7 d.**



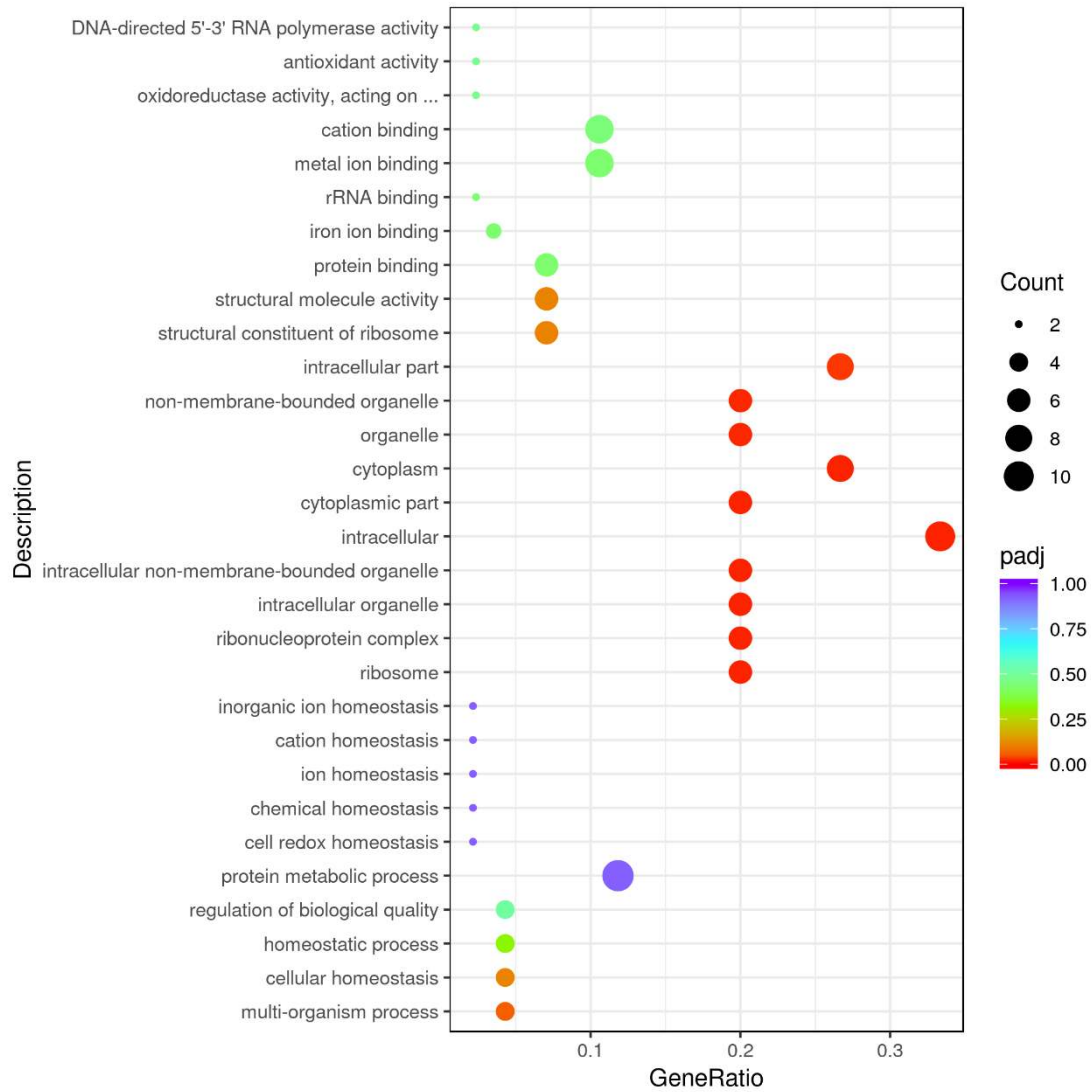
1048

1049 **Supplementary Fig. 62. Up-regulation Go enrichment (histogram) based on the**

1050 **transcriptomic analysis of PE degradation by *Ochrobactrum* sp. for 14 d. The**

1051 numbers above the column are corresponding genes number related to different

1052 pathways.



1053

1054 **Supplementary Fig. 63. Up-regulation GO enrichment (scatter plot) based on the**
1055 **transcriptomic analysis of PE degradation by *Ochrobactrum* sp. for 14 d.**

1056

1057

1058

1059

1060

1061

1062

1063

1064

1065 **Supplementary Table 1. Absolute quantification analysis about 16S rRNA**
1066 **sequences of top 5 bacterial genera within the microbial community degrading**
1067 **plastics.**

genus	Total OTU[*]	E1 OTUsize[#]	E2 OTUsize[#]	E3 OTUsize[#]
<i>Idiomarina</i>	2456196232	1377935941	581578306	496681985
<i>Marinobacter</i>	1380072016	595840950	369029555	415201511
<i>Exiguobacterium</i>	886323611	424309595	265900937	196113079
<i>Halomonas</i>	122456072	60195881	36040715	26219476
<i>Ochrobactrum</i>	34634341	17227886	9263026	8143429

1068 *OTU: operational taxonomic unit. #Three biological replicates.

1069

1070